HHS Public Access

Author manuscript

J Med Chem. Author manuscript; available in PMC 2026 July 07.

Published in final edited form as:

J Med Chem. 2026 June 25; 69(12): 14365–14389. doi:10.1021/acs.jmedchem.6c00065.

Lead Optimization of TgCDPK1 Inhibitors for the Treatment of Toxoplasmosis

Michael P. Mannino[⊥],
Department of Biochemistry and Molecular Biophysics, Washington University School of Medicine, St. Louis, Missouri 63110, United States

Anusha Gokanapalle[⊥],
Department of Biochemistry and Molecular Biophysics, Washington University School of Medicine, St. Louis, Missouri 63110, United States

Shrushti Patil[⊥],
Department of Molecular Microbiology, Washington University School of Medicine, St. Louis, Missouri 63110, United States

Anoopjit Singh Kooner[⊥],
Department of Biochemistry and Molecular Biophysics, Washington University School of Medicine, St. Louis, Missouri 63110, United States

Chhuttan Lal Meena,
Department of Biochemistry and Molecular Biophysics, Washington University School of Medicine, St. Louis, Missouri 63110, United States

Matthew Medcalf,
Department of Biochemistry and Molecular Biophysics, Washington University School of Medicine, St. Louis, Missouri 63110, United States

Igi Vilza,
Department of Molecular Microbiology, Washington University School of Medicine, St. Louis, Missouri 63110, United States

Jennifer Barks,
Department of Molecular Microbiology, Washington University School of Medicine, St. Louis, Missouri 63110, United States

Yong Fu,

Corresponding Authors L. David Sibley – Department of Molecular Microbiology, Washington University School of Medicine, St. Louis, Missouri 63110, United States; sibley@wustl.edu, **James W. Janetka** – Department of Biochemistry and Molecular Biophysics and Department of Molecular Microbiology, Washington University School of Medicine, St. Louis, Missouri 63110, United States; janetkaj@wustl.edu.

[⊥]Author Contributions

[⊥]M.P.M., A.G., S.P., and A.S.K. contributed equally to this work.

The authors declare the following competing financial interest(s): L.D.S. and J.W.J. are inventors on several patents and patent applications.

Accession Codes

9Z5L and 9Z5M, compounds TRC3264 and TRC2895. The authors have released the atomic coordinates and experimental data to the PDB.

Department of Molecular Microbiology, Washington University School of Medicine, St. Louis, Missouri 63110, United States

Jing Xia,
Department of Molecular Microbiology, Washington University School of Medicine, St. Louis, Missouri 63110, United States

Jay C. Nix,
Advanced Light Source, Lawrence Berkely National Laboratory, Berkeley, California 94720, United States

Chris Nelson,
Department of Pathology and Immunology, Washington University School of Medicine, St. Louis, Missouri 63110, United States

Daved Fremont,
Department of Pathology and Immunology, Washington University School of Medicine, St. Louis, Missouri 63110, United States

Arun Dhillon,
Department of Molecular Microbiology, Washington University School of Medicine, St. Louis, Missouri 63110, United States

L. David Sibley,
Department of Molecular Microbiology, Washington University School of Medicine, St. Louis, Missouri 63110, United States

James W. Janetka
Department of Biochemistry and Molecular Biophysics and Department of Molecular Microbiology, Washington University School of Medicine, St. Louis, Missouri 63110, United States

Abstract

Toxoplasma gondii is an important opportunistic pathogen that infects many individuals and threatens the health of those with compromised immunity. Current therapies are unable to eradicate chronic infections and pose risks of adverse reactions. Using X-ray structure-based drug design, we have developed a new series of biaryl-substituted pyrazolopyrimidine inhibitors of the essential parasite enzyme calcium-dependent protein kinase 1 (TgCDPK1). These inhibitors have excellent potency against the enzyme and *in vitro* antiparasitic activity. We further optimized the compounds for increased metabolic stability, lowered plasma protein binding, decreased efflux, and improved pharmacokinetics (PK). Several of the inhibitors had desirable PK with high oral bioavailability, low clearance, and extended half-life, leading to excellent compound exposure in the plasma and brain over a 24-h period. Three compounds were tested during acute infection in both immunocompetent and immunocompromised mice. We identified **16c** as a promising preclinical candidate to treat toxoplasmosis.

Graphical Abstract

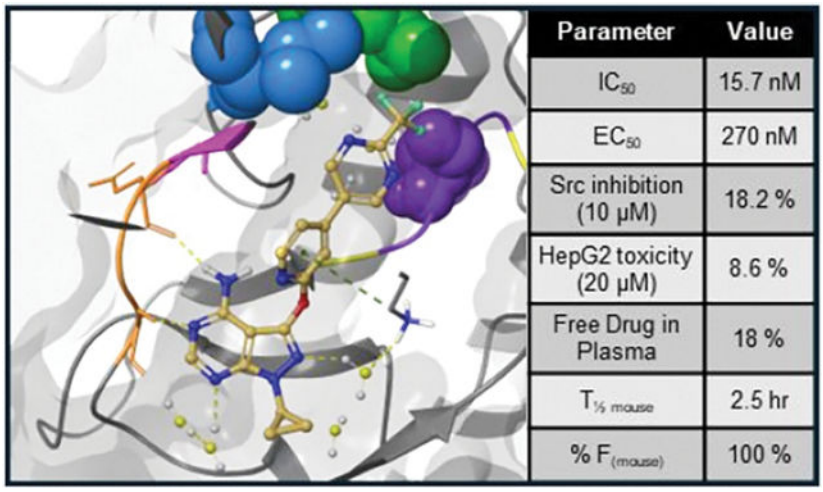

Parameter	Value
IC_{50}	15.7 nM
EC_{50}	270 nM
Src inhibition (10 μM)	18.2 %
HepG2 toxicity (20 μM)	8.6 %
Free Drug in Plasma	18 %
$T_{½\ mouse}$	2.5 hr
% $F_{(mouse)}$	100 %

INTRODUCTION

One third of the global human population is sero-positive for the apicomplexan parasite *Toxoplasma gondii* (*T. gondii*) suggesting it chronically infects a large fraction of the population.[1] The majority of people infected with *T. gondii* in North America and Europe have mild symptoms during acute infection such as enlarged lymph nodes and fever, although more severe cases can result in encephalitis leading to headache, seizure, altered mentation and focal neurologic signs.[2,3] In contrast, more virulent strains of *T. gondii* found in South America are associated with serious ocular disease in immunocompetent persons.[4–6] Toxoplasmosis is also more severe in organ transplant and cancer patients due to immunosuppression,[7] and in HIV-AIDS patients that are not under effective antiviral treatment and where T cell levels may be very low.[8,9] Congenital infection can result when previously naive women become infected during pregnancy and the risk of transplacental infection and the severity of outcome vary during pregnancy.[2,10]

Humans, and other intermediate hosts, are infected by the ingestion of oocysts present in contaminated food or water sources, or by ingestion of undercooked meat harboring tissue cysts that contain bradyzoites.[11] Acute infections are characterized by a fast growing form called the tachyzoite, which invades the host cell to form a parasitophorous vacuole. Within this protected compartment, the parasite replicates by binary fission before egressing from the host cell, leading to new rounds of infection.[12] A vigorous Th1 host immune response, culminating in production of interferon γ, suppresses tachyzoite growth and eliminates many parasites through various effector mechanisms.[13,14] In response, the parasite differentiates into a cyst-forming bradyzoite stage typically found in long-lived tissue such neurons in the CNS and retina or in muscle tissues. These chronic stages effectively evade the immune system, resulting in life long chronic infection of the host.[15]

The current clinical treatment for toxoplasmosis employs two repurposed antimalarial drugs, pyrimethamine and sulfadiazine, which synergistically inhibit folic acid metabolism, preventing parasite replication.[16] However, these drugs only act upon the actively replicating tachyzoite stage of the parasite but do not eliminate those in the chronic stage due to the

semidormant nature of bradyzoites.[16] Additionally, immunocompromised patients require extended or indefinite maintenance treatment.[17] These prolonged treatment regimens are problematic as these drugs are associated with adverse side effects and toxicity such as hematological toxicity, rash and leucopoenia, the latter related to off-target inhibition of endogenous folic acid metabolism.[18] For example, a study done from 2013–2019 found 503 reported cases of adverse events while treating toxoplasmosis, 59% of which featured either one or both drugs.[19] Other treatments targeting protein synthesis, DNA damage protection and electron transport chain function are available but are either less effective or exhibit similar toxicities.[16] Given these issues with prolonged treatment, there is a strong need for drug therapies that either directly target the bradyzoites in tissue cysts and/or have far diminished toxicity amendable for long-term treatment.

Micronemes are apical secretion organelles that release adhesin proteins and play a role in substrate and host cell of apicomplexan parasites.[20] In *T. gondii*, microneme secretion is regulated by a calcium-dependent protein kinase 1 (TgCDPK1), which is required for motility, host cell invasion and egress.[21] TgCDPK1 is a member of the CDPK family of kinases which are restricted to plants and protozoa.[22] TgCDPK1 shares many of the same structural elements with mammalian kinases but features a highly unusual Gly gatekeeper residue.[23,24] The gatekeeper residue sits just above the hinge region in the ATP-binding site and the side chain at this residue influences active site interaction with bulky ATP-mimetic inhibitors.[25] Most mammalian kinases contain larger residues such as Leu or Met, or intermediate residues such as Ser or Thr, at this position.[26] This important difference was initially exploited to selectively inhibit TgCDPK1 with ATP analogs bearing bulky substituents that project into the deep hydrophobic pocket afforded by the unique Gly gatekeeper.[21,23] These early studies validated the primary target of pyrazolopyrimidine (PP) inhibitors as CDPK1, and confirmed the essentiality of the glycine gatekeeper in determining specificity over mammalian kinases.

Since these initial discoveries, a variety of published studies by us and others have used the PP scaffold to generate more drug-like molecules to improve potency, metabolic stability, and target specificity.[23,25,27–32] For example, our previous PP lead compound (TRC2885), bearing an O-linked *o*-pyridyl group at the R_1 position,[27] performed well in the acute mouse model of toxoplasmosis but left room for improvement in pharmacokinetic (PK) properties, especially in duration of exposure above effective levels. Others have also reported efficacy of a different class of small molecule CDPK1 inhibitors for treating toxoplasmosis[32,33] and cryptosporidiosis.[34,35]

Utilizing newly derived crystal structures, we sought to expand upon TRC2885, aiming to improve its drug-like properties, such as volume of distribution and overall exposure, while maintaining its potency and nontoxic profile. Herein we describe our efforts in continuing the optimization of our PP, O-linked *o*-pyridyl scaffold by expanding the scope of substituents in the R_2 and R_3 position. Further optimization resulted in the discovery of new lead candidate (**16c**, MPM2008) that was able to cure acute toxoplasmosis in immunocompetent mice and prolong survival in immunodeficient mice.

RESULTS

Although the potency of previous lead compound TRC2885 was excellent (IC_{50} = 16 nM), it lacks structural attributes capable of establishing interactions in the TgCDPK1 active site known to be exploited by other compounds. Namely, a hydrogen bond (H-bond) donating group at R_2 forming an interaction with residues in the ribose-binding pocket, and an extended flat aryl group at the R_3 position projecting further into the deep hydrophobic pocket (Figure 1). Both features have previously proven to improve selectivity and potency.[30,31,36] Here, we pursued new rationally designed compounds which take advantage of such interactions to improve potency as well as for developing SAR for improving compound properties such as metabolic stability, plasma protein binding, and pharmacokinetics (PK). To this extent, we obtained cocrystal structures of TgCDPK1 with two compounds that we predicted may exploit interactions in the ribose binding pocket (**2a**, TRC3264) and the deep hydrophobic pocket (**1b**, TRC2895), Figure 1A. Both TRC2885 and **2a** have a C5 para-trifluoromethyl (CF_3) pyridyl group, while **1b** has an additional para phenyl moiety at R_3. Compound **2a** contains an *N*-methyl-4-aminocyclohexyl ring at R_2 compared to the cyclopropyl of TRC2885 and **1b**, Figure 1B.

The X-ray cocrystal structures of both compounds bound to TgCDPK1 demonstrated an αC-helix “out” inactive configuration and the predicted H-bonding at the hinge site, hydrogen bond donor from exocyclic N–H and hydrogen bond acceptor from pyrimidine nitrogen to the backbone amides of Glu129 and Tyr131, respectively (Figure 1C, Supporting Table 1). The *N*-methyl-4-aminocyclohexyl ring at R_2 position of **2a** projects into the ribose binding pocket, where its amino group interacts with a water molecule, which is part of a network of water molecules coordinated by Ser61, Lys80, Glu135, Glu178, Asn179, and Asp195. This amino group at R_2 also forms an H-bond with Lys59′s backbone. Both these sets of interactions are absent from the cyclopropyl-bearing compounds.

However, the *N*-methyl-4-aminocyclohexyl ring system is pointing away and is unable to take advantage of a previously highlighted interaction with the Glu135 side chain, an interaction that has been shown to improve selectivity over mammalian kinases.[31] The CF_3 group of **2a** is positioned to interact with the N–H amide backbone of Asp195, and a water molecule potentially forming a H-bond.[37] In **1b**, the second phenyl group replaces the CF_3 present in TRC2885 and **2a** and hence loses the potential interaction with Asp195. However, it reached deeper into the hydrophobic pocket lined by the residues Leu103, Leu114, His174, and Phe196. This orients the phenyl ring to have additional hydrophobic interactions with Leu114, Ph196, and Phe198 when compared to the CF_3 group of **2a** (Figure 1C). Projection into this pocket has previously been demonstrated to impart selectivity and potency.[32,36] The water molecules seen bridging Tyr131 and Gly134 with the PP ring of **1b** were observed to have high *B*-factors in the TgCDPK1-**2a** map and could not be modeled accurately. Collectively, these interactions take advantage of additional features beyond the selective Gly gatekeeper, which is the primary basis for the selectivity of CDPK1inhibitors.[21,23]

These new structural insights were leveraged in the generation of new antitoxoplasmosis lead compounds. In this vein we expanded the scope of compounds to focus on those with

R_2 groups capable of electrostatic interactions in the ribose-binding pocket, and R_3 aryl groups that project deeper into the hydrophobic pocket.

The synthesis of such compounds was achieved using advanced PP, O-linked pyridyl intermediates (described previously).[27] Linkage of R_3 aryl groups was realized by applying Suzuki reactions with the *p*-bromo, O-pyridyl PP intermediate with the corresponding aryl boronic acids/esters, Scheme 1A. Functionalization at the R_2 position was achieved through Mitsunobu reactions or addition of mesyl chloride under basic conditions. In the case of amine-bearing moieties, the Boc protected amino group was deprotected and further functionalized via acylation or reductive amination, Scheme 1B. All final compounds were purified by reverse-phase HPLC and purity was confirmed to be >95% by LCMS (see Supporting data) prior to biological assays.

Compounds were screened on their potency as TgCDPK1 inhibitors, their ability to inhibit parasitic proliferation and their metabolic stability when incubated with mouse and/or human liver microsomes. Inhibition of recombinant TgCDPK1 isolated from *Escherichia coli* was determined using an ELISA assay. The *T. gondii* growth assay was done incubating human foreskin fibroblast (HFF) cells with *β*-gal RH parasites in the presence of inhibitors. Both methods have been previously employed and described by our lab.[29] Compounds that demonstrated IC_{50} and EC_{50} values below 150 and 350 nM respectively were further analyzed to determine their metabolic stability. Compounds with stability half-lives >90 min were then selected for determination of other *in vitro* drug-like properties, such as efflux ratio, plasma protein binding and/or cytotoxicity. Compounds that featured good overall drug like properties were then selected for *in vivo* PK studies prior to animal model consideration.

As was observed in our previous publication,[27] *cis*- and *trans*-1,4-cyclohexyl alkylated amines at the R_2 position showed good inhibition in both the kinase and cell assays. With this in mind, we examined additional alkylated and acylated amine-bearing compounds. Compounds functionalized with smaller groups such as methyl, ethyl, acetyl and even isopropyl (**1a–6a** and **9a–10a**) showed comparable kinase inhibition between diastereomers. However, a preference for the *trans*-isomer was observed with longer alkyl groups or acyl groups containing additional heteroatoms (**7a–8a** and **11a–14a**). Molecular modeling using the **2a** crystal structure (PDB: 9Z5L) and these stereoisomers suggest that the *cis*-substituents steric clashes in the ribose binding pocket (Figure S2). Unfortunately, none of these functionalities demonstrated acceptable metabolic stability against mouse liver microsomes (MLM), Table 1. Wanting to further evaluate R_2 amino substituents, we synthesized a variety of alkylated and acylated 1,3-cyclohexyl amines. All four diastereomers of the free amine showed very similar potency against TgCDPK1 (**15a–18a**). However, like the 1,4-amino compounds, a stereo preference was observed when substituents were added. The steric sensitivity was even more noticeable in this series, showing 8- and 15-fold reduced inhibition when comparing R,R isomers to the far less desirable S,R and S,S series (**19a–22a**). Unfortunately, molecular modeling did not produce predictive docking or interactions for this series. Expansion of this series showed that acylated compounds display improved kinase inhibition compared to their alkylated counterparts (**25a–28a**). However, only the free amine and methyl sulfonamide moieties

showed acceptable cellular activity and MLM stability (**15a**, **17a** and **26a**). Although the free amine, compound **17a** showed an ideal potency and stability, MDCK-MDR1 efflux assays revealed it to be highly susceptible to efflux, with a $P_{b\ to\ a}$ ratio of 24.4. To address this concern, we synthesized similar 1,3-amino compounds utilizing pyran rings whose endocyclic oxygen is predicted to reduce the basicity of the free amine. These pyran compounds exhibited slightly reduced kinase and cellular potency compared to the cyclohexyl compounds (**15a–18a** vs **29a–31a**). The pyran compound **30a** (AJS2144) showed good potency, excellent MLM stability and importantly an increased resistance to efflux (efflux ratio improved to 6.6).

Similarly, we utilized the **1b** crystal structure to design compounds with an additional aryl group at the R_3 position, biaryl compounds, to take advantage of the deep hydrophobic pocket of TgCDPK1, Table 2. Unlike our starting point in the R_2 direction, (**1b**) allowed for improvement in terms of potency. To understand the available space in this deeper part of the hydrophobic pocket, we first set out to determine the effect of substituent location and length. Surprisingly even the simple addition of a para-methyl group drastically improved the enzymatic and cellular potency (**2b**). Comparing location and flexibility of substituents demonstrated that the para moieties had improved fit in the active site compared to meta, indicated by IC_{50} (**3b–6b**). This was even more apparent with more rigid substitutions such as cyano, possibly suggesting steric hindrance at the meta-position. Continuing to investigate the SAR of para-functional groups we noticed that although we achieved improved kinase and cellular potency, the metabolic stability of these compounds was poor (**5b** and **7b**). This was even the case with p-trideuteromethane (CD_3) which showed no improved stability compared to its hydrogen counterpart (**8b** vs **2b**). Addition of a para-fluorine atom demonstrated slightly improved MLM stability (**10a**). From this result we decided to investigate the effect of electron withdrawing groups. Bulky, heteroatom-containing groups such as sulfonamide or amide were unable to fit into the hydrophobic pocket (**11b** and **12b**). The para-CF_3 drastically improved the MLM stability while maintaining the compound's potency (**13b**). Similar stability was observed for other electron deficient phenyl groups, with the flanking meta difluoro para-CF_3 compound affording the best stability. It is important to note that these fluorinated lipophilic compounds exhibited reduced cellular potency, likely through decreased cell permeability (**14b–16b**). We then expanded the biaryl scope to 5-member heterocycles. Inhibitor potency was not substantially altered when changing between the 1, 2-linkages vs 1, 3-linkages for furan and thiophene rings (**17b** and **18b** vs **20b** and **21b**), however we observed *a* > 10-fold reduction in potency for 1, 3-linked pyrazol compared to the 1, 2-linkage (**19b** vs **22b**). The inclusion of a second heteroatom in thiazole and oxazole rings showed reduced enzymatic potency and drastically inferior cellular potency, perhaps suffering from reduced permeability (**23b–25b**). As was observed in the biphenyl series, appendages of the heterocycles which project deeper into the pocket showed a 10-fold improvement in enzymatic inhibition (**18b** vs **26b**, **27b** and **30b** vs **19b**). These improvements were mitigated when substituents were moved adjacent to the aryl-linkage (**28b** and **31b**). Compound **30b** in particular demonstrated outstanding potency in both theenzyme and cellular assays. However, unlike the phenyl compounds, stability of these compounds was not improved by adding electron withdrawing groups (**29b** and **31b**), which was found to be a major liability in this series of compounds. Attempts to address

this by capping free amines or adding additional substituents at all positions both resulted in reduced cellular potency (**31b** and **32b**). This may be a result of reduced permeability.

From our initial SAR screening we identified three lead compounds suitable for further testing; **30a** (AJS2144), **1a** (AM5013) and **16b** (CLM1086). These leads were found to have good selectivity against kinases with larger gatekeeper residues (Src, Thr and TgCDPK G128M, Met), and were not cytotoxic toward HepG2 cells (Figure 2C). Subsequently, both IV (3 mg/kg) and PO (10 mg/kg) dosing were performed in mice to elucidate a complete PK profile, Figure 2A,B. The compounds bearing exocyclic amines at R_2, **30a** and **1a**, featured rapid elimination indicated by their short half-lives, low exposure (AUC) and high clearance values. By comparison, the biaryl **16b** exhibited far slower elimination, demonstrated through its significantly longer half-life and reduced clearance. The continuous and variable increases in **16b** plasma concentration over 8 h in PO dosing compared to IV may be explained by slow oral absorption. Compound **16b** also displayed excellent drug exposure (AUC) and oral bioavailability (% F). From these studies, **16b** stood out as our lead candidate.

The primary concern of compound **16b** is its high levels of plasma protein binding (PPB), 99.7% bound. According to the free drug hypothesis, it is only the unbound fraction of drug that exerts a pharmacological effect. To address the highly bound nature of our lead compound, we decided to do additional optimization aimed at lowering the compound's lipophilicity while maintaining potency and metabolic stability. Additionally, we theorized that improving this parameter would also improve cellular permeability and potency. To achieve this outcome, we undertook three different approaches to generate compounds in three groups (Table 3): group A replacing the para-CF_3 group with less lipophilic groups (**1c–7c**), group B exchanging the R_2 group with less lipophilic ones (**8c–11c**) and group C replacing the 3,5-difluoro phenyl ring moiety with various nitrogen bearing 6-member heterocycles (**12c–20c**)).

As predicted, replacing the para-CF_3 group with less lipophilic ones greatly improved the cellular potency (EC_{50}) (**1c–3c**), Table 3. This outcome was not the case for the more polar and uncapped heteroatoms (**5c** and **6c**). Unfortunately, these derivatives were metabolically liable and did not substantially alter PPB. Since the heavily fluorinated **16b** exhibited excellent *in vitro* and *in vivo* stability (Table 2 and Figure 2), we next endeavored to maintain the 3,5-difluoro, 4-CF_3 phenyl moiety, while decreasing the lipophilicity at the R_2 group, Table 3. Substituent modification at this site showed a similar improvement in EC_{50} potency. Importantly, several of these compounds demonstrated similarly optimal MLM stability to **16b** (**8c** and **9c**). Although compound **9c** exhibited a PPB that was more appealing, we feared a similar efflux liability of the piperidine group as we observed with **17a**. We converted to the less basic morpholine group (**10c**) to avoid this pitfall, but unfortunately this modification reduced both cellular potency and MLM stability. Our next attempt to lower the lipophilicity of our biaryl compounds was to replace the 3,5-difluoro phenyl moiety with N-aromatic rings, while still featuring the para-CF_3 group, Table 3. We hypothesized that replacing the fluorine atoms with nitrogen would decrease the PPB while maintaining an electron deficient ring system, which may be important for metabolic stability. Despite a lack of improvement in cellular potency, pyridyl rings maintained very

good metabolic stability while simultaneously reducing the PPB (**12c** and **13c**). Replacing the CF_3 group with a single fluorine atom (**14c**) showed substantial improvement in PPB, although this change introduced MLM liability. Along the same lines **15c** exhibited a slight decrease in MLM stability. Replacing both fluorine atoms from **16b** with nitrogen atoms (pyrimidine, **16c**) vastly improved the compound properties. These changes greatly increased cellular potency while still maintaining optimized metabolic stability. Importantly this compound also exhibited excellent PPB, demonstrating a 60-fold reduction in plasma-bound compound compared to the **16b**.

Comparison of cLogP and pEC_{50} in these 3 groups indicates that group C afforded the most compounds with good Ligand Lipophilicity Efficiency (LLE) values, >2 (green circles, Figure 3). LLE is a metric which accounts for lipophilicity (cLogP) and efficacy (pEC_{50}) often used to optimize compound's drug-like properties and minimize off-target effects.[38–40] Encouraged by these results, we decided to synthesize additional pyrimidyl compounds, derivatizing either the para substituent on the pyrimidyl ring or changing the R_2 cyclopropyl group to other aliphatic rings that were known to be metabolically stable from our previous work,[27] Table 3. The cellular potency was maintained for most of these derivatives. Modifying the para-group introduced metabolic liability in most of the compounds, with the para-methyl derivative **20c** being the exception. This result was surprising as its 3,5-difluoro counterpart (**2b**) showed poor stability.

Pyrimidine compounds with modified R_2 substituent (**21c–23c**) consistently demonstrated better metabolic stability than those without the para-CF_3 group.

From the additional SAR evaluation, we selected three additional candidates for PK profiling to compare with the current lead **16b**. (Figure 4). As observed with the previous leads, these compounds exhibited good selectivity against kinases bearing large gatekeeper residues and were also noncytotoxic (Figure 4D). Compound **23c** (MPM2085) suffered from poor %F and was not investigated further. The half-lives, AUC, C_{max}, clearance and brain:plasma ratio were only slightly improved for **13c** (MPM1062) over **16c** (MPM2008), although **16c** did show better distribution (V_d). Although the PK profile of these newer compounds fall short of those from **16b**, their increased free fraction (both in plasma and brain, PPB and BPB) favor **16c** and **13c** over **16b** which may be important for inducing a pharmacological effect as stated in the free drug hypothesis (Figure 4C).[41] With this in mind, we continued forward with these three compounds.

Compounds **16b**, **13c**, and **16c** were then further studied to evaluate dose escalation and repeated dosing PK. We administered compounds **16b** and **13c** at doses of 10, 30, or 100 mg/kg as a single oral dose and monitored plasma and brain levels over 24 h (Figure S3). Compound **16b** showed dose-dependent increases on exposure in plasma and even higher levels in brain. Although these levels exceeded EC_{50} total for doses of 30 and 100 mg/kg, only the dose of 100 mg/kg approached the EC_{50} free level, a limitation that is due to high protein binding (Figure S3A). Compound **13c** also showed dose-dependent increased exposure in plasma and brain, although plasma levels generally exceed those of brain (Figure S3B). Also, **13c** showed enhanced clearance at 30 mg/kg and was not detectable

after 8 h. Importantly, the plasma and brain level of **13c** exceeded or approximated the EC_{50} free value, due to the slightly lower protein binding compared to **16b** (Figure S3).

We next evaluated the three lead compounds for repeated doing over 4 consecutive days. Based on the initial 24 h PK profiles for **16b** and **13c**, we decided to perform the 30 mg/kg dosing twice a day (i.e., BID) while 100 mg/kg was given once (i.e., QD), PO. Samples taken over 24 h for the first day vs the final fourth day were evaluated for plasma and brain exposure (Figure 5). In general, all three compounds exhibited similar profiles at day 1 and day 4 indicating they do not induce increased metabolism with repeated exposure, and they also do not accumulate to high levels in tissue. The profiles of **16b** and **13c** were similar in that the former compound failed to achieve exposure above the EC_{50} free level, while the later approximated this level for the first 8 h and then fell below it (Figure 5A,B). Interestingly, the 30 mg/kg BID dose for **13c** exhibited higher serum concentrations after 24 h compared to the 100 mg/kg QD dose at day 1, but they were essentially equivalent at day 4 (Figure 5B). A much-improved profile was observed for **16c** that was well above the EC_{50} free for the duration of 24 h at day 1 and day 4 (Figure 5C). In terms of brain exposure, **16b** performed much better than the other two compounds showing a greater concentration in brain than plasma at both day 1 and day 4, while **13c** and **16c** had ratios less than 1 (Figure 5). Notably, even though **16c** had the lowest brain levels overall, it was still able to achieve exposure at or above the EC_{50} free value (Figure 5C).

Efficacy Testing in Murine Models

Acute Infection Model. We tested efficacy of the compounds **16b**and **13c** in an acute infection model in C57/Bl6 mice given a LD_{90} challenge of ME49-Fluc tachyzoites by ip injection. Beginning at 4 days postinfection, compounds were dosed by oral gavage daily for 7 days at 30 mg/kg (BID) or 100 mg/kg (QD) vs vehicle control (Figure 6A). In the vehicle control group, animals began to lose weight by day 5–6 associated with expansion of parasite burden as seen by bioluminescence imaging (Figures 6B,C and S4A). The precipitous decline in weight resulted in high mortality (Figure 6D). Treated animals showed initial weight loss followed by recovery in the surviving animals (Figure 6B). (Figure 6C,D and S4A). Overall, there were few survivors and they all tested positive for ELISA confirming that they had been infected[42] (Table 4, Figure S4B). At 30 days post infection, remaining animals were sacrificed, brains removed and homogenized and inoculated onto HFF monolayers. (Table 4). The sole survivor treated with 30 mg/kg **16b** and the two survivors treated with 100 mg/kg **13c** both showed outgrowth on HFF monolayers confirming the mice were chronically infected.

We also tested **16c** (MPM2008) in the acute infection in comparison to sulfadiazine, which provides effective control in the murine model without the added side-effects of pyrimethamine (Figure 7A). As above, vehicle treated mice rapidly lost weight, showed elevated parasite growth as detected by bioluminescence, and most succumbed to infection (Figure 7B,C,D). Although mice treated with **16c** at 30 mg/kg BID showed transient weight loss and elevated infection, as evident by bioluminescence, animals treated with 100 mg/kg **16c** or sulfadiazine controlled the infection much better (Figures 7B,C and S5A). All animals from the treated groups survived and at 30 days post infection, brains were removed,

homogenized and used to inoculate on HFF monolayers for outgrowth to monitor chronic infection. All animals were infected as confirmed by ELISA (Table 4, Figure S5B). Brain homogenates from animals treated with **16c** at 30 mg/kg BID showed evidence of outgrowth on HFF monolayers in all 5 surviving animals, indicating they were chronically infected (Table 4). Most animals treated with sulfadiazine (3 of 5 animals) also showed evidence of chronic infection as seen by outgrowth on HFF monolayers (Table 4). However, brain homogenates from all 5 surviving mice treated with **16c** at 100 mg/kg failed to grow on HFF monolayers indicating they had been cured of infection (Table 4).

Immunocompromised Infection Model. Given the improved outcome of immunocompetent C57/Bl mice treated with **16c**, we decided to extend testing to a previously described immunocompromised model.[43] Ifngr1$^{-/-}$ mice lack the major pathway for control of toxoplasmosis and hence they rapidly succumb to challenge. Oral infection in this model results in rapid expansion and dissemination of tachyzoites and conversion to bradyzoites that can give rise to chronic infection. Hence, compounds need to control both the acute and chronic stages to prevent lethal outcome in this model.[42] We infected Ifngr1$^{-/-}$ mice by oral gavage with tissue cysts of ME49-FLUC to mimic the nature route of infection. Animals were treated with compounds by oral gavage for 14 days starting 48 h post infection (Figure 7E). Animals in the vehicle control group showed rapid weight decline and increased bioluminescence signals consistent with uncontrolled parasite expansion (Figures 7F,G and S6). Animals treated with **16c** at 30 mg/kg BID also lost weight, and showed enhanced bioluminescence, but with delayed kinetics relative to control (Figures 7F,G and S6). Treatment with **16c** at 100 mg/kg BID was slightly better at suppressing infection and much more substantial control was achieved by dosing twice per day in the **16c** 100 mg/kg BID group, as well as with sulfadiazine (Figures 7F,G and S6). All treatments significantly prolonged survival relative to control, and treatment with **16c** 100 mg/kg BID was significantly better than the single QD treatment (Figure 7H). Sulfadiazine showed a biphasic response with two animals succumbing early, while the three remaining animals persistent for the longest time, although overall survival was not significantly different from **16c** 100 mg/kg BID (Figure 7H). Despite significantly extended survival, eventually all animals succumbed to infection (Figure 7H).

DISCUSSION AND CONCLUSIONS

The treatment of chronic toxoplasmosis is a major concern in immune compromised individuals; primarily organ transplants, cancer and HIV-AIDS patients. The current standard of therapy employs synergistic inhibitors of folic acid metabolism, pyrimethamine and sulfadiazine.[17] Unfortunately these drugs are only effective against the acute tachyzoite stage and not the chronic bradyzoite stage within tissue cysts. These features result in lengthy treatment regimens up to 6 weeks for transiently immunocompromised patients and indefinitely in permanently compromised patients.[17] Additionally these drugs are known to have toxicities associated with reported adverse events, which are further complicated by the lengthy treatment regimens.[18] There is a vital need for antitoxoplasmosis therapeutics which can target the chronic parasitic-stage and/or demonstrate reduced toxicity in prolonged treatments.

TgCDPK1 inhibitors are emerging as potential antitoxoplasmosis drug candidates, large part due to the uniquely deep-pocket in the active site. Inspired by crystal structures of our previous compounds, we explored compound design based on the formation of interactions in the ribose-binding site and deep hydrophobic pocket. Compound groups exploiting the former featured exocyclic amines capable of forming electrostatic interactions at the R_2 position, while the latter group donned with additional aryl moieties projected deeper into the hydrophobic pocket at the R_3 projection. All compounds were evaluated by their potency in kinase- and cell-based parasite growth assays, as well as their metabolic stability against liver microsomes. These initial screening efforts afforded valuable SAR used for future lead optimization and improved understanding of these groups. SAR of the R_2 group (Table 1) demonstrated reduced cellular potency and stability for most N-functionalized amine derivatives (**15a** vs **23a** and **24a**), consistent with previous studies.[36] SAR observations of the R_3 group (Table 2) determined the structural restrictions of appending the biaryl moiety in the deep hydrophobic pocket. Molecules with substituents of proper length and position increased potency in 6-member, 5-member and fused-ring scaffolds (**1b** and **18b** vs **2b** and **26b**). Metabolic stability was optimized by decreasing the ring's electron density or by covering potential metabolic hotspots (**2b** < **13b** < **14b** < **16b**).

This initial screen led to the identification of 4 preliminary candidates for PK analysis (Figure 4) including **30a** (AJS2144), **1a** (AM5013), and **16b** (CLM1086). From these studies the R_3 biphenyl-bearing **16b** featured the best oral bioavailability (% F), clearance (Cl), half-life and exposure (AUC and Cmax) values among the four, identifying it as the clear lead compound. Lead optimization efforts were focused on improving **16b**'s high protein binding by reducing its lipophilicity. Endeavors were made through substituent modification, functionalizing with polar R_2 groups or changing to N-bearing ring moieties (Table 3). Although the former two were moderately successful, the best improvement in protein binding was demonstrated with inclusion of N-aryl rings, identifying **13c** (MPM1062) and **16c** (MPM2008) as new candidates. Accompanied by reasonable PK profiles, dose-escalation studies solidified the three optimal candidates (**16b**, **13c** and **16c**) for advanced *in vivo* testing.

The *in vivo* testing determined **16c** (MPM2008) to be by far the most efficacious of the three candidates, perhaps due to its higher free-drug concentration. This outcome was particularly evident in the acute model that featured increased survival and no outgrowth of brain homogenates on HFF monolayers, indicating a curative effect. Importantly, more rapid improvement in bioluminescence levels, recovery of body weight, and ability to prevent infection were all superior for **16c** (MPM2008) compared to sulfadiazine (Figure 7A). Additionally, both sulfadiazine and **16c** (MPM2008) were able to suppress *T. gondii* in the immunocompromised mouse model during treatment; however, all mice ultimately succumbed to the infection after treatment was stopped (Figure 7B). Although **16c** was unable to cure infection in immunocompromised mice, it demonstrated comparable efficacy with sulfadiazine. In contrast, previous studies using a related analog called TRC2885, demonstrated a partial cure in a chronic immunocompromised model of infection.[29] The reason for differences in outcome between these two analogs is unclear but may be related to differences in exposure due to the unbound protein fraction, CNS exposure, or differences

in leak levels of exposure that could lead to secondary targets such as MAPKL1, as has recently been shown for other PP analogs.[44] Additionally, although our current studies to do not directly assess the ability of **16c** to target bradyzoites within tissue cysts, they indicate that further improvements to this scaffold will be needed to eliminate chronic infection.

Collectively, these studies demonstrate that **16c** (MPM2008) can prevent establishment of infection when administered during the acute phase in immunocompetent mice and prolongs survival during extended infection in immunocompromised mice. Additionally, since **16c** (MPM2008) acts alone, unlike the current standard of care that requires multiple drugs, it is likely to elicit fewer adverse outcomes. As such, **16c** (MPM2008) may have improved properties as a potential antitoxo therapy in immunocompetent patients who require extended treatment.

EXPERIMENTAL SECTION

Parasite Strains and Culture

Experiments were conducted with the type 2 (ME49Δ*hx*::FLUC strain) that expresses firefly luciferase, as described previously.[45] Tachyzoites were grown in monolayers of human foreskin fibroblasts (HFF) maintained in complete medium (DMEM containing 10% FBS, 10 mM glutamine, and 10 μg/mL gentamycin) incubated at 37 °C in 5% CO_2. In vitro cultures were shown to be mycoplasma negative using the e-Myco plus kit (Intron Biotechnology).

Enzyme Expression and Purification

Full-length *T. gondii* CDPK1 enzyme was expressed with a C-terminal His tag in pET22b(+), as described previously.[21] For protein purification, CDPK1 was expressed in BL21 (DE3)V2RpAcYc-LIC +LamP *E. coli*, which contains the LamP phosphatase.[21] Protein expression and purification using HIS-select Nickel Affinity Gel were conducted as previously described.[27] Purified proteins were dialyzed against storage buffer (i.e., 50 mM Tris-HCL, pH7.5, 150 mM NaCl), assessed for purity and concentration by SDS-PAGE, and stored in 25% glycerol containing 0.5 mM DTT at −80 °C.

X-ray Crystallography Studies

TgCDPK1 was cloned into pET15-MHL vector and expressed as a His-tagged fusion protein in *E. coli* BL21 (DE3)-V2RpAcYc-LIC +LamP *E. coli* cells expressing LamP phosphatase, as reported previously.[24] Cells were grown overnight in Terrific Broth at 37 °C and diluted 1:100, followed by another period of growth until A_{600} reached 0.6–0.8. TgCDPK1expression was induced overnight at 15 °C by adding 0.3 mM IPTG. Co-crystallization of TgCDPK1 with TRC3264 and TRC2895 used the same setup and crystallization conditions as previously reported.[30] Diffraction data were collected at the Advanced Light Source. Lawrence Berkeley National Laboratories. The software program XDS (build 20240712)[46] was used for indexing, integration, and scaling of data was done by AIMLESS (version 0.7.4).[47] To build models, molecular replacement was done using a Phaser implementation in Phenix (version 1.21), which used 4IH8 as a search model.[48] Models were iteratively refined using Phenix[48] and Coot (version 0.9.8)[49] and validated

using the MolProbity online tool.[50] PyMol (version 3.0, Schrodinger, LLC. 2010) and ChimeraX (version 1.9) were used for structure visualization.[51]

Enzyme Assays

CDPK1 activity was monitored based on phosphorylation of syntide-2 peptide (Callbiochem) detected using mAb MS-6E6 (MBL Intl, Corp) by ELISA, using a previously described ELISA-assay.[27] Reactions were conducted at 30 °C for 45 min in 20 mM HEPES, pH 7.5, 10 mM $MgCl_2$, 1 mM DTT, 2.5 mM $CaCl_2$, 0.1 mM EGTA, 0.005% Tween 20. Kinase reactions included 25 μM ATP (the Km for the enzyme) and 35 nM of kinase per reaction. IC_{50} values were calculated from triplicate biological replicates, each containing duplicate wells from a dilution series from 20 μM to 0.13 nM containing 1% DMSO final, as described previously.[30] Individual IC_{50} values were determined using variable slope four parameter nonlinear curve fit in Prism (10.5.0) (GraphPad).

Human Src Activity

Human Src (hSrc) activity was monitored by phosphorylation of the Abltide peptide (EAIYAAPFAKKK, Enzo Life Sciences) and detection using a monoclonal antibody to phosphotyrosine (Sigma) using an ELISA protocol described previously.[27,30] Alternatively, hSrc activity was monitored by measuring ADP formed during the kinase reaction using SRC kinase Enzyme System and ADP-Glo Kinase Assay Kit (Promega). Kinase reactions were initiated by adding 100 ng/μL Active Src enzyme, 1 mg/mL Substrate, 2X Kinase buffer and 250 mM ATP solution to 10 μM of the compounds for 15 min at 30 °C. ADP-Glo reagent was used to terminate the reactions at room temperature for 40 min by depleting the residual ATP. ADP was converted to ATP by incubation in Kinase Detection Reagent for 30 min and ATP levels were measured using luciferase. Compounds were tested at 10 μM in duplicate, in two biological replicates. For compounds that showed >50% inhibition at 10 μM, serial dilutions from 10 μM to 0.5 nM were tested in duplicate to derive IC_{50} values.

In Vitro Growth Assays

HFF monolayers grown in 96 well plates were inoculated with 5×10^3 of luciferase expressing parasites containing dilutions of compounds ranging from 10 μM to 1.67 nM plus 0.1% DMSO, or 0.1% DMSO alone as a control. Parasites were allowed to replicate for 72 h and luciferase activity was monitored using the Luciferase Assay System (Promega, E1501). Plates were read with a Cytation3 Imaging Multimode plate reader (Biotek), as described previously.[27] Individual IC_{50} values were determined variable slope four parameter using nonlinear curve fit in Prism (10.5.0) (GraphPad).

Host Toxicity Assays

Hepatocellular carcinoma HepG2 cells (ATCC HB-8065) were grown in complete medium according to ATCC recommendation and maintained at 37 °C, 5% CO_2. Cells were plated at 15,000 cells/well and allowed to adhere for 4 h at 37 °C, 5% CO_2. Compounds diluted to 20 μM in 0.2% (v/v) DMSO, or DMSO alone, were then added and cells were incubated for an additional 72 h. Following the incubation period, samples were evaluated using a cell proliferation assay (CellTiter 96 Aqueous Non-Radioactive Cell Proliferation Assay,

Promega Corporation). As a positive control, mitomycin C (20 μM) was included in each plate. Reported values were derived from three independent experiments with two technical replicates each.

Animal Ethics Statement

Animals were obtained from Jackson Laboratories, or bred locally, and housed at Washington University in accordance with the U.S.A. Public Health Service Policy on Humane Care and Use of Laboratory Animals. Animals were maintained in an Association for Assessment and Accreditation of Laboratory Animal Care approved facilities and studies were approved by the Institutional Animal Studies Committee at the School of Medicine, Washington University in St. Louis (Protocol number 25–0038). ADME and Animal studies conducted at WuXi AppTec in China were performed in accordance approved institutional and national guidelines.

ADME Studies

Microsome Stability Assays. Microsome stability assays were conducted by WuXi AppTech China. Compounds were prepared at 10 μM in 1% DMSO and mouse liver microsomes were prepared from CD-1 mice and diluted to 0.5 mg/mL PBS. Compounds, and positive controls, were diluted to 1 μM and tested in a volume of 100 μL of microsomes (0.5 mg/mL final) containing 1 mM NADPH and incubated at 37 °C. At 5, 15, 30, 45 and 60 min, samples were quenched by adding 3:1 volumes of acetonitrile containing 250 nM tolbutamide. Samples were shaken for 10 min, centrifuged at 4000 rpm for 20 min at 4 °C and the supernatant analyzed by LC-MS/MS. Values for $T_{1/2}$ and Clint in mL min^{-1} kg^{-1} were calculated using first order kinetics

Protein Binding Assays. Protein binding assays were conducted by WuXi AppTech China. Compounds were added at a final concentration of 2 μM containing 0.5% DMSO to mouse plasma from male CD1 mice adjusted to pH 7.4. Samples were tested by dialysis using HT-dialysis plates (HTD 96, Thermo Fischer) equilibrated against 0.1 M sodium phosphate, 0.15 M sodium chloride, pH 7.2 (PBS). Samples were treated in triplicate for 4 h at 37 °C and 5%CO_2 with rotation at 100 rpm. Samples were analyzed from the donor (sample) and receiver (PBS) sides by LC/MS/MS and recovery, bound and unbound fractions calculated.

MDCK-MDR1 Efflux Assay. Efflux assays were conducted by WuXi AppTech China. Bidirectional permeability and efflux of compounds were tested in MDCK cells expressing the human MDR1 efflux pump. MDR1-MDCK cells were seeded on 96-well transport inserts and cultured for 4–7 days before being used for the transport experiment. Compounds were added at 2.0 μM final concentration (<0.1% DMSO) to the apical vs basolateral side of transport inserts. Samples were incubated for 2.5 h at 5% CO_2 37 °C and samples were taken from both the donor and receiver chambers and analyzed by LC/MS/MS. Transfer from apical to basolateral (A to B) and basolateral to apical (B to A) direction was expressed as the mean rate of exchange and used to determine the efflux ratio

PK Studies

Oral vs iv Trial. PK studies were conducted by WuXi AppTech China. For initial PK studies compounds were formulated at 1 mg/mL in 5% DMSO/50% PEG 400, 45% PBS pH 7.4. Compounds were dosed at 3 mg/kg by iv injection or 10 mg/kg by oral gavage into 3 CD-1 male mice each. Animals were sampled by blood draw at 0.08, 0.25, 0.5, 1, 2, 4, 8, and 24 h. Samples were extracted an analyzed by LC-MS/MS in comparison to standards of the parent compounds. Data were analyzed using Phoenix WinNonLIn 8.3.5. using a noncompartmentalized model with linear/log trapezoidal calculation method.

Escalating and Repeating Dose Studies. For dose escalation studies, and repeated dosing, compounds were formulated as above at 1 mg/mL (final 10 mg/kg) 6 mg/mL (final 30 mg/kg) or 20 mg/mL (for 100 mg/kg) for respective dosing. Groups of 3 CD1 male mice were dosed by oral gavage and sampled at 0.5, 1, 3, 8, and 24 h. For repeated dosing, animals were dosed BID (doses separated by 10 h) for vehicle control or 30 mg/kg compounds and QD for 100 mg/kg compound for 4 days. Separate groups of mice were used for monitoring the first 24 h (day 1) and the last 24 h (Day 4). A separate set of animals was also used for sampling of brain tissue at 24 h on Day 1 and Day 4. Brain homogenate was used to calculate tissue accumulation and Brain/Plasma ratio in ng/mL. Animals were monitored for weight and clinical chemistry (ALT, AST, CR, Urea, and CK) and no abnormalities were observed.

Acute Challenge Model

To monitor the ability of compound to suppress acute infection, 8–12 week old male or female C57BL/6 mice (JAX:000664) were challenged with 500–1000 tachyzoites of ME49Δ*hx*::FLUC strain parasites by i.p. injection. At 72 h postinfection, compounds (dissolved in 0.5% carboxy methyl cellulose (CMC)) were administered by oral gavage for a total of 7 days. In parallel, one group of animals served a vehicle control and another group was treated with sulfadiazine (0.25 g/L in the drinking water). Animals were monitored for weight loss (and sacrificed when weight loss reached >20%, or they were unable to reach food or water) and imaged for bioluminescence as described below. Animals were monitored for weight loss, bioluminescence imaging, and survival for 30 days. At the end of 30 days, surviving animals were sacrificed humanely and the brains removed and homogenized. A portion of each brain was inoculated on HFF monolayers grown in vitro and parasite outgrowth assess by plaque formation.

Immunocompromised Model

Studies using the immunocompromised infection model were conducted using a previously described model to monitor the ability of compounds to prevent reactivation of toxoplasmosis.[43] Male or female Ifngr1$^{-/-}$ mice (JAX:025394) were orally infected with 5 cysts of the type 2 ME49Δ*hx*::FLUC line, obtained from purification of chronically infected mouse brains.[42] At 48 h postinfection compounds (dissolved in 0.5% CMC) were administered by oral gavage for a total of 14 days. In parallel, one group of animals served a vehicle control and another group was treated with sulfadiazine (0.25 g/L in the drinking water). Animals were monitored for weight loss (and sacrificed when weight loss reached

>20%, or they were unable to reach food or water) and imaged for bioluminescence as described below.

Bioluminescence Imaging

Mice were anesthetized by inhalation with 2% isoflurane and injected i.p. with D-luciferin (Biosynth AG) (stock 15 mg/mL and administered as 10 μL per gram of body weight) just prior to imaging. Animals were monitored for bioluminescence using a Xenogen IVIS200 instrument. Data were analyzed using the Xenogen Living Image software (Caliper Life Sciences).

Synthetic Experimental Section

Commercially available reagents and anhydrous solvents were used without further purification unless otherwise specified. The mass spectra were recorded using a quadrupole mass spectrometer on an Agilent 1200, 1956 MSD (column Shim-pack XR-ODS 30 mm × 3.0 mm, 2.2 μm) operating in ES (+) ionization mode. Flash chromatography was performed on prepacked columns of silica gel (230–400 mesh, 40–63 um) by CombiFlash with ethyl acetate (EtOAc)/hexane or methanol (MeOH)/ dichloromethane (DCM), or by reverse phase using acetonitrile (ACN)/ water with 0.05% trifluoroacetic acid. Preparative HPLC was performed on SunFire C_{18} OBD 10 μm (30 mm × 250 mm) with acetonitrile (ACN)/ water with 0.05% trifluoroacetic acid as eluents to purify final compounds. All final compounds were isolated with greater than 95% purity based on HPLC UV% AUC as determined at 210 and 254 nm wavelengths. NMR spectra were recorded with a Varian 400 MHz or Bruker 600 MHz spectrometers at ambient temperature with chemical shifts δ recorded in ppm relative to residual solvent peak or TMS.

General Synthetic Procedure A

Reductive amination conditions applied to the alkylation of all appropriate amine containing compounds reported in Tables 1, 3 and 4, exemplified through the synthesis of *1-((1s,4s)-4-(ethylamino)cyclohexyl)-3-((4-(trifluoromethyl)pyridin-2-yl)oxy)-1H-pyrazolo[3,4-d]pyrimidin-4-amine* (**3a**). A solution of 1-((cis)-4-aminocyclohexyl)-3-((4-(trifluoromethyl)pyridine-2-yl)oxy)-1H-pyrazolo[3,4-*d*]pyrimidin-4-amine[29] (30.1 mg, 0.01 mmol, 1.0 equiv) in DCM (3 mL) was prepared and purged with argon. Acetaldehyde (5.0 M, 15.3 mL, 1.0 equiv), sodium triacetoxyborohydride (22.7 mg, 1.3 equiv) and acetic acid (4.59 mg, 1.0 equiv) were added and stirred at room temperature under argon. The reaction was neutralized with addition of sodium hydroxide solution (1 M), extracted with EtOAc, dried with magnesium sulfate and concentrated. The crude sample was purified via preparative HPLC.

General Synthetic Procedure B

Acylation conditions were applied to all appropriate amine containing compounds reported in Tables 1, 3 and 4, exemplified through the synthesis of *1-((cis-4-acetylamino)cyclohexyl)-3-((4-trifluoromethyl)pyridine-2-yl)oxy)-1H-pyrazolo[3,4-d]pyrimidin-4-amine* (**9a**). Acetyl chloride (10.41 mg, 0.18 mmol, 1.5 equiv) was added to a solution of 1-((cis)-4-aminocyclohexyl)-3-((4-(trifluoromethyl)pyridine-2-

yl)oxy)-1H-pyrazolo[3,4-*d*]pyrimidin-4-amine[29] (35.0 mg, 0.12 mmol, 1.0 equiv) in DCM (2 mL) and potassium carbonate (23.1 mg, 0.24 mmol, 2.0 equiv) and stirred under argon. Upon completion the solution was concentrated, and the resulting crude sample was purified via preparative HPLC.

General Synthetic Procedure C

Mitsunobu and Boc-removal conditions applied to formation of appropriate compounds reported in Tables 1, 3 and 4, exemplified through the synthesis of *1-((1R, 3R)-3-aminocyclohexyl)-3-((4-(trifluoromethyl)pyridine-2-yl)oxy)-1H-pyrazolo[3,4-d]pyrimidin-4-amine* (**15a**). A mixture of 1-((cis)-4-aminocyclohexyl)-3-((4(trifluoromethyl)pyridine-2-yl)oxy)-1H-pyrazolo[3,4-*d*]pyrimidin-4-amine[29] (1.0 g, 3.4 mmol, 1.0 equiv), triphenyl phosphine (1.41 g, 5.4 mmol, 1.5 equiv), (1R, 3S)-(3-hydroxy-cyclohexyl)-carbamic acid tert-butyl ester (1.0 g, 3.4 mmol, 1.0 equiv) and diisopropyl azodicarboxylate (1.06 mL, 5.4 mmol, 1.5 equiv) was prepared in dry THF (75 mL) and heated to 60 °C overnight under argon. Upon completion the solution was concentrated and purified via flash silica chromatography. Some of the isolated sample (450 mg, 0.91 mmol, 1.0 equiv) was dissolved in 4 N HCl/dioxane (10 mL) and stirred. Upon completion the reaction was concentrated and the crude sample was purified via preparative HPLC.

General Synthetic Procedure D

Suzuki reaction conditions were applied to produce the appropriate compounds in Tables 2, 3 and 4, exemplified through the synthesis of *1-cyclopropyl-3-((4-(p-tolyl)pyridin-2-yl)oxy)-1H-pyrazolo[3,4-d]pyrimidin-4-amine* (**2b**). The mixture of 3-((4-bromopyridin-2-yl) oxy)-1-cyclopropyl-1H-pyrazolo[3,4-*d*] pyrimidin-4-amine (50 mg, 0.144 mmol, 1.0 equiv), the aqueous solution (0.5 mL) of Cs_2CO_3 (140 mg, 0.432 mmol, 3.0 equiv) and p-tolylboronic acid (29.4 mg 0.216 mmol, 1.5 equiv) in 1, 4-dioxane (3.5 mL) was degassed for 15 min. Thereafter, tetrakis (triphenylphosphine) palladium (0) (8.32 mg, 0.0072 mmol, 0.05 equiv) was added to the mixture and stirred at 90–110 °C under argon for 2–8 h. The reaction mixture was cooled to room temperature, diluted with water, extracted with ethyl acetate, concentrated and purified through flash silica chromatography. Isolated **2b**, as with most compounds, were further purified via preparative HPLC.

1-((1s,4s)-4-(Ethylamino)cyclohexyl)-3-((4-(trifluoromethyl)pyridin-2-yl)oxy)-1H-pyrazolo[3,4-*d*]pyrimidin-4-amine (3a). Synthesized using general procedure A. Yield: 1.1 mg, 15.6%. ^{1}H NMR (400 MHz, CD_3OD) δ 8.38 (d, J = 5.2 Hz, 1H), 8.31 (d, J = 5.2 Hz, 1H), 7.63 (s, 1H), 7.53 (d, J = 5.3 Hz, 1H), 5.03 (s, 1H), 3.08 (q, J = 7.3 Hz, 1H), 2.35–2.25 (m, 2H), 2.13–1.96 (m, 6H), 1.33–1.26 (m, 5H). LC/MS (ESI) m/z: $[M + H]^+$ calcd. for $C_{19}H_{22}F_3N_7O$, 421.18; found 422.72.

1-((trans-4-Ethylamino)cyclohexyl)-3-((4-trifluoromethyl)pyridine-2-yl)oxy)-1H-pyrazolo[3,4-*d*]pyrimidin-4-amine (4a). Synthesized using general procedure A. Yield: 9.1 mg, 4.3%. ^{1}H NMR (400 MHz, CD_3OD) δ 8.40 (d, J = 5.3 Hz, 1H), 8.36 (s, 1H), 7.67 (s, 1H), 7.55 (d, J = 5.2 Hz, 1H), 4.87–4.76 (m, 1H), 3.26–3.17 (m, 1H), 3.12 (q, J = 7.2 Hz, 2H), 2.30 (d, J = 12.1 Hz, 2H), 2.22–2.00 (m, 4H), 1.72–1.56 (m, 2H),

1.32 (t, J = 7.3 Hz, 3H). ^{13}C NMR (600 MHz, MeOD) δ 163.9, 162.7, 162.5, 154.7, 152.5, 152.2, 151.0, 150.4, 143.4, 143.2, 117.5, 110.4, 92.6, 56.4, 56.2, 41.4, 30.5, 28.9, 11.7. LC/MS (ESI) m/z: $[M + H]^+$ calcd. for $C_{19}H_{22}F_3N_7O$, 421.18; found 422.72.

1-((cis-4-Isopropylamino)cyclohexyl)-3-((4-trifluoromethyl)pyridine-2-yl)oxy)-1H-pyrazolo[3,4-*d*]pyrimidin-4-amine (5a). Synthesized using general procedure A. Yield: 2.2 mg, 24.2%. ^{1}H NMR (400 MHz, $(CD_3)_2SO$) δ 8.39 (d, J = 5.3 Hz, 1H), 8.37 (s, 1H), 7.64 (s, 1H), 7.54 (dd, J = 5.3, 1.4 Hz, 1H), 5.09 (q, J = 4.1 Hz, 1H), 3.52 (h, J = 6.5 Hz, 1H), 3.44 (q, J = 4.3 Hz, 1H), 2.46–2.31 (m, 2H), 2.17–1.97 (m, 6H), 1.33 (d, J = 6.5 Hz, 6H). ^{13}C NMR (600 MHz, $(CD_3)_2SO$) δ 164.1, 152.4, 151.7, 150.4, 149.2, 143.5, 143.2, 125.3, 122.6, 121.0, 119.5, 117.3, 110.2, 92.9, 53.6, 53.0, 48.6, 28.6, 25.8, 19.3. LC/MS (ESI) m/z: $[M + H]^+$ calcd. for $C_{20}H_{24}F_3N_7O$ 435.20; found 436.76.

1-((trans-4-Isopropylamino)cyclohexyl)-3-((4-trifluoromethyl)pyridine-2-yl)oxy)-1H-pyrazolo[3,4-*d*]pyrimidin-4-amine (6a). Synthesized using general procedure A. Yield: 27.5 mg, 71.1%. ^{1}H NMR (399 MHz, CD_3OD) δ 8.40 (d, J = 5.2 Hz, 1H), 8.37 (s, 1H), 7.66 (s, 1H), 7.54 (dd, J = 5.5, 1.4 Hz, 1H), 4.89–4.78 (m, 1H), 3.53 (p, J = 6.5 Hz, 1H), 2.32–2.23 (m, 2H), 2.21–2.05 (m, 4H), 1.65 (qd, J = 12.5, 4.3 Hz, 2H), 1.34 (d, J = 6.5 Hz, 6H). ^{13}C NMR (600 MHz, CD_3OD) δ 163.8, 162.4, 153.5, 152.6, 151.9, 150.4, 149.0, 143.5, 143.2, 138.6, 125.2, 117.6, 110.5, 110.5, 92.5, 56.4, 53.4, 48.5, 30.5, 28.9, 19.4. LC/MS (ESI) m/z: $[M + H]^+$ calcd. for $C_{20}H_{24}F_3N_7O$ 435.20; found 437.10.

1-((cis-4-Cyclopropylmethylamino)cyclohexyl)-3-((4-trifluoromethyl)pyridine-2-yl)oxy)-1H-pyrazolo[3,4-*d*]pyrimidin-4-amine (7a). Synthesized using general procedure A. Yield: 3.2 mg, 12.5%. ^{1}H NMR (400 MHz, CD_3OD) δ ppm 0.35–0.41 (m, 2 H) 0.66–0.74 (m, 2 H) 1.01–1.09 (m, 1 H) 1.98–2.15 (m, 6 H) 2.28–2.34 (m, 2 H) 2.92 (d, J = 7.40 Hz, 2 H) 3.35 (s, 1 H) 5.04 (br. s., 1 H) 7.53 (d, J = 5.06 Hz, 1 H) 7.63 (s, 1 H) 8.32 (s, 1 H) 8.39 (d, J = 5.45 Hz, 1 H). ^{13}C NMR (600 MHz, CD_3OD) δ 164.2, 163.0, 162.7, 162.5, 162.3, 155.9, 153.2, 152.6, 152.3, 151.2, 150.4, 143.4, 143.2, 126.6, 124.8, 123.0, 121.2, 120.9, 119.0, 117.1, 115.1, 110.1, 93.0, 56.3, 53.0, 51.2, 28.5, 25.8, 8.2, 4.6. LC/MS (ESI) m/z: $[M + H]^+$ calcd. for $C_{21}H_{24}F_3N_7O$, 447.47; found 448.66.

1-((trans-4-Cyclopropylmethylamino)cyclohexyl)-3-((4-trifluoromethyl)pyridine-2-yl)oxy)-1H-pyrazolo[3,4-*d*]pyrimidin-4-amine (8a). Synthesized using general procedure A. Yield: 18.5 mg, 66%. ^{1}H NMR (400 MHz, CD_3OD) δ 8.40 (d, J = 5.2 Hz, 1H), 8.31 (s, 1H), 7.67 (s, 1H), 7.54 (d, J = 5.2 Hz, 1H), 4.84–4.74 (m, 1H), 3.26–3.17 (m, 1H), 2.96 (d, J = 7.5 Hz, 2H), 2.30 (d, J = 12.6 Hz, 2H), 2.19–2.00 (m, 4H), 1.73–1.57 (m, 2H), 1.13–1.04 (m, 1H), 0.78–0.64 (m, 2H), 0.46–0.37 (m, 2H). ^{13}C NMR (600 MHz, CD_3OD) δ 164.0, 156.5, 153.7, 151.6, 150.4, 143.6, 143.4, 143.2, 138.5, 124.8, 123.0, 117.3, 110.3, 102.9, 92.8, 56.6, 55.9, 51.2, 30.6, 28.9, 8.4, 4.6. LC/MS (ESI) m/z: $[M + H]^+$ calcd. for $C_{21}H_{24}F_3N_7O$, 447.20; found 448.66.

1-((cis-4-Acetylamino)cyclohexyl)-3-((4-trifluoromethyl)pyridine-2-yl)oxy)-1H-pyrazolo[3,4-*d*]pyrimidin-4-amine (9a). Synthesized using general procedure B. Yield: 15 mg, 71.4%. ^{1}H NMR (400 MHz, CD_3OD) δ 8.41 (d, J = 5.2 Hz, 1H), 8.36 (d, J = 0.7 Hz, 1H), 7.67 (s, 1H), 7.54 (d, J = 5.2 Hz, 1H), 4.00–

3.93 (m, 1H), 2.26–2.13 (m, 2H), 2.01–1.87 (m, 8H), 1.83–1.71 (m, 2H). LC/MS (ESI) *m*/*z*: $[M + H]^+$ calcd. for $C_{19}H_{20}F_3N_7O_2$, 435.16; found 436.69.

1-((trans-4-Acetylamino)cyclohexyl)-3-((4-trifluoromethyl)pyridine-2-yl)oxy)-1H-pyrazolo[3,4-*d*]pyrimidin-4-amine (10a). Synthesized using general procedure B. Yield: 2.5 mg, 53.1%. ^{1}H NMR (400 MHz, CD_3OD) δ 8.41 (d, J = 5.1 Hz, 1H), 8.36 (s, 1H), 7.69 (s, 1H), 7.54 (d, J = 5.2 Hz, 1H), 4.79 (p, J = 7.6 Hz, 1H), 3.77–3.65 (m, 1H), 2.11–2.01 (m, 6H), 1.93 (s, 3H), 1.56–1.40 (m, 2H). ^{13}C NMR (400 MHz, CD_3OD) δ 171.55, 162.53, 151.61, 150.95, 150.16, 149.03, 146.75, 116.08, 116.05, 109.01, 108.97, 90.89, 55.01, 44.45, 38.97, 27.94, 26.66, 21.12. LC/MS (ESI) *m*/*z*: $[M + Na]^+$ calcd. for $C_{19}H_{20}F_3N_7O_2$, 435.16; found 459.1

1-((cis-4-Methylcarbamo)cyclohexyl)-3-((4-trifluoromethyl)pyridine-2-yl)oxy)-1H-pyrazolo[3,4-*d*]pyrimidin-4-amine (11a). Synthesized using general procedure B. Yield: 1.4 mg, 34.2%. ^{1}H NMR (400 MHz, CD_3OD) δ 8.42 (d, J = 5.2 Hz, 1H), 8.36 (s, 1H), 7.69 (s, 1H), 7.60–7.53 (m, 1H), 4.90–4.79 (m, 1H), 3.82–3.71 (m, 1H), 3.62 (s, 3H), 2.28–2.13 (m, 2H), 2.02–1.93 (m, 2H), 1.93–1.85 (m, 2H), 1.83–1.73 (m, 2H). ^{13}C NMR (400 MHz, CD_3OD) δ 163.9, 153.0, 152.4, 151.5, 150.4, 148.2, 139.7, 125.2, 123.8, 117.5, 110.5, 92.3, 56.7, 52.3, 49.6, 49.4, 49.3, 49.2, 49.0, 48.8, 48.6, 48.4, 47.0, 29.8, 27.9, 27.9. LC/MS (ESI) *m*/*z*: $[M + H]^+$ calcd. for $C_{19}H_{20}F_3N_7O_3$, 451.41; found 452.82.

1-((trans-4-Methylcarbamo)cyclohexyl)-3-((4-trifluoromethyl)pyridine-2-yl)oxy)-1H-pyrazolo[3,4-*d*]pyrimidin-4-amine (12a). Synthesized using general procedure B. Yield: 1.6 mg, 36.7%. ^{1}H NMR (400 MHz, CD_3OD) d 8.40 (d, J = 5.2 Hz, 1H), 8.33 (d, J = 1.7 Hz, 1H), 7.69 (s, 1H), 7.54 (d, J = 5.2 Hz, 1H), 4.83–4.70 (m, 1H), 3.62 (s, 3H), 3.52–3.41 (m, 1H), 2.12–2.01 (m, 6H), 1.56–1.38 (m, 2H). LC/MS (ESI) *m*/*z*: $[M + H]^+$ calcd. for $C_{19}H_{21}F_3N_8O_2$, 450.17; found 453.10.

1-((cis-4-(*N*-methylureido))cyclohexyl)-3-((4-trifluoromethyl)pyridine-2-yl)oxy)-1H-pyrazolo[3,4-*d*]pyrimidin-4-amine (13a). Synthesized using general procedure B. Yield: 1.2 mg, 18%. ^{1}H NMR (400 MHz, CD_3OD) δ 8.41 (d, J = 5.2 Hz, 1H), 8.36 (s, 1H), 7.66 (s, 1H), 7.55 (dd, J = 5.3, 1.5 Hz, 1H), 4.91–4.81 (m, 1H), 3.96–3.83 (m, 1H), 2.68 (s, 3H), 2.21–2.09 (m, 2H), 1.97–1.85 (m, 4H), 1.84–1.73 (m, 2H). ^{13}C NMR (600 MHz, CD_3OD) δ 166.8, 164.0, 161.3, 153.0, 152.4, 151.5, 150.4, 148.1, 143.2, 117.5, 117.5, 110.4, 110.4, 92.3, 56.9, 47.9, 45.4, 40.6, 30.4, 27.9, 26.8. LC/MS (ESI) *m*/*z*: $[M + H]^+$ calcd. for $C_{19}H_{21}F_3N_8O_2$, 450.17; found 451.75.

1-((trans-4-(*N*-methylureido))cyclohexyl)-3-((4-trifluoromethyl)pyridine-2-yl)oxy)-1H-pyrazolo[3,4-*d*]pyrimidin-4-amine (14a). Synthesized using general procedure B. Yield: 12 mg, 56.5%. ^{1}H NMR (400 MHz, CD_3OD) d 8.41 (d, J = 5.2 Hz, 1H), 8.34 (s, 1H), 7.69 (s, 1H), 7.54 (d, J = 5.2 Hz, 1H), 4.83–4.69 (m, 1H), 3.63–3.47 (m, 1H), 2.68 (s, 3H), 2.16–1.97 (m, 6H), 1.51–1.36 (m, 2H). ^{13}C NMR (600 MHz, CD_3OD) δ 163.8, 161.2, 153.5, 152.3, 151.8, 150.4, 148.9, 143.5, 143.1, 125.3, 122.6, 117.5, 117.5, 110.5, 110.4, 92.4, 57.4, 49.3, 33.1, 31.8, 26.9. LC/MS (ESI) *m*/*z*: $[M + H]^+$ calcd. for $C_{19}H_{21}F_3N_8O_2$, 450.17; found 452.20

1-((1R,3R)-3-Aminocyclohexyl)-3-((4-(trifluoromethyl)pyridine-2-yl)oxy)-1H-pyrazolo[3,4-*d*]pyrimidin-4-amine (15a). Synthesized using general procedure C. Yield: 392 mg, 25.3% over 2 steps. ^{1}H NMR (600 MHz, CD_3OD) δ 8.32 (s, 2H), 7.57 (s, 1H), 7.42 (s, 1H), 5.19 (s, 1H), 3.76 (s, 1H), 2.37 (s, 1H), 2.16–1.53 (m, 7H). ^{13}C NMR (600 MHz, MeOD) δ 163.4, 153.2, 151.9, 150.6, 149.4, 143.2, 143.0, 142.8, 142.5, 126.3, 124.5, 122.7, 120.9, 117.5, 110.5, 92.3, 53.0, 48.0, 34.5, 30.8, 29.8, 20.2. LC/MS (ESI) *m*/*z*: $[M + H]^+$ calcd. for $C_{17}H_{18}F_3N_7O$, 393.15; found 394.20.

1-((1R,3S)-3-Aminocyclohexyl)-3-((4-(trifluoromethyl)pyridine-2-yl)oxy)-1H-pyrazolo[3,4-*d*]pyrimidin-4-amine (16a). Synthesized using general procedure C. Yield: 156 mg, 18.3% over 2 steps. ^{1}H NMR (600 MHz, CD_3OD) δ 8.41 (d, J = 5.0 Hz, 1H), 8.36 (s, 1H), 7.67 (s, 1H), 7.55 (d, J = 4.9 Hz, 1H), 4.92 (t, J = 12.0 Hz, 1H), 3.44–3.36 (m, 1H), 2.37 (d, J = 11.4 Hz, 1H), 2.13–2.01 (m, 4H), 1.92–1.82 (m, 1H), 1.68–1.57 (m, 1H), 1.49–1.37 (m, 1H). ^{13}C NMR (600 MHz, CD_3OD) δ 163.8, 154.4, 152.3, 150.9, 150.5, 143.4, 143.2, 117.5, 110.5, 92.7, 55.6, 50.2, 36.7, 31.7, 30.6, 23.1. LC/MS (ESI) *m*/*z*: $[M + H]^+$ calcd. for $C_{17}H_{18}F_3N_7O$ 393.15; found 394.20.

1-((1S,3R)-3-Aminocyclohexyl)-3-((4-(trifluoromethyl)pyridine-2-yl)oxy)-1H-pyrazolo[3,4-*d*]pyrimidin-4-amine (17a). Synthesized using general procedure C. Yield: 322 mg, 28.4% over 2 steps. ^{1}H NMR (600 MHz, CD_3OD) δ 8.45–8.19 (m, 2H), 7.61 (s, 1H), 7.49 (s, 1H), 3.38 (s, 1H), 2.38 (s, 1H), 2.18–1.75 (m, 6H), 1.58 (s, 1H), 1.44 (s, 1H). ^{13}C NMR (600 MHz, MeOD) δ 191.7, 182.0, 180.3, 180.1, 178.7, 178.5, 171.5, 171.3, 171.0, 170.8, 154.5, 152.7, 150.9, 149.1, 145.6, 138.6, 120.6, 83.7, 78.3, 64.7, 59.9, 58.6, 51.2. LC/MS (ESI) *m*/*z*: $[M + H]^+$ calcd. for $C_{17}H_{18}F_3N_7O$, 393.15; found 394.20.

1-((1S,3S)-3-Aminocyclohexyl)-3-((4-(trifluoromethyl)pyridine-2-yl)oxy)-1H-pyrazolo[3,4-*d*]pyrimidin-4-amine (18a). Synthesized using general procedure C. Yield: 463 mg, 26.9% over 2 steps. ^{1}H NMR (600 MHz, CD_3OD) δ 8.42 (d, J = 5.2 Hz, 1H), 8.40 (s, 1H), 7.69 (s, 1H), 7.56 (d, J = 5.1 Hz, 1H), 5.32 (p, J = 5.0 Hz, 1H), 3.86 (tt, J = 8.7, 4.0 Hz, 1H), 2.51–2.44 (m, 1H), 2.15–2.06 (m, 2H), 2.05–1.94 (m, 2H), 1.92–1.83 (m, 1H), 1.82–1.74 (m, 1H), 1.70–1.62 (m, 1H). ^{13}C NMR (600 MHz, CD_3OD) δ 163.8, 153.1, 152.4, 152.0, 150.5, 148.7, 143.5, 143.2, 117.6, 110.5, 92.5, 53.2, 48.1, 34.5, 30.8, 29.9, 20.2. LC/MS (ESI) *m*/*z*: $[M + H]^+$ calcd. for $C_{17}H_{18}F_3N_7O$, 393.15; found 394.20.

1-((1R,3R)-3-Ethylaminocyclohexyl)-3-((4-(trifluoromethyl)pyridine-2-yl)oxy)-1H-pyrazolo[3,4-*d*]pyrimidin-4-amine (19a). Synthesized using general procedure A. Yield: 3.9 mg, 19.5%. ^{1}H NMR (600 MHz, CD_3OD) δ 8.41 (d, J = 5.3 Hz, 1H), 8.34 (s, 1H), 7.68 (dt, J = 1.2, 0.6 Hz, 1H), 7.55 (ddd, J = 5.1, 1.4, 0.6 Hz, 1H), 5.29 (p, J = 4.9 Hz, 1H), 3.82 (tt, J = 9.3, 4.1 Hz, 1H), 3.07 (q, J = 7.2 Hz, 2H), 2.58–2.50 (m, 1H), 2.19—2.02 (m, 3H), 1.99–1.91 (m, 1H), 1.89–1.74 (m, 2H), 1.67–1.58 (m, 1H), 1.27 (t, J = 7.3 Hz, 3H). ^{13}C NMR (600 MHz, CD_3OD) δ 163.9, 162.3, 162.0, 161.8, 161.6, 154.8, 152.8, 151.9, 151.1, 150.5, 143.5, 143.3, 117.5, 110.5, 92.6, 54.4, 53.0, 41.3, 33.1, 30.8, 28.7, 20.3, 11.5. LC/MS (ESI) *m*/*z*: $[M + H]^+$ calcd. for $C_{19}H_{22}F_3N_7O$, 421.18; found 422.72.

1-((1R,3S)-3-Ethylaminocyclohexyl)-3-((4-(trifluoromethyl)pyridine-2-yl)oxy)-1H-pyrazolo[3,4-*d*]pyrimidin-4-amine (20a). Synthesized using general procedure A. Yield: 2 mg, 12.5%. ^{1}H NMR (400 MHz, CD_3OD) δ 8.39 (d, J = 5.3 Hz, 1H), 8.26 (s, 1H), 7.66 (s, 1H), 7.52 (d, J = 5.3 Hz, 1H), 3.41–3.36 (m, 1H), 3.11 (q, J = 6.7 Hz, 2H), 2.45–2.39 (m, 1H), 2.18 (d, J = 12.5 Hz, 1H), 2.11–1.82 (m, 5H), 1.66–1.57 (m, 1H), 1.42–1.35 (m, 1H), 1.30 (t, J = 7.2 Hz, 3H). LC/MS (ESI) m/z: $[M + H]^+$ calcd. for $C_{19}H_{22}F_3N_7O$, 421.18; found 422.48.

1-((1S,3R)-3-Ethylaminocyclohexyl)-3-((4-(trifluoromethyl)pyridine-2-yl)oxy)-1H-pyrazolo[3,4-*d*]pyrimidin-4-amine (21a). Synthesized using general procedure A. Yield: 8.2 mg, 34.7%. ^{1}H NMR (600 MHz, CD_3OD) δ 8.40 (d, J = 5.1 Hz, 1H), 8.36 (s, 1H), 7.67 (s, 1H), 7.56–7.54 (m, 1H), 4.96–4.90 (m, 1H), 3.38 (tt, J = 12.0, 3.9 Hz, 1H), 3.11 (q, J = 7.3 Hz, 2H), 2.48–2.43 (m, 1H), 2.21–2.16 (m, 1H), 2.09–2.02 (m, 3H), 1.94–1.84 (m, 1H), 1.67–1.57 (m, 1H), 1.40 (qd, J = 12.6, 3.6 Hz, 1H), 1.30 (t, J = 7.3 Hz, 3H). ^{13}C NMR (600 MHz, CD_3OD) δ 163.8, 162.0, 161.7, 154.0, 152.6, 152.1, 150.4, 149.9, 143.5, 143.3, 117.6, 110.5, 92.6, 56.4, 55.7, 41.2, 35.2, 31.9, 29.1, 23.0, 11.7. LC/MS (ESI) m/z: $[M + H]^+$ calcd. for $C_{19}H_{22}F_3N_7O$, 421.18; found 422.78.

1-((1S,3S)-3-Ethylaminocyclohexyl)-3-((4-(trifluoromethyl)pyridine-2-yl)oxy)-1H-pyrazolo[3,4-*d*]pyrimidin-4-amine (22a). Synthesized using general procedure A. Yield: 2 mg, 5.6%. ^{1}H NMR (400 MHz, CD_3OD) δ 8.41 (d, J = 5.2 Hz, 1H), 8.36 (s, 1H), 7.68 (s, 1H), 7.58–7.53 (m, 1H), 5.35–5.27 (m, 1H), 3.83 (m, 1H), 3.06 (q, J = 7.2 Hz, 2H), 2.54 (m, 1H), 2.18–2.04 (m, 3H), 2.00–1.90 (m, 1H), 1.87–1.75 (m, 2H), 1.67–1.56 (m, 1H), 1.26 (t, J = 7.3 Hz, 3H). ^{13}C NMR (400 MHz, CD_3OD) δ 163.9, 152.0, 150.4, 143.2, 117.5, 110.5, 92.6, 54.3, 53.0, 41.3, 33.0, 30.8, 28.7, 20.3, 11.5. LC/MS (ESI) m/z: $[M + H]^+$ calcd. for $C_{19}H_{22}F_3N_7O$, 421.18; found 422.78.

1-((1R,3R)-3-(Cyclopropylmethylamino)cyclohexyl)-3-((4-(trifluoromethyl)pyridine-2-yl)oxy)-1H-pyrazolo[3,4-*d*]pyrimidin-4-amine (23a). Synthesized using general procedure A. Yield: 12.6 mg, 55.1%. ^{1}H NMR (600 MHz, CD_3OD) δ 8.41 (d, J = 5.2 Hz, 1H), 8.37 (s, 1H), 7.68 (dt, J = 1.5, 0.7 Hz, 1H), 7.58–7.53 (m, 1H), 5.34 (p, J = 4.6 Hz, 1H), 3.89 (tt, J = 10.1, 4.1 Hz, 1H), 2.95–2.86 (m, 2H), 2.60–2.52 (m, 1H), 2.18–2.05 (m, 3H), 1.99–1.91 (m, 1H), 1.90–1.74 (m, 2H), 1.67–1.57 (m, 1H), 1.07–0.97 (m, 1H), 0.68–0.60 (m, 2H), 0.39–0.33 (m, 2H). ^{13}C NMR (600 MHz, CD_3OD) δ 163.9, 162.3, 162.0, 153.9, 152.4, 152.1, 150.4, 149.6, 143.5, 143.2, 117.5, 110.5, 92.6, 54.2, 53.2, 50.9, 33.0, 30.7, 28.7, 20.3, 8.1, 4.6, 4.5. LC/MS (ESI) m/z: $[M + H]^+$ calcd. for $C_{21}H_{24}F_3N_7O$, 447.20; found 448.79.

1-((1R,3S)-3-(Cyclopropylmethylamino)cyclohexyl)-3-((4-(trifluoromethyl)pyridine-2-yl)oxy)-1H-pyrazolo[3,4-*d*]pyrimidin-4-amine (24a). Synthesized using general procedure A. Yield: 1.3 mg, 6.9%. ^{1}H NMR (400 MHz, CD_3OD) δ 8.39 (d, J = 5.3 Hz, 1H), 8.30 (s, 1H), 7.67 (s, 1H), 7.54 (d, J = 5.3 Hz, 1H), 3.40–3.35 (m, 1H), 2.95 (dd, J = 7.7, 2.7 Hz, 2H), 2.48–2.41 (m, 1H), 2.19 (d, J = 12.5 Hz, 1H), 2.10–2.01 (m, 3H), 1.95–1.82 (m, 1H), 1.61 (d,

J = 13.5 Hz, 1H), 1.47–1.35 (m, 1H), 1.12–1.02 (m, 1H), 0.71 (q, *J* = 5.6 Hz, 2H), 0.40 (q, *J* = 4.8 Hz, 2H). LC/MS (ESI) *m*/*z*: $[M + H]^+$ calcd. for $C_{21}H_{24}F_3N_7O$, 447.20; found 448.85.

1-((1R,3R)-3-(Methanesulfonamino)cyclohexyl)-3-((4-(trifluoromethyl)pyridine-2-yl)oxy)-1H-pyrazolo[3,4-*d*]pyrimidin-4-amine (25a). Synthesized using general procedure B. Yield: 26.6 mg, 72.5%. ^{1}H NMR (600 MHz, CD_3OD) *δ* 8.42 (d, *J* = 5.3 Hz, 1H), 8.36 (s, 1H), 7.69 (s, 1H), 7.55 (dd, *J* = 5.2, 1.5 Hz, 1H), 5.20–5.14 (m, 1H), 3.92 (p, *J* = 4.2 Hz, 1H), 2.94 (s, 3H), 2.23 (ddd, *J* = 13.6, 10.1, 3.7 Hz, 1H), 2.16–2.10 (m, 1H), 2.01–1.94 (m, 2H), 1.83–1.71 (m, 4H). ^{13}C NMR (600 MHz, MeOD) *δ* 163.7, 162.4, 162.1, 153.3, 152.5, 151.7, 150.5, 148.5, 117.6, 110.5, 92.2, 53.9, 50.6, 40.7, 37.9, 32.0, 31.8, 20.8. LC/MS (ESI) *m*/*z*: $[M + H]^+$ calcd. for $C_{18}H_{20}F_3N_7O_3S$, 471.13; found 472.10.

1-((1R,3S)-3-(Methanesulfonamino)cyclohexyl)-3-((4-(trifluoromethyl)pyridine-2-yl)oxy)-1H-pyrazolo[3,4-*d*]pyrimidin-4-amine (26a). Synthesized using general procedure B. Yield: 6.0 mg, 38.7%. ^{1}H NMR (400 MHz, CD_3OD) *δ* 8.41 (d, *J* = 5.2 Hz, 1H), 8.34 (s, 1H), 7.68 (s, 1H), 7.57–7.51 (m, 1H), 4.88–4.81 (m, 1H), 3.46 (tt, *J* = 11.8, 4.1 Hz, 1H), 2.96 (s, 3H), 2.31 (d, *J* = 12.3 Hz, 1H), 2.06 (d, *J* = 13.2 Hz, 1H), 1.98–1.90 (m, 2H), 1.85–1.74 (m, 1H), 1.65–1.51 (m, 1H), 1.33 (d, *J* = 4.1 Hz, 2H). ^{13}C NMR (600 MHz, CD_3OD) *δ* 163.9, 154.1, 152.3, 151.9, 150.4, 150.1, 143.5, 125.3, 117.4, 110.4, 110.4, 92.5, 56.5, 52.7, 41.5, 40.6, 34.1, 31.9, 23.9. LC/MS (ESI) *m*/*z*: $[M + H]^+$ calcd. for $C_{18}H_{20}F_3N_7O_3S$, 471.13; found 472.20.

1-((1R,3R)-3-(*N*-methylureido)cyclohexyl)-3-((4-(trifluoromethyl)pyridine-2-yl)oxy)-1H-pyrazolo[3,4-*d*]pyrimidin-4-amine (27a). Synthesized using general procedure B. Yield: 18.6 mg, 60.0%. ^{1}H NMR (600 MHz, CD_3OD) *δ* 8.42 (d, *J* = 5.2 Hz, 1H), 8.35 (s, 1H), 7.71–7.69 (m, 1H), 7.54 (dd, *J* = 5.3, 1.4 Hz, 1H), 5.09–5.02 (m, 1H), 4.13 (p, *J* = 4.1 Hz, 1H), 2.70 (s, 3H), 2.22–2.16 (m, 1H), 2.08–2.02 (m, 1H), 2.01–1.93 (m, 2H), 1.86–1.81 (m, 1H), 1.78–1.71 (m, 1H), 1.70–1.65 (m, 2H). ^{13}C NMR (600 MHz, MeOD) *δ* 163.7, 161.7, 161.5, 161.2, 153.0, 152.5, 151.5, 150.4, 148.0, 117.5, 110.5, 92.2, 54.4, 46.7, 37.4, 32.3, 31.0, 26.8, 21.1. LC/MS (ESI) *m*/*z*: $[M + H]^+$ calcd. for $C_{19}H_{21}F_3N_8O_2$, 450.17; found 451.20.

1-((1R,3S)-3-(*N*-methylureido)cyclohexyl)-3-((4-(trifluoromethyl)pyridine-2-yl)oxy)-1H-pyrazolo[3,4-*d*]pyrimidin-4-amine (28a). Synthesized using general procedure B. Yield: 9.6 mg, 56.4%. ^{1}H NMR (400 MHz, CD_3OD) *δ* 8.41 (d, *J* = 5.2 Hz, 1H), 8.35 (s, 1H), 7.68 (s, 1H), 7.56–7.52 (m, 1H), 4.89–4.82 (m, 1H), 3.74–3.65 (m, 1H), 2.67 (s, 3H), 2.22 (m, 1H), 2.02–1.90 (m, 2H), 1.88–1.74 (m, 2H), 1.63–1.51 (m, 1H), 1.36–1.15 (m, 2H). ^{13}C NMR (600 MHz, CD_3OD) *δ* 163.8, 161.0, 153.3, 152.5, 151.5, 150.4, 148.7, 143.5, 143.1, 125.3, 122.5, 117.5, 117.5, 110.5, 110.4, 92.3, 56.8, 49.3, 39.8, 33.3, 32.2, 26.9, 24.1. LC/MS (ESI) *m*/*z*: $[M + H]^+$ calcd. for $C_{19}H_{21}F_3N_8O_2$, 450.17; found 451.17.

1-((1S,3S)-3-(Tetrahydro-2H-pyran-3-ylamine)-3-((4-(trifluoromethyl)pyridine-2-yl)oxy)-1H-pyrazolo[3,4-*d*]pyrimidin-4-amine (29a). Synthesized using general procedure C. Yield: 407.8 mg, quant. ^{1}H NMR (400 MHz, CD_3OD-d_4) *δ* 2.37 (d, *J* =

14.01 Hz, 1 H) 2.65–2.75 (m, 1 H) 3.75–3.94 (m, 4 H) 4.09–4.16 (m, 1 H) 5.31–5.40 (m, 1 H) 7.55 (d, J = 4.67 Hz, 1 H) 7.67 (s, 1H) 8.38–8.43 (m, 2 H). ^{13}C NMR (600 MHz, CD_3OD) δ 163.9, 162.5, 155.2, 153.6, 152.3, 152.0, 150.4, 143.5, 143.2, 125.3, 122.5, 117.5, 117.4, 110.5, 110.4, 93.0, 70.8, 69.0, 49.7, 47.8, 31.6. LC/MS (ESI) m/z: $[M + H]^+$ calcd.for $C_{16}H_{16}F_3N_7O_2$, 395.13; found 396.64.

1-((1S,3R)-3-(Tetrahydro-2H-pyran-3-ylamine)-3-((4-(trifluoromethyl)pyridine-2-yl)oxy)-1H-pyrazolo[3,4-*d*]pyrimidin-4-amine (30a). Synthesized using general procedure C. Yield: 376 mg, quant. ^{1}H NMR (400 MHz, CD_3OD) δ 8.44 (d, J = 5.3 Hz, 1H), 8.36 (s, 1H), 7.70 (s, 1H), 7.58 (d, J = 5.3 Hz, 1H), 5.17–5.06 (m, 1H), 4.13–4.02 (m, 2H), 3.87–3.75 (m, 1H), 3.63–3.56 (m, 2H), 2.65–2.60 (m, 1H), 2.39–2.27 (m, 1H).^{13}C NMR (600 MHz, CD_3OD) δ 163.4, 162.5, 162.3, 155.3, 153.2, 152.3, 152.1, 150.3, 143.8, 143.6, 143.3, 132.1, 129.9, 128.0, 117.6, 110.7, 92.6, 90.3, 70.8, 69.2, 51.9, 46.5, 32.2. LC/MS (ESI) m/z: $[M + H]^+$ calcd for $C_{16}H_{16}F_3N_7O_2$, 395.13; found 396.2.

1-((1S,3S)-3-(Tetrahydro-2H-pyran-3-ylamine)-3-((4-(trifluoromethyl)pyridine-2-yl)oxy)-1H-pyrazolo[3,4-*d*]pyrimidin-4-amine (31a). Synthesized using general procedure C. Yield: 312.1 mg, 96.9%. ^{1}H NMR (400 MHz, CD_3OD) δ 8.34 (d, J = 5.2 Hz, 1H), 8.16 (s, 1H), 7.64–7.59 (m, 1H), 7.46–7.40 (m, 1H), 5.14–5.03 (m, 1H), 3.99–3.90 (m, 1H), 3.83–3.75 (m, 1H), 3.70–3.63 (m, 1H), 3.61–3.54 (m, 1H), 3.30–3.22 (m, 1H), 2.53–2.40 (m, 1H), 2.08–1.98 (m, 1H). ^{13}C NMR (600 MHz, CD_3OD) δ 164.1, 158.9, 157.7, 154.8, 150.7, 150.4, 143.6, 143.2, 142.9, 142.6, 125.3, 122.6, 117.0, 116.9, 110.1, 110.1, 110.0, 110.0, 93.1, 73.3, 71.0, 50.6, 49.9, 46.9, 36.1. LC/MS (ESI) m/z: $[M + H]^+$ calcd. for $C_{16}H_{16}F_3N_7O_2$, 395.13; found 396.2.

1-((1S,3S)-3-((N-methanesulfonyl)tetrahydro-2H-pyran-3-ylamine)-3-((4-(trifluoromethyl)pyridine-2-yl)oxy)-1H-pyrazolo[3,4-*d*]pyrimidin-4-amine (32a). Synthesized using general procedure B. Yield: 19.5 mg, 59.3%. ^{1}H NMR (400 MHz, CD_3OD) δ 8.43 (d, J = 5.3 Hz, 1H), 8.38 (s, 1H), 7.69 (s, 1H), 7.56 (d, J = 5.2 Hz, 1H), 4.00 (dd, J = 11.3, 4.0 Hz, 1H), 3.95–3.84 (m, 2H), 3.79–3.69 (m, 2H), 2.95 (d, J = 1.1 Hz, 3H), 2.58–2.47 (m, 1H), 2.30–2.20 (m, 1H). ^{13}C NMR (600 MHz, CD_3OD) δ 163.7, 162.2, 153.4, 152.7, 152.6, 150.5, 149.1, 143.5, 143.2, 125.2, 117.7, 117.6, 110.6, 110.6, 92.5, 72.2, 70.6, 51.9, 41.0, 40.4, 35.1. LC/MS (ESI) m/z: $[M + H]^+$ calcd. for $C_{17}H_{18}F_3N_7O_4S$, 473.11; found 474.10.

1-Cyclopropyl-3-((4-(p-tolyl)pyridin-2-yl)oxy)-1H-pyrazolo[3,4-*d*]pyrimidin-4-amine (2b). Synthesized using general procedure D. Yield: 30 mg, 58%. ^{1}H NMR (400 MHz, $(CD_3)_2SO$) δ 8.09–8.25 (m, 2H), 7.73–7.85 (m, J = 8.17 Hz, 2H), 7.46–7.62 (m, 2H), 7.27–7.42 (m, J = 7.79 Hz, 2H), 2.38 (s, 3H), 0.84–1.13 (m, 4H). ^{13}C NMR (400 MHz, $(CD_3)_2SO$) δ 163.2, 157.1, 156.6, 154.7, 151.0, 148.6, 147.7, 139.4, 133.7, 129.8, 129.2, 126.8, 126.8, 117.4, 108.9, 92.2, 28.5, 20.8, 6.0, 6.0. LC/MS (ESI) m/z: $[M + H]^+$ calcd. for $C_{20}H_{18}N_6O$, 358.41; found 359.2.

(4-(2-((4-Amino-1-cyclopropyl-1H-pyrazolo[3,4-*d*]pyrimidin-3-yl) oxy)pyridin-4-yl)phenyl)methanol (3b). Synthesized using general procedure D. Yield: 20 mg, 37.1%. ^{1}H NMR (400 MHz, $(CD_3)_2SO$) δ 8.20 (s, 1H), 8.17 (d, J = 5.06 Hz, 1H), 7.83 (d, J = 8.17

Hz, 2H), 7.46–7.55 (m, 3H), 5.32 (s, 1H), 4.58 (d, J = 5.45 Hz, 2H), 3.71 (tt, J = 3.80, 7.10 Hz, 1H), 1.08 (d, J = 2.72 Hz, 2H), 0.87–1.05 (m, 2H). ^{13}C NMR (400 MHz, $(CD_3)_2SO$) δ 169.0, 169.0, 163.6, 157.5, 157.0, 155.1, 151.5, 149.0, 148.1, 144.7, 135.3, 127.6, 127.1, 118.0, 109.5, 92.6, 62.9, 29.0, 6.4, 6.4. LC/MS (ESI) m/z: $[M + H]^+$ calcd. for $C_{20}H_{18}N_6O_2$, 374.15; found 375.15.

(3-(2-((4-Amino-1-cyclopropyl-1H-pyrazolo[3,4-*d*]pyrimidin-3-yl)oxy) pyridin-4-yl)phenyl)methanol (4b). Synthesized using general procedure D. Yield: 25 mg, 48%. ^{1}H NMR (400 MHz, $(CD_3)_2SO$) δ 8.15–8.25 (m, 2H), 7.79 (s, 1H), 7.71 (d, J = 7.40 Hz, 1H), 7.41–7.56 (m, 4H), 5.33 (br. s., 1H), 4.56–4.67 (m, 2H), 3.71 (td, J = 3.65, 7.10 Hz, 1H), 0.93–1.14 (m, 4H). ^{13}C NMR (400 MHz, $(CD_3)_2SO$) δ 163.1, 157.1, 156.6, 154.7, 151.3, 148.6, 147.7, 143.7, 136.5, 129.1, 127.7, 125.3, 124.9, 117.7, 109.3, 92.1, 62.7, 28.6, 6.0, 6.0. LC/MS (ESI) m/z: $[M + H]^+$ calcd. for $C_{20}H_{18}N_6O_2$, 374.15; found 375.15.

4-(2-((4-Amino-1-cyclopropyl-1H-pyrazolo[3,4-*d*]pyrimidin-3-yl)oxy)pyridin-4-yl)benzonitrile (5b). Synthesized using general procedure D. Yield: 22 mg, 41%. ^{1}H NMR (400 MHz, $(CD_3)_2SO$) δ 8.17–8.34 (m, 2H), 8.05 (q, J = 8.56 Hz, 4H), 7.53–7.73 (m, 2H), 6.78 (br. s., 1H), 5.75 (s, 1H), 3.63–3.82 (m, 1H), 0.93–1.19 (m, 4H). ^{13}C NMR (400 MHz, $(CD_3)_2SO$) δ 163.4, 157.3, 156.8, 154.9, 149.4, 148.6, 148.2, 141.4, 133.3, 133.3, 128.2, 128.2, 118.8, 118.1, 112.3, 110.2, 92.4, 28.8, 6.2, 6.2. LC/MS (ESI) m/z: $[M + H]^+$ calcd. for $C_{20}H_{15}N_7O$, 369.39; found 370.1.

3-(2-((4-Amino-1-cyclopropyl-1H-pyrazolo[3,4-*d*]pyrimidin-3-yl)oxy)pyridin-4-yl)benzonitrile (6b). Synthesized using general procedure D. Yield: 32 mg, 60%. ^{1}H NMR (400 MHz, $(CD_3)_2SO$) δ 8.38 (s, 1H), 8.18–8.25 (m, 3H), 7.98 (d, J = 7.79 Hz, 1H), 7.70–7.79 (m, 1H), 7.58–7.66 (m, 2H), 6.77 (br. s., 1H), 3.71 (br. s., 1H), 0.98–1.17 (m, 4H). ^{13}C NMR (400 MHz, $(CD_3)_2SO$) δ 168.9, 163.4, 157.3, 156.8, 154.9, 149.2, 148.6, 148.2, 138.0, 133.3, 132.0, 131.0, 130.7, 118.7, 118.0, 112.6, 110.0, 92.3, 28.8, 6.2. LC/MS (ESI) m/z: $[M + H]^+$ calcd. for $C_{20}H_{15}N_7O$, 369.38, found, 370.1.

4-(2-((4-Amino-1-cyclopropyl-1H-pyrazolo[3,4-*d*]pyrimidin-3-yl)oxy)pyridin-4-yl)phenol (7b). Synthesized using general procedure D. Yield: 20 mg, 67%. ^{1}H NMR (400 MHz, $(CD_3)_2SO$) δ 9.92 (br. s., 1H), 8.18 (s, 1H), 8.08 (d, J = 5.06 Hz, 1H), 7.61–7.77 (m, J = 8.56 Hz, 2H), 7.33–7.47 (m, 2H), 6.77–6.95 (m, J = 8.56 Hz, 2H), 3.69 (td, J = 3.55, 7.30 Hz, 1H), 0.94–1.13 (m, 4H). ^{13}C NMR (400 MHz, $(CD_3)_2SO$) δ 168.7, 168.6, 163.2, 159.1, 157.1, 156.6, 154.7, 151.0, 148.7, 147.5, 128.3, 127.1, 116.9, 116.0, 108.0, 92.2, 28.5, 6.0, 6.0. LC/MS (ESI) m/z: $[M + H]^+$ calcd. for $C_{19}H_{16}N_2O_2$, 360.2; found 361.

4-(2-((4-Amino-1-cyclopropyl-1H-pyrazolo[3,4-*d*]pyrimidin-3-yl)oxy)pyridin-4-yl)phenol (8b). Synthesized using general procedure D. Yield: 20 mg, 67%. ^{1}H NMR (400 MHz, CD_3OD) δ 8.32 (s, 1H), 8.20 (d, J = 5.3 Hz, 1H), 7.70–7.62 (m, 3H), 7.57–7.50 (m, 1H), 7.38–7.30 (m, 2H), 3.82 (tt, J = 7.4, 3.8 Hz, 1H), 1.25–1.19 (m, 2H), 1.14–1.08 (m, 2H). ^{13}C NMR (400 MHz, CD_3OD) δ 163.7, 163.1, 154.6, 154.2, 153.5, 152.7, 150.1, 148.8, 141.3, 135.4, 131.0, 128.0, 119.9, 111.0, 92.4, 30.4, 6.9. LC/MS (ESI) m/z: $[M + H]^+$ calcd. for $C_{20}H_{15}D_3N_6O$, 361.42; found 362.30.

3-((4-(4-Chlorophenyl)pyridin-2-yl)oxy)-1-cyclopropyl-1H-pyrazolo[3,4-*d*]pyrimidin-4-amine (9b). Synthesized using general procedure D. Yield: 10 mg, 31.25%. ^{1}H NMR (400 MHz, $CDCl_3$) δ 8.13–8.36 (m, 2H), 7.60 (br. s., 1H), 7.48 (br. s., 1H), 7.33–7.45 (m, 2H), 3.72–4.00 (m, 1H), 1.32 (br. s., 2H), 1.25 (br. s., 1H), 1.16 (d, J = 6.23 Hz, 2H). ^{13}C NMR (400 MHz, $CDCl_3$) δ 173.8, 173.8, 162.1, 153.0, 152.6, 151.9, 148.2, 146.7, 136.3, 135.3, 129.6, 129.6, 128.3, 128.3, 119.5, 110.4, 91.9, 29.8, 6.6. LC/MS (ESI) *m*/*z*: $[M + H]^+$ calcd. for $C_{19}H_{15}ClN_6O$, 378.8; found 379.1.

1-Cyclopropyl-3-((4-(4-fluorophenyl)pyridin-2-yl)oxy)-1H-pyrazolo[3,4-*d*]pyrimidin-4-amine (10b). Synthesized using general procedure D. Yield: 60 mg, 95%. ^{1}H NMR (400 MHz, $(CD_3)_2SO$) δ 8.20 (br.s., 2H), 7.93 (br.s., 2H), 7.52 (br.s., 2H), 7.38 (br.s., 2H), 3.71 (br.s., 1H), 1.08 (br.s., 2H), 1.02 (br.s., 2H). ^{13}C NMR (400 MHz, $(CD_3)_2SO$) δ 168.9, 163.4, 157.3, 156.8, 154.9, 150.2, 148.7, 148.0, 133.3, 129.6, 129.5, 117.8, 116.5, 116.3, 109.4, 92.4, 28.8, 6.2,6.2. LC/MS (ESI) *m*/*z*: $[M + H]^+$ calcd. for $C_{19}H_{15}FN_6O$, 362.13; found 363.1.

4-(2-((4-Amino-1-cyclopropyl-1H-pyrazolo[3,4-*d*]pyrimidin-3-yl)oxy)pyridin-4-yl)-*N*-methyl benzenesulfonamide (11b). Synthesized using general procedure D. Yield: 13 mg, 20%. ^{1}H NMR (400 MHz, $(CD_3)_2SO$) δ 8.18–8.27 (m, 2H), 8.04–8.14 (m, *J* = 7.79 Hz, 2H), 7.89–7.98 (m, *J* = 8.17 Hz, 2H), 7.60 (br. s., 3H), 6.71 (br. s., 1H), 3.67–3.77 (m, 1H), 2.46 (d, *J* = 4.67 Hz, 3H), 1.08 (br. s., 2H), 1.02 (d, *J* = 6.23 Hz, 2H). ^{13}C NMR (400 MHz, $(CD_3)_2SO$) δ 168.9, 163.4, 157.3, 156.8, 154.9, 149.8, 148.6, 148.2, 140.7, 140.2, 128.2, 127.7, 118.2, 110.1, 92.4, 40.3, 40.1, 39.9, 39.7, 39.3, 39.1, 28.9, 28.8, 6.2. LC/MS (ESI) *m*/*z*: $[M + H]^+$ calcd. for $C_{20}H_{19}N_7O_3S$, 437.48 found 437.48.

4-(2-((4-Amino-1-cyclopropyl-1H-pyrazolo[3,4-*d*]pyrimidin-3-yl)oxy)pyridin-4-yl)benzamide (12b). Synthesized using general procedure D. Yield: 13 mg, 20%. ^{1}H NMR (400 MHz, $(CD_3)_2SO$) δ 8.17–8.22 (m, 2H), 8.10 (br. s., 1H), 7.99–8.06 (m, *J* = 8.17 Hz, 2H), 7.92–7.98 (m, *J* = 8.17 Hz, 2H), 7.58 (d, *J* = 1.56 Hz, 2H), 7.48 (br. s., 1H), 3.70 (td, *J* = 3.41, 7.20 Hz, 1H), 0.95–1.11 (m, 4H). ^{13}C NMR (400 MHz, $(CD_3)_2SO$) δ 168.7, 167.2, 163.2, 157.1, 156.6, 154.7, 150.2, 148.5, 147.8, 139.2, 135.0, 128.3, 126.9, 120.8, 117.8, 109.6, 92.2, 28.6, 6.0, 6.0. LC/MS (ESI) *m*/*z*: $[M + H]^+$ calcd. for $C_{20}H_{17}N_7O_2$, 387.40; found 387.40.

1-Cyclopropyl-3-((4-(4-(trifluoromethyl)phenyl)pyridin-2-yl)oxy)-1H-pyrazolo[3,4-*d*]pyrimidin-4-amine (13b). Synthesized using general procedure D. Yield: 63 mg, 88%. ^{1}H NMR (400 MHz, $CDCl_3$) δ 8.39 (s, 1H), 8.33 (d, *J* = 5.45 Hz, 1H), 7.77 (d, *J* = 2.73 Hz, 4H), 7.47 (s, 1H), 7.37 (d, *J* = 5.45 Hz, 1H), 5.78 (br. s., 2H), 3.69 (tt, *J* = 3.50, 7.20 Hz, 1H), 1.28 (br. s., 2H), 1.12 (d, *J* = 5.84 Hz, 2H). ^{13}C NMR (400 MHz, $CDCl_3$) δ 162.8, 157.1, 156.9, 155.0, 151.6, 149.0, 148.6, 140.9, 131.4, 127.5, 127.5, 126.2, 126.2, 126.2, 118.8, 110.2, 92.8, 28.8, 6.4, 6.4. LC/MS (ESI) *m*/*z*: $[M + H]^+$ calcd. for $C_{20}H_{15}F_3N_6O$, 412.13; found 413.1.

1-Cyclopropyl-3-((4-(3,4,5-trifluorophenyl)pyridin-2-yl)oxy)-1H-pyrazolo[3,4-*d*]pyrimidin-4-amine (14b). Synthesized using general procedure D. Yield: 20 mg, 34%. ^{1}H NMR (400 MHz, $CDCl_3$) δ 8.35 (s, 1H), 8.28 (d, *J* = 5.45 Hz, 1H),

7.35 (s, 1H), 7.20–7.30 (m, 3H), 5.84 (br. s., 2H), 3.66 (td, J = 3.65, 7.10 Hz, 1H), 1.21–1.27 (m, 2H), 1.05–1.14 (m, 2H). ^{13}C NMR (400 MHz, $CDCl_3$) δ 162.8, 157.2, 156.9, 155.0, 153.0, 150.5, 149.8, 148.9, 148.8, 133.5, 118.3, 111.6, 111.5, 111.4, 111.3, 109.8, 92.7, 28.8, 6.5, 6.5. LC/MS (ESI) m/z: $[M + H]^+$ calcd. for $C_{19}H_{13}F_3N_6O$, 398.35; found 399.1.

1-Cyclopropyl-3-((4-(3,5-difluoro-4-chlorophenyl)pyridin-2-yl)oxy)-1H-pyrazolo[3,4-*d*]pyrimidin-4-amine (15b). Synthesized using general procedure D. Yield: 20 mg, 33.5%. ^{1}H NMR (400 MHz, $CDCl_3$) δ 8.15–8.31 (m, 2H), 7.59 (s, 1H), 7.16–7.39 (m, 3H), 3.76 (td, J = 3.55, 7.30 Hz, 1H), 1.04–1.34 (m, 4H). ^{13}C NMR (400 MHz, $CDCl_3$) δ 174.1, 174.0, 162.1, 160.9, 152.1, 151.2, 148.7, 147.6, 119.2, 111.1, 111.1, 110.9, 110.8, 110.4, 77.6, 77.3, 49.8, 49.6, 49.4, 49.2, 49.0, 30.0, 6.8. LC/MS (ESI) m/z: $[M + H]^+$ calcd. for $C_{19}H_{13}ClF_2N_6O$, 414.80; found 416.2.

1-Cyclopropyl-3-((4-(3,5-difluoro-4-(trifluoromethyl)phenyl)pyridin-2-yl)oxy)-1H-pyrazolo[3,4-*d*]pyrimidin-4-amine (16b). Synthesized using general procedure D. Yield: 16 mg, 25%. ^{1}H NMR (400 MHz, $CDCl_3$) δ 8.25 (d, J = 5.06 Hz, 1H), 8.19 (s, 1H), 7.97 (s, 1H), 8.00 (s, 1H), 7.72 (s, 1H), 7.66 (d, J = 5.06 Hz, 1H), 3.59–3.79 (m, 1H), 0.89–1.12 (m, 4H). ^{13}C NMR (400 MHz, $CDCl_3$) δ 168.8, 168.8, 163.5, 157.3, 156.8, 154.9, 148.5, 148.4, 147.1, 144.2, 118.0, 112.4, 112.4, 112.2, 112.2, 110.4, 92.3, 40.3, 40.1, 39.9, 39.7, 39.3, 39.1, 28.8, 6.2. LC/MS (ESI) m/z: $[M + H]^+$ calcd. for $C_{20}H_{13}F_5N_6O$, 448.36; found 449.1.

1-Cyclopropyl-3-((4-(furan-2-yl)pyridin-2-yl)oxy)-1H-pyrazolo[3,4-*d*]pyrimidin-4-amine (17b). Synthesized using general procedure D. Yield: 30 mg, 62%. ^{1}H NMR (400 MHz, $(CD_3)_2SO$) δ 8.20 (s, 1H), 8.13 (d, J = 5.06 Hz, 1H), 7.86–7.97 (m, 1H), 7.46–7.53 (m, 1H), 7.44 (s, 1H), 7.37 (d, J = 3.50 Hz, 1H), 6.72 (dd, J = 1.75, 3.31 Hz, 1H), 3.70 (td, J = 3.41, 7.20 Hz, 1H), 0.87–1.16 (m, 4H). ^{13}C NMR (400 MHz, $(CD_3)_2SO$) δ 168.6, 163.1, 157.1, 156.6, 154.7, 150.2, 148.4, 147.9, 145.2, 140.5, 114.2, 112.7, 110.8, 105.3, 92.1, 28.5, 6.0. LC/MS (ESI) m/z: $[M + H]^+$ calcd. for $C_{17}H_{14}N_6O_2$, 334.34; found 335.1.

1-Cyclopropyl-3-((4-(thiophen-2-yl)pyridin-2-yl)oxy)-1H-pyrazolo[3,4-*d*]pyrimidin-4-amine (18b). Synthesized using general procedure D. Yield: 13 mg, 26%. ^{1}H NMR (400 MHz, $(CD_3)_2SO$) δ 8.33 (s, 1H), 8.12 (d, J = 4.67 Hz, 1H), 7.88 (br. s., 1H), 7.78 (d, J = 4.28 Hz, 1H), 7.48 (br. s., 2H), 7.24 (br. s., 1H), 3.77 (br. s., 1H), 1.06 (d, J = 14.79 Hz, 4H) ^{13}C NMR (400 MHz, $(CD_3)_2SO$) δ 173.7, 168.9, 163.2, 149.6, 148.2, 144.8, 139.8, 129.2, 129.2, 127.5, 116.7, 107.8, 92.1, 30.9, 29.2, 6.3. LC/MS (ESI) m/z: $[M + H]^+$ calcd. for $C_{17}H_{14}N_6OS$, 350.13; found 351.1.

3-((4-(1H-Pyrazol-5-yl)pyridin-2-yl)oxy)-1-cyclopropyl-1H-pyrazolo[3,4-*d*]pyrimidin-4-amine (19b). Synthesized using general procedure D. Yield: 10 mg, 20%. ^{1}H NMR (400 MHz, CD_3OD) δ 8.17–8.22 (m, 2H), 7.77 (s, 1H), 7.73 (s, 1H), 7.63 (br. s., 1H), 6.87 (br. s., 1H), 3.65–3.63 (dd, J = 3.70, 6.42 Hz, 1H), 1.18 (br. s., 2H), 1.08 (d, J = 7.01 Hz, 2H). ^{13}C NMR (400 MHz, CD_3OD) δ 164.7, 159.6, 158.4, 158.3, 158.3, 156.2, 151.6, 149.4, 132.2, 132.1, 118.9, 115.0, 109.9, 105.2, 30.2, 7.5, 7.5. LC/MS (ESI) m/z: $[M + H]^+$ calcd. for $C_{16}H_{14}N_8O$, 334.12; found 335.65.

1-Cyclopropyl-3-((4-(furan-3-yl)pyridin-2-yl)oxy)-1H-pyrazolo[3,4-*d*]pyrimidin-4-amine (20b). Synthesized using general procedure D. Yield: 33 mg, 68%. ^{1}H NMR (400 MHz, $(CD_3)_2SO$) δ 8.52 (s, 1H), 8.20 (s, 1H), 8.10 (d, J = 5.06 Hz, 1H), 7.84 (s, 1H), 7.41–7.55 (m, 2H), 7.16 (s, 1H), 3.58–3.80 (m, 1H), 0.93–1.14 (m, 4H). ^{13}C NMR (400 MHz, $(CD_3)_2SO$) δ 168.9, 163.4, 157.3, 156.8, 154.9, 148.9, 147.8, 145.3, 143.7, 142.6, 123.7, 116.9, 109.8, 108.7, 108.3, 92.3, 28.7, 6.2. LC/MS (ESI) m/z: $[M + H]^+$ calcd. for $C_{17}H_{14}N_6O_2$, 334.12; found 335.2.

1-Cyclopropyl-3-((4-(thiophen-3-yl)pyridin-2-yl)oxy)-1H-pyrazolo[3,4-*d*]pyrimidin-4-amine (21b). Synthesized using general procedure D. Yield: 16 mg, 31%. ^{1}H NMR (400 MHz, $(CD_3)_2SO$) δ 8.32 (br. s., 2H), 8.13 (d, J = 4.67 Hz, 1H), 7.74 (br. s., 2H), 7.58 (br. s., 2H), 3.76 (br. s., 1H), 1.22 (br. s., 1H), 1.06 (d, J = 14.79 Hz, 3H). ^{13}C NMR (400 MHz, $(CD_3)_2SO$) δ 168.9, 168.8, 168.8, 163.3, 153.5, 151.7, 149.8, 148.0, 146.1, 138.4, 128.2, 126.3, 125.5, 117.6, 108.8, 29.1, 6.3. LC/MS (ESI) m/z: $[M + H]^+$ calcd. for $C_{17}H_{14}N_6OS$, 350.4; found 351.1.

3-((4-(1H-Pyrazol-4-yl)pyridin-2-yl)oxy)-1-cyclopropyl-1H-pyrazolo[3,4-*d*]pyrimidin-4-amine (22b). Synthesized using general procedure D. Yield: 16 mg, 33%. ^{1}H NMR (400 MHz, $(CD_3)_2SO$) δ 13.21 (br. s., 1H), 8.50 (s, 1H), 8.09–8.25 (m, 2H), 8.03 (d, J = 5.06 Hz, 1H), 7.21–7.50 (m, 3H), 3.63–3.86 (m, 1H), 0.95–1.15 (m, 4H). ^{13}C NMR (400 MHz, $(CD_3)_2SO$) δ 168.4, 163.0, 156.9, 156.4, 154.4, 152.7, 151.6, 148.6, 147.3, 144.2, 127.4, 118.3, 116.2, 107.0, 91.9, 39.9, 39.7, 39.3, 39.1, 38.9, 38.7, 30.5, 28.3, 5.8. LC/MS (ESI) m/z: $[M + H]^+$ calcd. for $C_{16}H_{14}N_8O$, 334.13; found 335.2.

1-Cyclopropyl-3-((4-(thiozo-2-yl)pyridin-2-yl)oxy)-1H-pyrazolo[3,4-*d*]pyrimidin-4-amine (23b). Synthesized using general procedure D. Yield: 6.2 mg, 27.5%. ^{1}H NMR (400 MHz, $(CD_3)_2SO$) δ 8.23 (d, J = 5.2 Hz, 1H), 8.19 (s, 1H), 8.08 (d, J = 3.2 Hz, 1H), 8.02 (d, J = 3.2 Hz, 1H), 7.69 (d, J = 5.3 Hz, 1H), 7.67 (s, 1H), 3.74–3.68 (m, 1H), 1.10–0.97 (m, 4H). ^{13}C NMR (400 MHz, $(CD_3)_2SO$) δ 164.32, 163.60, 157.52, 157.07, 155.17, 148.88, 148.65, 145.13, 143.79, 123.63, 117.07, 108.86, 92.55, 29.05, 6.43. LC/MS (ESI) m/z: $[M + H]^+$ calcd. for $C_{16}H_{13}N_7OS$, 351.39; found 352.1.

1-Cyclopropyl-3-((4-(isothiozo-4-yl)pyridin-2-yl)oxy)-1H-pyrazolo[3,4-*d*]pyrimidin-4-amine (24b). Synthesized using general procedure D. Yield: 13 mg, 58.17%. ^{1}H NMR (400 MHz, $(CD_3)_2SO$) δ 9.74 (s, 1H), 9.25 (s, 1H), 8.36 (s, 1H), 8.19 (d, J = 5.4 Hz, 1H), 7.71 (s, 1H), 7.67 (d, J = 5.3 Hz, 1H), 3.80–3.75 (m, 1H), 1.11–1.01 (m, 4H). ^{13}C NMR (400 MHz, $(CD_3)_2SO$) δ 219.14, 163.47, 159.50, 157.12, 154.38, 153.49, 152.54, 150.08, 148.50, 148.48, 143.57, 136.50, 118.38, 109.86, 92.33, 29.42, 6.54. LC/MS (ESI) m/z: $[M + H]^+$ calcd. for $C_{16}H_{13}N_7OS$, 351.39; found 352.2.

1-Cyclopropyl-3-((4-(isooxazo-4-yl)pyridin-2-yl)oxy)-1H-pyrazolo[3,4-*d*]pyrimidin-4-amine (25b). Synthesized using general procedure D. Yield: 12.5 mg, 58.17%. ^{1}H NMR (400 MHz, $(CD_3)_2SO$) δ 8.36 (d, J = 5.9 Hz, 1H), 8.23 (d, J = 5.4 Hz, 1H), 7.86 (s, 1H), 7.75 (d, J = 7.8 Hz, 1H), 7.69 (d, J = 9.0 Hz, 3H), 7.42 (t, J = 7.1 Hz, 1H), 7.32 (t, J = 7.5 Hz, 1H), 3.81–3.75 (m, J = 8.7, 4.7, 2.4 Hz, 1H), 1.13–0.99 (m, 4H). ^{13}C NMR (400 MHz, $(CD_3)_2SO$) δ 163.33, 155.12,

152.42, 148.56, 140.91, 128.57, 126.70, 124.21, 122.53, 115.85, 112.00, 107.24, 92.33, 29.43, 6.54. LC/MS (ESI) *m*/*z*: $[M + H]^+$ calcd. for $C_{16}H_{13}N_7O_2$, 335.33; found 336.2.

1-Cyclopropyl-3-((4-(5-methylthiophen-2-yl)pyridin-2-yl)oxy)-1H-pyrazolo[3,4-*d*]pyrimidin-4-amine (26b). Synthesized using general procedure D. Yield: 18 mg, 34%. ^{1}H NMR (400 MHz, CD_3OD) δ 8.22 (br. s., 1H), 8.12 (d, J = 3.89 Hz, 1H), 7.58 (br. s., 1H), 7.41 (br. s., 1H), 7.34 (br. s., 1H), 6.82 (br. s., 1H), 3.63 (br. s., 1H), 2.53 (br. s., 2H), 1.22 (br. s., 2H), 1.10 (d, J = 6.23 Hz, 2H). ^{13}C NMR (400 MHz, CD_3OD) δ 156.4, 147.6, 147.6, 143.4, 126.9, 126.5, 116.6, 107.2, 47.6, 46.7, 28.5, 15.0, 6.1, 6.1. LC/MS (ESI) *m*/*z*: $[M + H]^+$ calcd. for $C_{18}H_{16}N_6OS$, 364.64; found 365.2.

1-Cyclopropyl-3-((4-(5-chlorothiophen-2-yl)pyridin-2-yl)oxy)-1H-pyrazolo[3,4-*d*]pyrimidin-4-amine (27b). Synthesized using general procedure D. Yield: 10 mg, 18.2%. ^{1}H NMR (400 MHz, $CDCl_3$) δ 8.39 (s, 1H), 8.20 (d, J = 5.3 Hz, 1H), 7.33–7.30 (m, 2H), 7.23 (dd, J = 5.4, 1.5 Hz, 1H), 6.99–6.95 (m, 1H), 3.73–3.65 (m, 1H), 1.32–1.22 (m, 3H), 1.18–1.07 (m, 2H). ^{13}C NMR (400 MHz, $CDCl_3$) δ 173.81, 156.90, 148.57, 127.74, 125.49, 116.59, 107.56, 28.82, 6.45. LC/MS (ESI) *m*/*z*: $[M + H]^+$ calcd. for $C_{17}H_{13}ClN_6OS$, 384.84; found 385.1.

1-Cyclopropyl-3-((4-(3-chlorothiophen-2-yl)pyridin-2-yl)oxy)-1H-pyrazolo[3,4-*d*]pyrimidin-4-amine (28b). Synthesized using general procedure D. Yield: 19 mg, 34%. ^{1}H NMR (400 MHz, $CDCl_3$) δ 8.25 (d, J = 5.4 Hz, 1H), 8.21 (s, 1H), 7.67 (s, 1H), 7.55 (dd, J = 5.3, 1.5 Hz, 1H), 7.45 (d, J = 5.3 Hz, 1H), 7.08 (d, J = 5.3 Hz, 1H), 3.91–3.79 (m, 1H), 1.37–1.29 (m, 2H), 1.22–1.11 (m, 2H). ^{13}C NMR (400 MHz, $CDCl_3$) δ 161.68, 152.98, 151.83, 151.06, 148.08, 146.57, 144.86, 131.64, 130.39, 126.74, 124.72, 120.29, 111.13, 91.71, 29.87, 6.57. LC/MS (ESI) *m*/*z*: $[M + H]^+$ calcd. for $C_{17}H_{13}ClN_6OS$, 384.84; found 385.1.

1-Cyclopropyl-3-((4-(5-(trifluoromethyl)thiophen-2-yl)pyridin-2-yl)oxy)-1H-pyrazolo[3,4-*d*]pyrimidin-4-amine (29b). Synthesized using general procedure D. Yield: 15 mg, 24%. ^{1}H NMR (400 MHz, $(CD_3)_2SO$) δ 8.20 (s, 1H), 8.19 (s, 1H), 7.96–8.01 (m, 1H), 7.87 (dd, J = 0.78, 3.89 Hz, 1H), 7.60 (s, 1H), 7.57 (dd, J = 1.56, 5.45 Hz, 1H), 6.78 (br. s., 1H), 3.71 (td, J = 3.41, 7.20 Hz, 1H), 0.98–1.11 (m, 4H); ^{13}C NMR (400 MHz, $(CD_3)_2SO$) δ 168.8, 168.8, 163.4, 157.3, 156.8, 154.9, 148.5, 148.4, 144.5, 142.9, 131.8, 131.8, 130.0, 127.6, 116.8, 108.6, 92.4, 40.3, 40.1, 39.9, 39.7, 39.3, 39.1, 28.8, 6.2. LC/MS (ESI) *m*/*z*: $[M + H]^+$ calcd. for $C_{18}H_{13}F_3N_6OS$, 418.40; found 419.1.

3-((4-(1H-3-(Trifluoromethyl)pyrazol-5-yl)pyridin-2-yl)oxy)-1-cyclopropyl-1H-pyrazolo[3,4-*d*]pyrimidin-4-amine (30b). Synthesized using general procedure D. Yield: 20 mg, 34.5%. ^{1}H NMR (400 MHz, CD_3OD) δ 8.33 (s, 1H), 8.27 (d, J = 5.3 Hz, 1H), 7.71 (s, 1H), 7.63 (d, J = 5.3 Hz, 1H), 7.28 (s, 1H), 3.82 (tt, J = 7.4, 3.7 Hz, 1H), 1.32–1.19 (m, 2H), 1.16–1.05 (m, 2H). ^{13}C NMR (600 MHz, CD_3OD) δ 164.2, 163.1, 162.9, 162.6, 155.4, 154.1, 152.0, 149.6, 141.9, 123.5, 121.7, 119.0, 118.2, 117.0, 109.8, 104.3, 92.9, 30.3, 6.9. LC/MS (ESI) *m*/*z*: $[M + H]^+$ calcd. for $C_{17}H_{13}F_3N_8O$, 402.12; found 403.20.

3-((4-(*N*-Methyl-3-(trifluoromethyl)pyrazol-5-yl)pyridin-2-yl)oxy)-1-cyclopropyl-1H-pyrazolo[3,4-*d*]pyrimidin-4-amine (31b). Synthesized using general procedure D. Yield: 48 mg, 80%. ^{1}H NMR (400 MHz, CD_3OD) δ 8.38–8.29 (m, 2H), 7.60 (s, 1H), 7.47 (dd, J = 5.2, 1.4 Hz, 1H), 6.96 (s, 1H), 4.08 (s, 3H), 3.83 (tt, J = 7.3, 3.8 Hz, 1H), 1.25–1.19 (m, 2H), 1.15–1.09 (m, 2H). ^{13}C NMR (400 MHz, CD_3OD) δ 163.5, 154.4, 153.7, 152.2, 150.5, 150.4, 149.4, 143.3, 142.4, 123.9, 121.4, 113.2, 106.6, 106.6, 106.6, 106.6, 92.6, 39.2, 30.4, 6.9. LC/MS (ESI) m/z: $[M + H]^+$ calcd. for $C_{18}H_{15}F_3N_8O$, 416.37; found 417.20.

1-Cyclopropyl-3-((4-(3,5-dimethyl-isooxazo-4-yl)pyridin-2-yl)oxy)-1H-pyrazolo[3,4-*d*]pyrimidin-4-amine (32b). Synthesized using general procedure D. Yield: 86.7 mg, 82.8%. ^{1}H NMR (400 MHz, $CDCl_3$) δ 8.28 (d, J = 5.2 Hz, 1H), 8.22 (s, 1H), 8.06 (d, J = 5.4 Hz, 0H), 7.51 (s, 0H), 7.39 (dd, J = 5.5, 1.5 Hz, 0H), 7.28–7.23 (m, 2H), 7.14 (dd, J = 5.2, 1.4 Hz, 1H), 3.90–3.77 (m, 1H), 1.37–1.26 (m, 2H), 1.21–1.12 (m, 2H). ^{13}C NMR (400 MHz, $CDCl_3$) δ 225.08, 174.31, 167.19, 161.62, 157.90, 152.89, 151.81, 150.96, 148.21, 146.53, 144.08, 125.05, 121.19, 116.44, 113.74, 112.18, 91.67, 29.88, 12.06, 11.05, 6.61, 6.59. LC/MS (ESI) m/z: $[M + H]^+$ calcd. for $C_{18}H_{17}N_7O_2$, 363.38; found 364.2.

1-Cyclopropyl-3-((4-(3,5-difluoro-4-methylphenyl)pyridine-2-yl)oxy)-1H-pyrazolo[3,4-*d*]pyrimidin-4-amine (1c). Synthesized using general procedure D. Yield: 10.0 mg, 17.8%. ^{1}H NMR (400 MHz, $(CD_3)_2SO$) δ 8.19 (br. s., 2H), 7.50–7.80 (m, 5H), 6.71 (br. s., 1H), 3.70 (br. s., 1H), 2.20 (br. s., 3H), 1.06 (br. s., 2H), 1.00 (br. s., 2H). ^{13}C NMR (400 MHz, $(CD_3)_2SO$) δ 169.1, 169.1, 163.7, 157.5, 157.0, 155.1, 151.9, 148.9, 148.3, 136.9, 117.9, 110.4, 110.1, 109.9, 92.6, 40.6, 40.4, 40.2, 40.0, 39.7, 39.5, 39.3, 29.0, 7.4, 6.4. LC/MS (ESI) m/z: $[M + H]^+$ calcd. for $C_{20}H_{16}F_2N_6O$, 394.39; found 395.2.

1-Cyclopropyl-3-((4-(3,5-difluoro-4-methoxyphenyl)pyridin-2-yl)oxy)-1H-pyrazolo[3,4-*d*]pyrimidin-4-amine (2c). Synthesized using general procedure D. Yield: 37.5 mg, 31.5%. ^{1}H NMR (400 MHz, $CDCl_3$) δ 8.38 (s, 1H), 8.28 (d, J = 5.3 Hz, 1H), 7.36 (s, 1H), 7.27 (d, J = 1.5 Hz, 1H), 7.26 (s, 2H), 7.23–7.17 (m, 2H), 4.08 (s, 3H), 3.80–3.52 (m, 1H), 1.35—1.20 (m, 2H), 1.22–0.96 (m, 2H). ^{13}C NMR (400 MHz, $CDCl_3$) δ 174.35, 162.84, 157.11, 156.92, 155.01, 150.37, 148.98, 148.60, 118.20, 111.15, 110.92, 109.52, 92.75, 61.88, 53.44, 28.82. LC/MS (ESI) m/z: $[M + H]^+$ calcd. for $C_{20}H_{16}F_2N_6O_2$, 410.38; found 411.505.

1-Cyclopropyl-3-((4-(3,5-difluoro-4-methoxyphenyl)pyridin-2-yl)oxy)-1H-pyrazolo[3,4-*d*]pyrimidin-4-amine (3c). Synthesized using general procedure D. Yield: 7.7 mg, 8.5%. ^{1}H NMR (400 MHz, $CDCl_3$) δ 11.40 (s, 1H), 8.24 (s, 1H), 8.21 (d, J = 5.4 Hz, 1H), 7.47–7.41 (m, 2H), 7.35 (dd, J = 5.5, 1.6 Hz, 1H), 7.26 (s, 3H), 7.20–7.11 (m, 2H), 3.91–3.78 (m, 2H), 3.71–3.58 (m, 5H), 1.96–1.88 (m, 5H), 1.38–1.31 (m, 3H), 1.23–1.12 (m, 3H). ^{13}C NMR (400 MHz, $CDCl_3$) δ 164.44, 162.20, 154.82, 153.23, 152.03, 151.40, 151.13, 148.06, 147.23, 124.04, 118.27, 110.82, 110.68, 108.85, 91.78, 51.28, 29.80, 25.75, 6.55. LC/MS (ESI) m/z: $[M + H]^+$ calcd. for $C_{23}H_{21}F_2N_7O$, 449.47; found 450.20.

1-Cyclopropyl-3-((4-(3,5-difluoro-4-thioansiole)pyridin-2-yl)oxy)-1H-pyrazolo[3,4-*d*]pyrimidin-4-amine (4c). Synthesized using general procedure D. Yield: 7.7 mg, 6.3%. ^{1}H NMR (400 MHz, CD_3OD) δ 8.33 (s, 1H), 8.28 (d, J = 5.3 Hz, 1H), 7.52 (s, 1H), 7.40–7.36 (m, 1H), 7.07 (s, 1H), 7.05 (s, 1H), 3.86–3.79 (m, 1H), 2.56 (s, 3H), 1.27–1.19 (m, 2H), 1.16–1.07 (m, 2H). LC/MS (ESI) m/z: $[M + H]^+$ calcd. for $C_{20}H_{16}F_2N_6OS$, 426.45; found 427.2.

1-Cyclopropyl-3-((4-(3,5-difluoro-4-analine)pyridin-2-yl)oxy)-1H-pyrazolo[3,4-*d*]pyrimidin-4-amine (5c). Synthesized using general procedure D. Yield: 7.7 mg, 6.8%. ^{1}H NMR (400 MHz, CD_3OD) δ 8.31 (s, 1H), 8.16 (d, J = 5.4 Hz, 1H), 7.60 (s, 1H), 7.49 (dd, J = 5.4, 1.6 Hz, 1H), 7.39 (dd, J = 7.7, 2.4 Hz, 2H), 3.85–3.76 (m, 1H), 1.26–1.19 (m, 2H), 1.16–1.09 (m, 2H). LC/MS (ESI) m/z: $[M + H]^+$ calcd. for $C_{19}H_{15}F_2N_7O$, 395.37; found 396.20.

1-Cyclopropyl-3-((4-(3,5-difluoro-4-phenol)pyridin-2-yl)oxy)-1H-pyrazolo[3,4-*d*]pyrimidin-4-amine (6c). Synthesized using general procedure D. Yield: 3.1 mg, 2.6%. ^{1}H NMR (400 MHz, $(CD_3)_2SO$) δ 10.74 (s, 1H), 8.21 (s, 1H), 8.12 (d, J = 5.3 Hz, 1H), 7.67 (dd, J = 8.2, 1.7 Hz, 2H), 7.57–7.49 (m, 2H), 3.78–3.62 (m, 1H), 1.08–1.05 (m, 2H), 1.03–0.97 (m, 2H). LC/MS (ESI) m/z: $[M + H]^+$ calcd. for $C_{19}H_{14}F_2N_6O_2$, 396.36; found 397.52.

1-Cyclopropyl-3-((4-(3,5-difluoro-4-cyanophenyl)pyridin-2-yl)oxy)-1H-pyrazolo[3,4-*d*]pyrimidin-4-amine (7c). Synthesized using general procedure D. Yield: 15 mg, 10.7%. ^{1}H NMR (400 MHz, $(CD_3)_2SO$) δ 8.46 (br. s., 1H), 8.29 (d, J = 4.67 Hz, 1H), 8.06 (d, J = 9.34 Hz, 2H), 7.76 (s, 1H), 7.70 (d, J = 5.06 Hz, 1H), 3.78 (br. s., 1H), 0.93–1.17 (m, 4H). ^{13}C NMR (400 MHz, $(CD_3)_2SO$) δ 169.0, 164.5, 163.5, 162.0, 161.9, 155.1, 153.9, 149.8, 148.7, 147.4, 145.5, 145.3, 118.5, 112.0, 111.8, 111.7, 110.8, 92.3, 92.2, 29.3, 6.5, 6.5. LC/MS (ESI) m/z: $[M + H]^+$ calcd. for $C_{20}H_{13}F_2N_7O$, 405.369; found 406.1.1.

1-Methylsulfonyl-3-((4-(3,5-difluoro-4-(trifluoromethyl)phenyl)pyridin-2-yl)oxy)-1H-pyrazolo[3,4-*d*]pyrimidin-4-amine (8c). Synthesized using general procedure B. Yield: 19.8 mg, 24.8%. ^{1}H NMR (400 MHz, $(CD_3)_2SO$) δ 8.39 (s, 1H), 8.35 (d, J = 5.3 Hz, 1H), 8.02 (d, J = 11.7 Hz, 3H), 7.86 (s, 1H), 7.78 (d, J = 1.5 Hz, 1H), 2.52 (s, 3H). ^{13}C NMR (400 MHz, $(CD_3)_2SO$) δ 220.05, 169.44, 162.72, 157.73, 153.65, 148.89, 111.46, 94.02, 42.04. LC/MS (ESI) m/z: $[M + H]^+$ calcd. for $C_{18}H_{11}F_5N_6O_3S$, 486.38; found 487.1.

1-(R)-(Pideridin-3-yl)-3-((4-(3,5-difluoro-4-(trifluoromethyl)phenyl)pyridin-2-yl)oxy)-1H-pyrazolo[3,4-*d*]pyrimidin-4-amine (9c). Synthesized using general procedure C. Yield: 20.9 mg, 59.7%. ^{1}H NMR (400 MHz, CD_3OD) δ 8.38 (s, 1H), 8.31 (d, J = 5.3 Hz, 1H), 7.74–7.71 (m, 2H), 7.70 (s, 1H), 7.64 (dd, J = 5.4, 1.5 Hz, 1H), 5.21–5.13 (m, 1H), 3.63 (d, J = 4.4 Hz, 1H), 3.56 (dd, J = 12.7, 9.3 Hz, 1H), 3.42–3.35 (m, 1H), 3.14 (ddd, J = 13.1, 10.7, 3.5 Hz, 1H), 2.23 (m, 2H), 2.17–2.06 (m, 1H), 2.01–1.87 (m, 1H). ^{13}C NMR (400 MHz, CD_3OD) δ 164.1, 162.9, 162.5, 160.3, 154.8, 153.1, 153.1, 151.3, 150.4, 149.6, 145.6, 145.5, 145.4, 120.1, 113.1, 113.0, 112.8, 112.8, 111.9, 92.9, 52.0, 47.0, 44.7, 28.9, 21.7. LC/MS (ESI) m/z: $[M + H]^+$ calcd. for $C_{22}H_{18}F_5N_7O$, 491.43; found 492.20.

1-(Morpholin-2-yl)-3-((4-(3,5-difluoro-4-(trifluoromethyl)phenyl)pyridin-2-yl)oxy)-1H-pyrazolo[3,4-*d*]pyrimidin-4-amine (10c). Synthesized using general procedure C. Yield: 4.9 mg, 5.0%. ^{1}H NMR (400 MHz, $(CD_3)_2SO$) δ 9.24 (s, 2H), 8.27 (d, J = 4.5 Hz, 2H), 8.01 (d, J = 11.6 Hz, 2H), 7.77 (s, 1H), 7.71 (d, J = 5.3 Hz, 1H), 6.18–6.08 (m, 1H), 4.05 (d, J = 12.7 Hz, 2H), 3.94 (t, J = 11.7 Hz, 2H), 3.78–3.66 (m, 1H), 3.61 (d, J = 12.3 Hz, 1H), 3.32—3.24 (m, 1H), 3.21–3.09 (m, 1H). ^{13}C NMR (600 MHz, $(CD_3)_2SO$) δ 163.40, 160.79, 159.09, 157.75, 157.56, 155.47, 151.14, 148.69, 147.53, 144.35, 118.60, 112.67, 112.51, 110.84, 92.90, 76.92, 62.78, 44.10, 42.08. LC/MS (ESI) m/z: $[M + H]^+$ calcd. for $C_{21}H_{16}F_5N_7O_2$, 493.4; found 494.20.

1-(4-Pyranyl)-3-((4-(3,5-difluoro-4-(trifluoromethyl)phenyl)pyridin-2-yl)oxy)-1H-pyrazolo[3,4-*d*]pyrimidin-4-amine (11c). Synthesized using general procedure C. Yield: 27.8 mg, 51.8%. ^{1}H NMR (400 MHz, $CDCl_3$) δ 11.55 (s, 1H), 8.36 (d, J = 5.3 Hz, 1H), 8.22 (s, 1H), 7.51 (s, 1H), 7.41 (dd, J = 5.3, 1.5 Hz, 1H), 7.31 (d, J = 10.1 Hz, 2H), 7.11 (s, 1H), 5.01–4.88 (m, 1H), 4.22–4.01 (m, 2H), 3.68–3.49 (m, 2H), 2.41–2.22 (m, 2H), 2.01–1.90 (m, 2H). ^{13}C NMR (400 MHz, $CDCl_3$) δ 224.42, 174.03, 152.93, 151.39, 150.09, 148.86, 146.38, 119.42, 111.64, 111.37, 110.81, 91.29, 66.74, 54.35, 31.88. LC/MS (ESI) m/z: $[M + H]^+$ calcd. for $C_{22}H_{17}F_5N_6O_2$, 492.41; found 493.20.

1-Cyclopropyl-3-((4-(4-(trifluoromethyl)pyrid-2-yl)pyridin-2-yl)oxy)-1H-pyrazolo[3,4-*d*]pyrimidin-4-amine (12c). Synthesized using general procedure D. Yield: 4.6 mg, 11.1%. ^{1}H NMR (400 MHz, $CDCl_3$) δ 8.97 (d, J = 5.1 Hz, 1H), 8.38 (d, J = 5.3 Hz, 1H), 8.22 (s, 1H), 8.03 (s, 1H), 7.97 (s, 1H), 7.87 (dd, J = 5.3, 1.4 Hz, 1H), 7.64 (d, J = 4.9 Hz, 1H), 3.88–3.78 (m, 1H), 1.36–1.28 (m, 2H), 1.21–1.14 (m, 2H). LC/MS (ESI) m/z: $[M + H]^+$ calcd. for $C_{19}H_{14}F_3N_7O$, 413.36; found 414.59.

1-Cyclopropyl-3-((4-(4-(trifluoromethyl)pyrid-3-yl)pyridin-2-yl)oxy)-1H-pyrazolo[3,4-*d*]pyrimidin-4-amine (13c). Synthesized using general procedure D. Yield: 28.9 mg, 35.2%. ^{1}H NMR (400 MHz, $(CD_3)_2SO$) δ 9.25 (s, 1H), 8.58–8.51 (m, 1H), 8.27 (d, J = 5.3 Hz, 1H), 8.19 (s, 1H), 8.09 (d, J = 8.2 Hz, 1H), 7.71 (s, 1H), 7.69–7.64 (m, 1H), 3.74–3.64 (m, 1H), 1.09–1.03 (m, 2H), 1.02–0.96 (m, 2H). LC/MS (ESI) m/z: $[M + H]^+$ calcd. for $C_{19}H_{14}F_3N_7O$, 413.36; found 414.59.

1-Cyclopropyl-3-((4-(4-fluoro-pyrid-3-yl)pyridin-2-yl)oxy)-1H-pyrazolo[3,4-*d*]pyrimidin-4-amine (14c). Synthesized using general procedure D. Yield: 49.0 mg, 67.5%. ^{1}H NMR (400 MHz, $(CD_3)_2SO$) δ 8.77 (s, 1H), 8.49 (td, J = 8.2, 2.7 Hz, 1H), 8.30 (s, 1H), 8.22 (d, J = 5.3 Hz, 1H), 7.65 (s, 1H), 7.62 (dd, J = 5.3, 1.6 Hz, 1H), 7.38 (dd, J = 8.6, 2.7 Hz, 1H), 3.80–3.71 (m, 1H), 1.12–1.06 (m, 2H), 1.05–0.98 (m, 2H). ^{13}C NMR (400 MHz, $(CD_3)_2SO$) δ 220.06, 163.45, 162.89, 148.43, 147.55, 146.73, 131.32, 118.34, 110.12, 92.42, 29.30, 6.50. LC/MS (ESI) m/z: $[M + H]^+$ calcd. for $C_{18}H_{14}FN_7O$, 363.36; found 364.71.

1-Cyclopropyl-3-((4-(4-(trifluoromethyl)-5-fluoropyrid-3-yl)pyridin-2-yl)oxy)-1H-pyrazolo[3,4-*d*]pyrimidin-4-amine (15c). Synthesized using general procedure D. Yield: 41.5 mg, 47.7%. ^{1}H NMR (400 MHz, CD_3OD) δ 8.96 (s, 1H), 8.37–8.32 (m, 3H), 7.78 (s, 1H), 7.68 (dd, J = 5.3, 1.6 Hz, 1H), 3.93–3.79 (m, 1H), 1.28–1.21 (m,

2H), 1.16–1.09 (m, 2H). ^{13}C NMR (600 MHz, CD_3OD) δ 164.72, 164.48, 162.21, 158.08, 156.27, 153.21, 152.12, 150.73, 149.20, 147.45, 147.31, 143.07, 138.31, 136.97, 136.72, 124.00, 123.87, 119.53, 110.98, 91.73, 29.91, 6.61. LC/MS (ESI) *m*/*z*: $[M + H]^+$ calcd. for $C_{19}H_{13}F_4N_7O$, 431.35; found 432.1.

1-Cyclopropyl-3-((4-(4-(trifluoromethyl)pyrimid-3,5-yl)pyridin-2-yl)oxy)-1H-pyrazolo[3,4-*d*]pyrimidin-4-amine (16c). Synthesized using general procedure D. Yield: 29.8 mg, 25.0%. ^{1}H NMR (400 MHz, $(CD_3)_2SO$) δ 9.56 (s, 2H), 8.32 (d, J = 5.3 Hz, 1H), 8.28 (s, 1H), 7.83 (s, 1H), 7.76 (dd, J = 5.4, 1.5 Hz, 1H), 3.79–3.71 (m, 1H), 1.11–1.05 (m, 2H), 1.05–0.99 (m, 2H). ^{13}C NMR (400 MHz, $(CD_3)_2SO$) δ163.43, 157.42, 154.76, 153.76, 153.12, 149.76, 148.81, 144.53, 132.91, 118.84, 111.03, 92.42, 29.43, 6.53. LC/MS (ESI) *m*/*z*: $[M + H]^+$ calcd. for $C_{18}H_{13}F_3N_8O$, 414.35; found 415.20.

1-Cyclopropyl-3-((4-(4-methoxy-pyrimid-3,5-yl)pyridin-2-yl)oxy)-1H-pyrazolo[3,4-*d*]pyrimidin-4-amine (17c). Synthesized using general procedure D. Yield: 69.7 mg, 64.3%. ^{1}H NMR (400 MHz, CD_3OD) δ 9.13 (s, 2H), 8.36 (s, 1H), 8.21 (dd, J = 5.3, 0.7 Hz, 1H), 7.67 (s, 1H), 7.64 (dd, J = 5.3, 1.5 Hz, 1H), 3.83–3.74 (m, 1H), 1.12–1.06 (m, 2H), 1.06–1.00 (m, 2H). ^{13}C NMR (600 MHz, CD_3OD) δ 219.73, 169.46, 166.04, 163.39, 158.52, 149.99, 148.43, 145.84, 124.51, 117.67, 109.28, 55.43, 48.43, 48.22, 48.01, 29.40, 6.49. LC/MS (ESI) *m*/*z*: $[M + H]^+$ calcd. for $C_{18}H_{16}N_8O_2$, 376.38; found 377.20.

1-Cyclopropyl-3-((4-(4-(*N*,*N*-dimethylamine)-pyrimid-3,5-yl)pyridin-2-yl)oxy)-1H-pyrazolo[3,4-*d*]pyrimidin-4-amine (18c). Synthesized using general procedure D. Yield: 1.7 mg, 14.2%. ^{1}H NMR (400 MHz, $CDCl_3$) δ 8.62 (s, 2H), 8.36 (s, 1H), 8.23 (d, J = 5.3 Hz, 1H), 7.34 (s, 1H), 7.27–7.23 (m, 1H), 3.72–3.60 (m, 1H), 3.26 (s, 6H), 1.31–1.21 (m, 2H), 1.17–1.05 (m, 2H). ^{13}C NMR (600 MHz, $CDCl_3$) δ 162.90, 162.25, 157.23, 156.85, 155.93, 155.00, 149.11, 148.51, 147.97, 117.91, 116.60, 107.45, 92.81, 77.25, 77.03, 76.82, 37.26, 28.83, 6.45. LC/MS (ESI) *m*/*z*: $[M + H]^+$ calcd. for $C_{19}H_{19}N_9O$, 389.42; found 390.20.

1-Cyclopropyl-3-((4-(4-cyclopropyl-pyrimid-3,5-yl)pyridin-2-yl)oxy)-1H-pyrazolo[3,4-*d*]pyrimidin-4-amine (19c). Synthesized using general procedure D. Yield: 30.7 mg, 40.0%. ^{1}H NMR (400 MHz, $CDCl_3$) δ 8.80 (s, 2H), 8.33–8.29 (m, 2H), 7.42 (s, 1H), 7.31–7.27 (m, 1H), 3.69–3.58 (m, 1H), 2.36–2.26 (m, 1H), 1.26–1.05 (m, 4H). ^{13}C NMR (600 MHz, $CDCl_3$) δ 173.41, 162.81, 157.32, 156.82, 154.84, 148.94, 146.85, 127.33, 117.85, 109.29, 92.61, 77.27, 77.06, 76.84, 28.84, 18.35, 11.64, 6.46. LC/MS (ESI) *m*/*z*: $[M + H]^+$ calcd. for $C_{20}H_{18}N_8O$, 386.42; found 387.20.

1-Cyclopropyl-3-((4-(4-methyl-pyrimid-3,5-yl)pyridin-2-yl)oxy)-1H-pyrazolo[3,4-*d*]pyrimidin-4-amine (20c). Synthesized using general procedure D. Yield: 6.4 mg, 10.4%. ^{1}H NMR (400 MHz, $CDCl_3$) δ 8.92 (s, 2H), 8.39 (s, 1H), 8.38–8.34 (m, 1H), 7.50 (s, 1H), 7.35 (dd, J = 5.2, 1.5 Hz, 1H), 3.73–3.62 (m, 1H), 2.83 (s, 3H), 1.30–1.20 (m, 2H), 1.19–1.05 (m, 2H). ^{13}C NMR (600 MHz, $CDCl_3$) δ 169.28, 162.82, 157.15, 156.97, 155.04, 149.03, 146.63, 127.91, 118.11, 109.64, 28.87, 25.93, 6.47. LC/MS (ESI) *m*/*z*: $[M + H]^+$ calcd. for $C_{18}H_{16}N_8O$, 360.38; found 361.2.

1-((S)-Pyran-3-yl)-3-((4-(4-(trifluoromethyl)-pyrimid-3,5-yl)pyridin-2-yl)oxy)-1H-pyrazolo[3,4-*d*]pyrimidin-4-amine (21c). Synthesized using general procedure C. Yield: 13.6 mg, 24.7%. ^{1}H NMR (400 MHz, $CDCl_3$) δ 9.19 (s, 2H), 8.43 (d, J = 5.2 Hz, 1H), 8.21 (s, 1H), 7.59 (s, 1H), 7.48 (dd, J = 5.2, 1.5 Hz, 1H), 4.96–4.85 (m, 1H), 4.10–4.03 (m, 1H), 4.01–3.93 (m, 1H), 3.79 (t, J = 10.5 Hz, 1H), 3.56–3.41 (m, 1H), 2.35–2.16 (m, 2H), 1.92–1.82 (m, 2H). ^{13}C NMR (600 MHz, $CDCl_3$) δ 162.18, 156.09, 152.96, 151.22, 150.75, 149.35, 146.57, 145.58, 132.69, 119.35, 110.81, 91.42, 69.80, 67.75, 53.67, 28.80, 25.02. LC/MS (ESI) *m*/*z*: $[M + H]^+$ calcd. for $C_{20}H_{17}F_3N_8O_2$, 458.41; found 459.20.

1-Cyclopropylmethyl-3-((4-(4-(trifluoromethyl)-pyrimid-3,5-yl)pyridin-2-yl)oxy)-1H-pyrazolo[3,4-*d*]pyrimidin-4-amine (22c). Synthesized using general procedure C. Yield: 20.8 mg, 34.4%. ^{1}H NMR (400 MHz, $CDCl_3$) δ 9.18 (s, 2H), 8.45 (d, J = 5.2 Hz, 1H), 8.19 (s, 1H), 7.60 (s, 1H), 7.48 (dd, J = 5.2, 1.5 Hz, 1H), 4.21 (d, J = 7.2 Hz, 2H), 1.41–1.27 (m, 1H), 0.64–0.57 (m, 2H), 0.49–0.42 (m, 2H). ^{13}C NMR (600 MHz, $CDCl_3$) δ 162.26, 156.10, 153.14, 151.19, 150.66, 149.45, 146.90, 145.49, 132.73, 119.32, 110.91, 91.13, 52.63, 11.03, 4.12. LC/MS (ESI) *m*/*z*: $[M + H]^+$ calcd. for $C_{19}H_{15}F_3N_8O$, 428.38; found 429.20.

1-(4,4-Difluorocyclohexyl)-3-((4-(4-(trifluoromethyl)-pyrimid-3,5-yl)pyridin-2-yl)oxy)-1H-pyrazolo[3,4-*d*]pyrimidin-4-amine (23c). Synthesized using general procedure C. Yield: 33.3 mg, 46%. ^{1}H NMR (400 MHz, $CDCl_3$) δ 11.66 (s, 1H), 9.18 (s, 2H), 8.43 (d, J = 5.2 Hz, 1H), 8.21 (s, 1H), 7.53 (s, 1H), 7.48 (dd, J = 5.2, 1.5 Hz, 1H), 6.92 (s, 1H), 2.41–2.23 (m, 4H), 2.13–1.88 (m, 4H). ^{13}C NMR (600 MHz, $CDCl_3$) δ 162.25, 156.10, 153.08, 151.22, 150.37, 149.39, 146.60, 145.66, 132.65, 119.45, 110.95, 91.52, 54.41, 32.50, 32.25, 32.00, 27.84, 27.75. LC/MS (ESI) *m*/*z*: $[M + H]^+$ calcd. for $C_{21}H_{17}F_5N_8O$, 492.41; found 493.20.

Supplementary Material

Refer to Web version on PubMed Central for supplementary material.

ACKNOWLEDGMENTS

Jennifer Barks, Washington University in St. Louis, provided general cell culture support. Dr. Zhou Huang (Washington University in St Louis) and Dr. Rick Stegman (WUSM Structural Biology Core at Washington University in St. Louis) assisted with crystallography studies. This work was supported by a grant from NIH (AI164473). Beamlines of the Advanced Light Source, a DOE Office of Science User Facility under Contract DE-AC02–05CH11231, are supported in part by the ALS-ENABLE Program funded by the National Institutes of Health, National Institute of General Medical Sciences, Grant P30 GM124169.

ABBREVIATIONS USED

ADME	absorption, distribution, metabolism, excretion
AUC	area under the curve
BID	dosing twice per day
CD_3	trideuteromethyl

CF_3	trifluoromethyl
dpi	days post infection
% F	oral bioavailability
HFF	human foreskin fibroblast
HLM	human liver microsomes
IV	intravenous
LLE	ligand lipophilicity efficiency
MDCK-MDR1	Madin-Darby Canine Kidney (MDCK) cells expressing MDR1 gene
MLM	mouse liver microsome
PK	Pharmacokinetic
PO	oral gavage
PP	pyrazolopyrimidine
PPB	Plasma protein binding
QD	dosing once per day
SAR	Structure activity relationship
TgCDPK1	*Toxoplasma gondii* calcium dependent protein kinase 1
T. gondii	Toxoplasma gondii
V_d	volume of distribution

REFERENCES

(1). Molan A; Nosaka K; Hunter M; Wang W Global status of Toxoplasma gondii infection: systematic review and prevalence snapshots. Trop. Biomed. 2019, 36 (4), 898–925. [PubMed: 33597463]

(2). McLeod R; Van Tubbergen C; Montoya JG; Petersen E Human Toxoplasma infection. In Toxoplasma gondii: A Model Apicomplexan - Perspectives and Methods; Weiss LM; Kim s, Eds.; Elsevier, 2014; pp 99–159.

(3). Montoya JG; Liesenfeld O Toxoplasmosis. Lancet 2004, 363, 1965–1976. [PubMed: 15194258]

(4). Khan A; Jordan C; Muccioli C; Vallochi AL; Rizzo LV; Belfort R Jr.; Vitor RW; Silveira C; Sibley LD Genetic divergence of Toxoplasma gondii strains associated with ocular toxoplasmosis Brazil. Emerging Infect. Dis. 2006, 12, 942–949.

(5). Melamed J Contributions to the history of ocular toxoplasmosis in Southern Brazil. Mem. Inst. Oswaldo Cruz 2009, 104, 358–363. [PubMed: 19430664]

(6). Pfaff AW; de-la-Torre A; Rochet E; Brunet J; Sabou M; Sauer A; Bourcier T; Gomez-Marin JE; Candolfi E New clinical and experimental insights into Old World and neotropical ocular toxoplasmosis. Int. J. Parasitol. 2014, 44, 99. [PubMed: 24200675]

(7). Israelski DM; Remington JS Toxoplasmosis in the non-AIDS immunocompromised host. Curr. Clin. Top. Infect. Dis. 1993, 13, 322–356. [PubMed: 8397917]

(8). Luft BJ; Remington JS Toxoplasmic encephalitis in AIDS. Clin. Infect. Dis. 1992, 15, 211–222. [PubMed: 1520757]

(9). Mariuz P; Bosler EM; Luft BJ Toxoplasmosis in individuals with AIDS. Infect. Dis. Clin. North. Am. 1994, 8, 365–381. [PubMed: 8089465]

(10). Montoya JG; Remington JS Management of *Toxoplasma gondii* infection during preganacy. Clin. Infect. Dis. 2008, 47, 554–566. [PubMed: 18624630]

(11). Dubey JP Toxoplasmosis of Animals and Humans; CRC Press, 2010.

(12). Blader IJ; Coleman BI; Chen CT; Gubbels MJ Lytic Cycle of *Toxoplasma gondii*: 15 Years Later. Annu. Rev. Microbiol. 2015, 69, 463–485. [PubMed: 26332089]

(13). Coombes JL; Hunter CA Immunity to *Toxoplasma gondii*–into the 21st century. Parasite Immunol. 2015, 37 (3), 105–107. [PubMed: 25682704]

(14). Dupont CD; Christian DA; Hunter CA Immune response and immunopathology during toxoplasmosis. Semin. Immunopathol. 2012, 34 (6), 793–813. [PubMed: 22955326]

(15). Knoll LJ; Tomita T; Weiss LM Bradyzoite development. In Toxoplasma gondii: The model apicomplexan: perspectives and methods, 2nd ed.; Weiss LM; Kim K, Eds.; Academic Press, 2014; pp 521–551.

(16). Dunay IR; Gajurel K; Dhakal R; Liesenfeld O; Montoya JG Treatment of Toxoplasmosis: Historical Perspective, Animal Models, and Current Clinical Practice. Clin Microbiol Rev. 2018, 31 (4), No. e00057–17, DOI: 10.1128/CMR.00057-17. [PubMed: 30209035]

(17). Rosenthal PJ Toxoplasmosis. In Current Medical Diagnosis and Treatment; Papadakis MA; McPhee SJ; Rabow MW; McQuaid KR; Gandhi M, Eds.; McGraw Hill, 2024; Vol. 6, p 37.

(18). Liu S; Cai M; Liu Z; Gao W; Li J; Li Y; Abudouxukuer X; Zhang J Comprehensive Insights into the Development of Antitoxoplasmosis Drugs: Current Advances, Obstacles, and Future Perspectives. J. Med. Chem. 2024, 67 (23), 20740–20764. [PubMed: 39589152]

(19). Shammaa AM; Powell TG; Benmerzouga I Adverse outcomes associated with the treatment of Toxoplasma infections. Sci. Rep. 2021, 11 (1), No. 1035. [PubMed: 33441899]

(20). Carruthers VB; Tomley FM Microneme proteins in apicomplexans. Subcell. Biochem. 2008, 47, 33–45. [PubMed: 18512339]

(21). Lourido S; Shuman J; Zhang C; Shokat KM; Hui R; Sibley LD Calcium-dependent protein kinase 1 is an essential regulator of exocytosis in Toxoplasma. Nature 2010, 465, 359–362. [PubMed: 20485436]

(22). Billker O; Lourido S; Sibley LD Calcium-dependent signaling and kinases in apicomplexan parasites. Cell Host Microbe 2009, 5, 612–622. [PubMed: 19527888]

(23). Ojo KK; Larson ET; Keyloun KR; Castaneda LJ; DeRoucher AE; KInampudi KK; Kim JE; Arakaki TL; Murphy RC; Zhang L; et al. *Toxoplasma gondii* calcium-dependent protein kinase 1 is a target for selective kinase inhibitors. Nat. Struct. Mol. Biol. 2010, 17, 602–607. [PubMed: 20436472]

(24). Wernimont AK; Artz JD; Finerty P; Lin Y; Amani M; Allali-Hassani A; senisterra G; Vedadi M; Tempel W; Mackenzie F; et al. Structures of apicomplexan calcium-dependent protein kinases reveal mechanism of activation by calcium. Nat. Struct. Mol. Biol. 2010, 17, 596–601. [PubMed: 20436473]

(25). Hui R; El Bakkouri M; Sibley LD Designing selective inhibitors for calcium-dependent protein kinases in apicomplexans. Trends Pharmacol. Sci. 2015, 36 (7), 452–460. [PubMed: 26002073]

(26). Manning G; Whyte DB; Martinez R; Hunter T; Sudarsanam S The protein kinase complement of the human genome. Science 2002, 298 (5600), 1912–1934. [PubMed: 12471243]

(27). Janetka JW; Hopper AT; Yang Z; Barks J; Dhason MS; Wang Q; Sibley LD Optimizing Pyrazolopyrimidine Inhibitors of Calcium Dependent Protein Kinase 1 for Treatment of Acute and Chronic Toxoplasmosis. J. Med. Chem. 2020, 63 (11), 6144–6163. [PubMed: 32420739]

(28). Lourido S; Tang K; Sibley LD Distinct signalling pathways control Toxoplasma egress and host-cell invasion. EMBO J. 2012, 31 (24), 4524–4534. [PubMed: 23149386]

(29). Lourido S; Zhang C; Lopez MS; Tang K; Barks J; Wang Q; Wildman SA; Shokat KM; Sibley LD Optimizing small molecule inhibitors of calcium-dependent protein kinase 1 to prevent infection by *Toxoplasma gondii*. J. Med. Chem. 2013, 56 (7), 3068–3077. From NLM [PubMed: 23470217]

(30). Rutaganira FU; Barks J; Dhason MS; Wang Q; Lopez MS; Long S; Radke JB; Jones NG; Maddirala AR; Janetka JW; et al. Inhibition of Calcium Dependent Protein Kinase 1 (CDPK1) by Pyrazolopyrimidine Analogs Decreases Establishment and Reoccurrence of Central Nervous System Disease by *Toxoplasma gondii*. J. Med. Chem. 2017, 60, 9976. [PubMed: 28933846]

(31). Larson ET; Ojo KK; Murphy RC; Johnson SM; Zhang Z; Kim JE; Leibly DJ; Fox AM; Reid MC; Dale EJ; et al. Multiple determinants for selective inhibition of apicomplexan calcium-dependent protein kinase CDPK1. J. Med. Chem. 2012, 55 (6), 2803–2810. [PubMed: 22369268]

(32). Vidadala RSR; Rivas KL; Ojo KK; Hulverson MA; Zambriski JA; Bruzual I; Schultz TL; Huang W; Zhang Z; Scheele S; et al. Development of an Orally Available and Central Nervous System (CNS) Penetrant Toxoplasma gondii Calcium-Dependent Protein Kinase 1 (TgCDPK1) Inhibitor with Minimal Human Ether-a-go-go-Related Gene (hERG) Activity for the Treatment of Toxoplasmosis. J. Med. Chem. 2016, 59 (13), 6531–6546. [PubMed: 27309760]

(33). de Sousa MCF; Imhof D; Hänggeli KPA; Choi R; Hulverson MA; Arnold SLM; Van Voorhis WC; Fan E; Roberto S-S; Ortega-Mora LM; et al. Efficacy of the bumped kinase inhibitor BKI-1708 against the cyst-forming apicomplexan parasites Toxoplasma gondii and Neospora caninum in vitro and in experimentally infected mice. Int. J. Parasitol. 2024, 25, No. 100553.

(34). Waldron-Young E; Wijitrmektong W; Choi R; Whitman GR; Hulverson MA; Charania R; Keelaghan A; Li L; Srinual S; Nikhar S; et al. Pyridopyrimidinones as a new chemotype of calcium dependent protein kinase 1 (CDPK1) inhibitors for Cryptosporidium. Mol. Biochem. Parasitol. 2024, 260, No. 111637.

(35). Hulverson MA; Choi R; Vidadala RSR; Whitman GR; Vidadala VN; Ojo KK; Barrett LK; Lynch JJ; Marsh K; Kempf DJ; et al. Pyrrolopyrimidine Bumped Kinase Inhibitors for the Treatment of Cryptosporidiosis. ACS Infect. Dis. 2021, 7 (5), 1200–1207. [PubMed: 33565854]

(36). Murphy RC; Ojo KK; Larson ET; Castellanos-Gonzalez A; Perera BG; Keyloun KR; Kim JE; Bhandari JG; Muller NR; Verlinde CL; et al. Discovery of potent and selective inhibitors of calcium-dependent protein kinase 1 (CDPK1) from C. parvum and T. gondii. ACS Med. Chem. Lett. 2010, 1 (7), 331–335. [PubMed: 21116453]

(37). Wang M; Garrison N; Nguyen PM; Prasad A; Wang Y; Kwon HK; Kim G; Siegler MA; Lectka T Can the -CF(3) Group Act as a Tight, Well-Defined Hydrogen Bond Acceptor? A Clear Crystallographic CF(2)-F···H-N(+) Interaction Says Yes. J. Org. Chem. 2024, 89 (13), 9681–9685. [PubMed: 38965938]

(38). Cavalluzzi MM; Mangiatordi GF; Nicolotti O; Lentini G Ligand efficiency metrics in drug discovery: the pros and cons from a practical perspective. Expert Opin. Drug Discovery 2017, 12 (11), 1087–1104.

(39). Johnson TW; Gallego RA; Edwards MP Lipophilic Efficiency as an Important Metric in Drug Design. J. Med. Chem. 2018, 61 (15), 6401–6420. [PubMed: 29589935]

(40). Lobo S Is there enough focus on lipophilicity in drug discovery? Expert Opin. Drug Discovery 2020, 15 (3), 261–263.

(41). Summerfield SG; Yates JWT; Fairman DA Free Drug Theory – No Longer Just a Hypothesis? Pharm. Res. 2022, 39 (2), 213–222. [PubMed: 35112229]

(42). Wang Q; Sibley LD Assays for Monitoring *Toxoplasma gondii* Infectivity in the Laboratory Mouse. Methods Mol. Biol. 2020, 2071, 99–116. [PubMed: 31758448]

(43). Radke JB; Melillo B; Mittal P; Sharma M; Sharma A; Fu Y; Uddin T; Gonse A; Comer E; Schreiber SL; et al. Bicyclic azetidines target acute and chronic stages of *Toxoplasma gondii* by inhibiting parasite phenylalanyl t-RNA synthetase. Nat. Commun. 2022, 13 (1), No. 459. [PubMed: 35075105]

(44). Montgomery JA; Alday PH; Choi R; Khim M; Staker BL; Hulverson MA; Ojo KK; Fan E; Van Voorhis WC; Doggett JS Bumped Kinase Inhibitors Inhibit both Toxoplasma gondii MAPKL1 and CDPK1. ACS Infect Dis 2025, 11 (6), 1552–1562. [PubMed: 40407244]

(45). Tobin CM; Knoll LJ A patatin-like protein protects *Toxoplasma gondii* from degradation in a nitric oxide-dependent manner. Infect. Immun. 2012, 80 (1), 55–61. [PubMed: 22006568]

(46). Kabsch W Xds. Acta Crystallogr., Sect. D:Biol. Crystallogr. 2010, 66 (Pt 2), 125–132. [PubMed: 20124692]

(47). Evans PR; Murshudov GN How good are my data and what is the resolution? Acta Crystallogr., Sect. D:Biol. Crystallogr. 2013, 69 (Pt7), 1204–1214. [PubMed: 23793146]

(48). Liebschner D; Afonine PV; Baker ML; Bunkoczi G; Chen VB; Croll TI; Hintze B; Hung LW; Jain S; McCoy AJ; et al. Macromolecular structure determination using X-rays, neutrons and electrons: recent developments in Phenix. Acta Crystallogr., Sect. D:Struct. Biol. 2019, 75 (Pt 10), 861–877. [PubMed: 31588918]

(49). Emsley P; Cowtan K COOT: model-building tools for molecular graphics. Acta Crystallogr., Sect. D:Biol. Crystallogr. 2004, 60, 2126–2132. [PubMed: 15572765]

(50). Davis IW; Murray LW; Richardson JS; Richardson DC MOLPROBITY: structure validation and all-atom contact analysis for nucleic acids and their complexes. Nucleic Acids Res. 2004, 32, W615–619. [PubMed: 15215462]

(51). Meng EC; Goddard TD; Pettersen EF; Couch GS; Pearson ZJ; Morris JH; Ferrin TE UCSF ChimeraX: Tools for structure building and analysis. Protein Sci. 2023, 32 (11), No. e4792. [PubMed: 37774136]

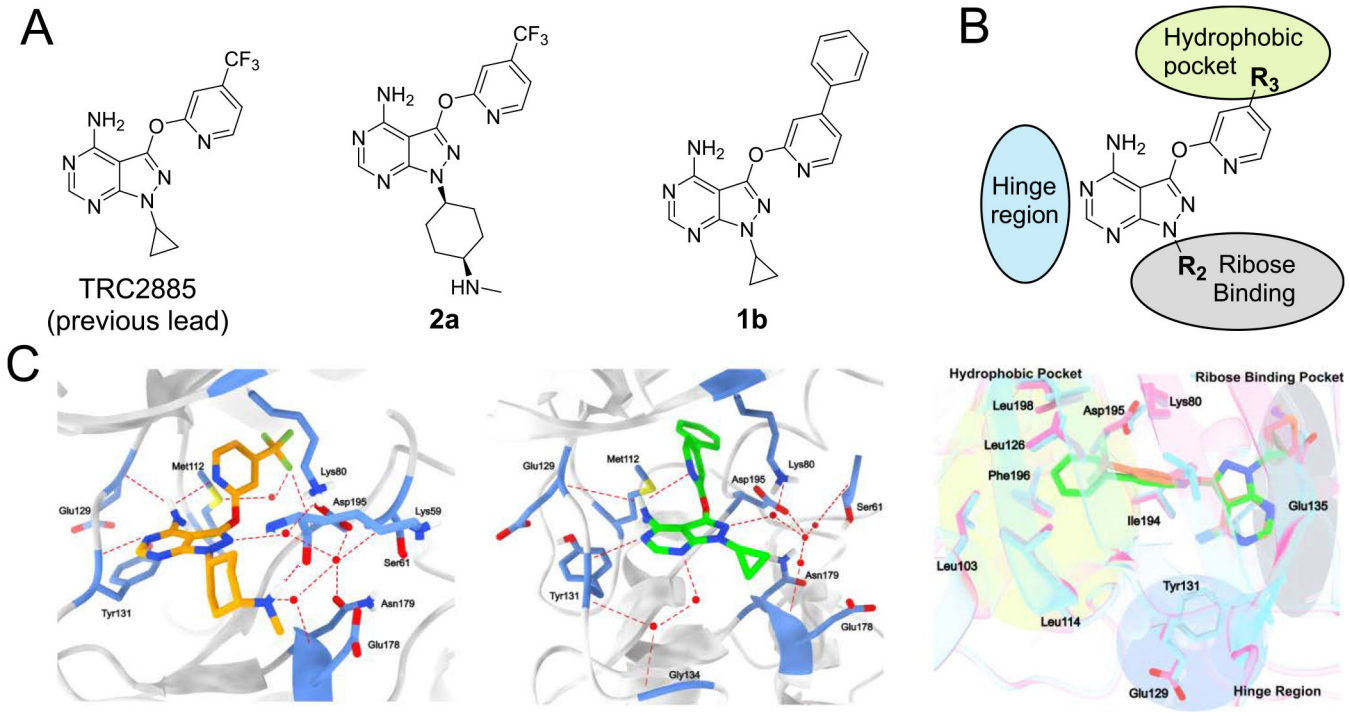

Figure 1.

Depiction of key structural details between PP compounds and TgCDPK1 active site. (A) Structure of previous lead TRC2885, and of the compounds used to obtain crystal structures (**2a** and **1b**). (B) Structural map of PP R_2 and R_3 derivatives and their active site interaction space. (C) Crystal structure of TgCDPK1 in complex with (left) **2a** (PDB: 9Z5L, orange, left), and (middle) **1b** (PDB: 9Z5M, green). Interactions between TgCDPK1 and bound ligands were analyzed using LigPlot[1] (Figure S1) and electron density maps in Coot.[2] Overlay (right) of TgCDPK1-**2a** (pink amino acid residues; orange ligand) and TgCDPK1-**1b** (cyan amino acid residues; green ligand) structures showing the extent of hydrophobic pocket penetration by **1b**.

A

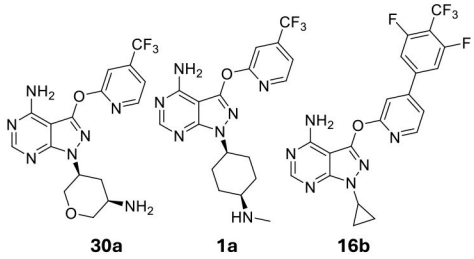

	30a	1a	16b
PPB[c] (% bound)	26.2 %	57.5 %	99.7 %
Half-life[a]	1.6 hr	0.9 hr	5.4 hr
AUC[a] (ng·h/mL)	1150	1860	16320
Cmax[b] (ng/mL)	997	509	1430
%F	66.4 %	94.5 %	100 %
Cl[b] (mL/min/kg)	94.7	87.0	8.0
Vd[b] (L/kg)	4.4	2.8	2.8

B

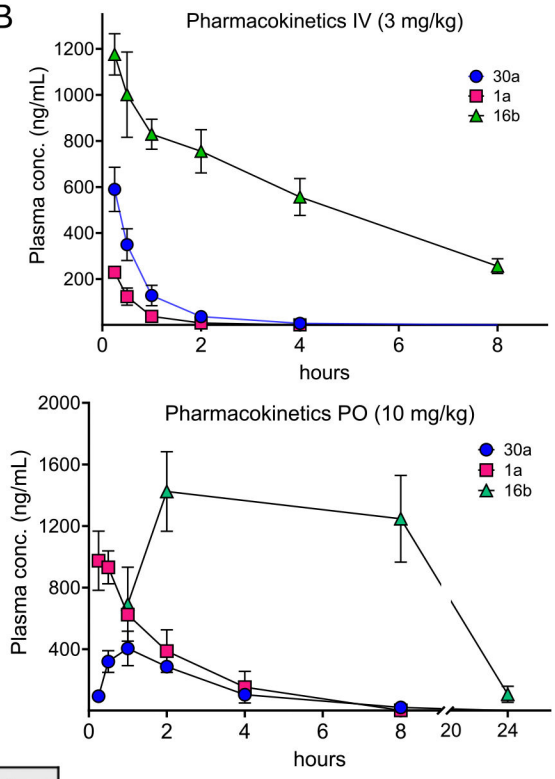

C Inhibitor specificity and cytotoxicity

Compound	Src inhibition at 10 μM (%)	G128M inhibition at 20 μM (%)	HepG2 cytotoxicity at 20 μM (%)
30a	23.3	5.13 ± 1.8	7.0
1a	39.7 ± 3.5	17.2 ± 7.8	3.2 ± 6.2
16b	0.84 ± 9.6	10.6 ± 4.9	8.5 ± 4.3

Figure 2.

Pharmacokinetic data of initial lead compounds. (A) Table of mouse (CD-1) pharmacokinetic characterization of lead compounds, $n = 3$. a = PO, 10 mg/kg, b = IV, 3 mg/kg, c = determined from *in vitro* assay. (B) Compound plasma concentration curves of the lead compounds from either PO (bottom) or IV (top) administration. (C) Compound % enzyme inhibition of Src (10 μM) and TgCDPK G128 M mutant (20 μM), and % HepG2 cytotoxicity (20 μM). Data are reported as duplicates and triplicates ± standard deviation.

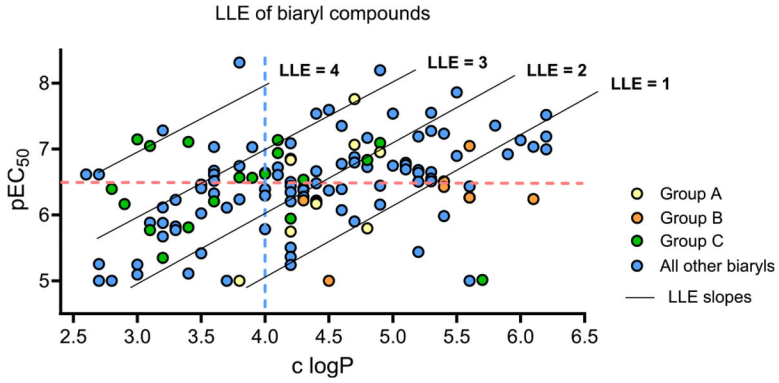

Figure 3.

Lead optimization. Scatter plot of biaryl compound's pEC_{50} vs c LogP. Black solid lines are LLE values (LLE = cLogP – pEC_{50}), above the red dotted line are ideal pEC50 (<300 nM) and to the left of the blue dotted line are compounds with ideal c Log P values (<4).

A

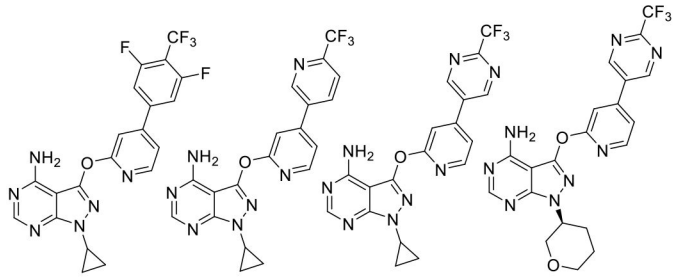

	16b	13c	16c	23c[e]
Half-life[a]	5.4 hr	3.5 hr	2.5 hr	0.7 hr
AUC[a] (ng·h/mL)	16,320	15,700	12,245	1260
Cmax[b] (ng/mL)	1,430	3,660	1,959	2897
Cl[b] (mL/min/kg)	8.02	12.4	29.6	10.8
Vd[b] (L/kg)	2.8	0.8	2.8	ND
%F	100 %	100 %	100 %	41%
BPB[c] (% bound)	99.9 %	95.8 %	87.4 %	ND
brain:plasma[d]	3.3	0.40	0.31	ND

B

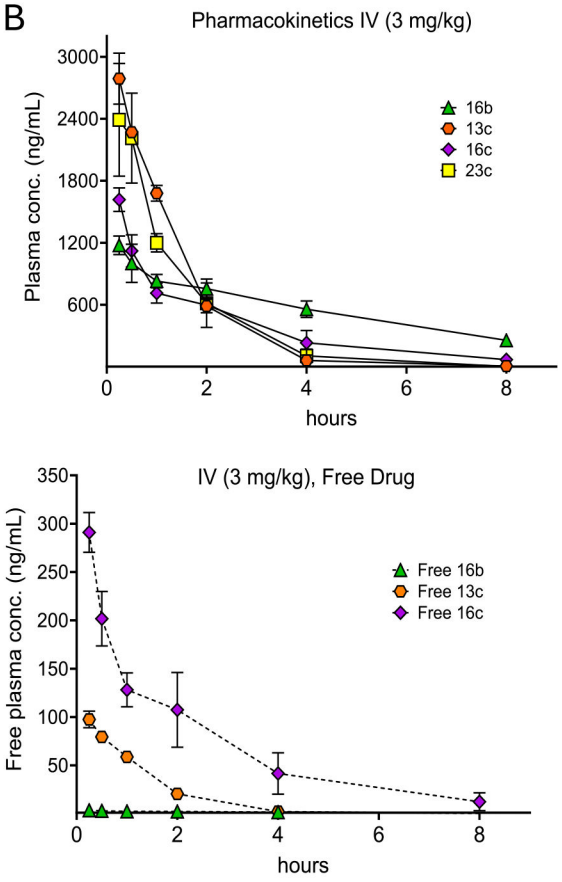

C Pharmacokinetics of Free Fraction

Compound	AUC_u[a] (ng·h/mL)	Cl_u[b] (mL/min/kg)	Vd_u[b] (L/kg)
16b	48.9	2,673.3	936.66
13c	549.5	354.3	22.89
16c	2,204.1	164.4	15.44

D Inhibitor specificity and cytotoxicity

Compound	Src inhibition at 10 μM (%)	G128M inhibition at 20 μM (%)	HepG2 cytotoxicity at 20 μM (%)
16b	0.84 ± 9.6	10.6 ± 4.9	8.5 ± 4.34
13c	21.2 ± 7.0	6.52 ± 1.9	6.3
16c	18.2 ± 2.8	13.6 ± 4.3	8.6

Figure 4.

Pharmacokinetic data of optimized lead compounds. (A) Table of mouse (CD-1) pharmacokinetic characterization of lead compounds, $n = 3$. a = PO, 10 mg/kg, b = IV, 3 mg/kg and c = determined *in vitro*, d = PO, 100 mg/kg; brain concentration determined at 24 h. (B) Compound plasma concentration curves of total drug (top) and free drug (bottom) from IV administration. e = compound PK was determined as a part of a cassette with other compounds. (C) Tables of pharmacokinetic values based on free fraction. (D) Compound % enzyme inhibition of Src (10 μM) and TgCDPK G128 M mutant (20 μM), and % HepG2 cytotoxicity (20 μM). Data are reported as duplicates and triplicates ± standard deviation. ND = not determined. BPB is brain protein binding.

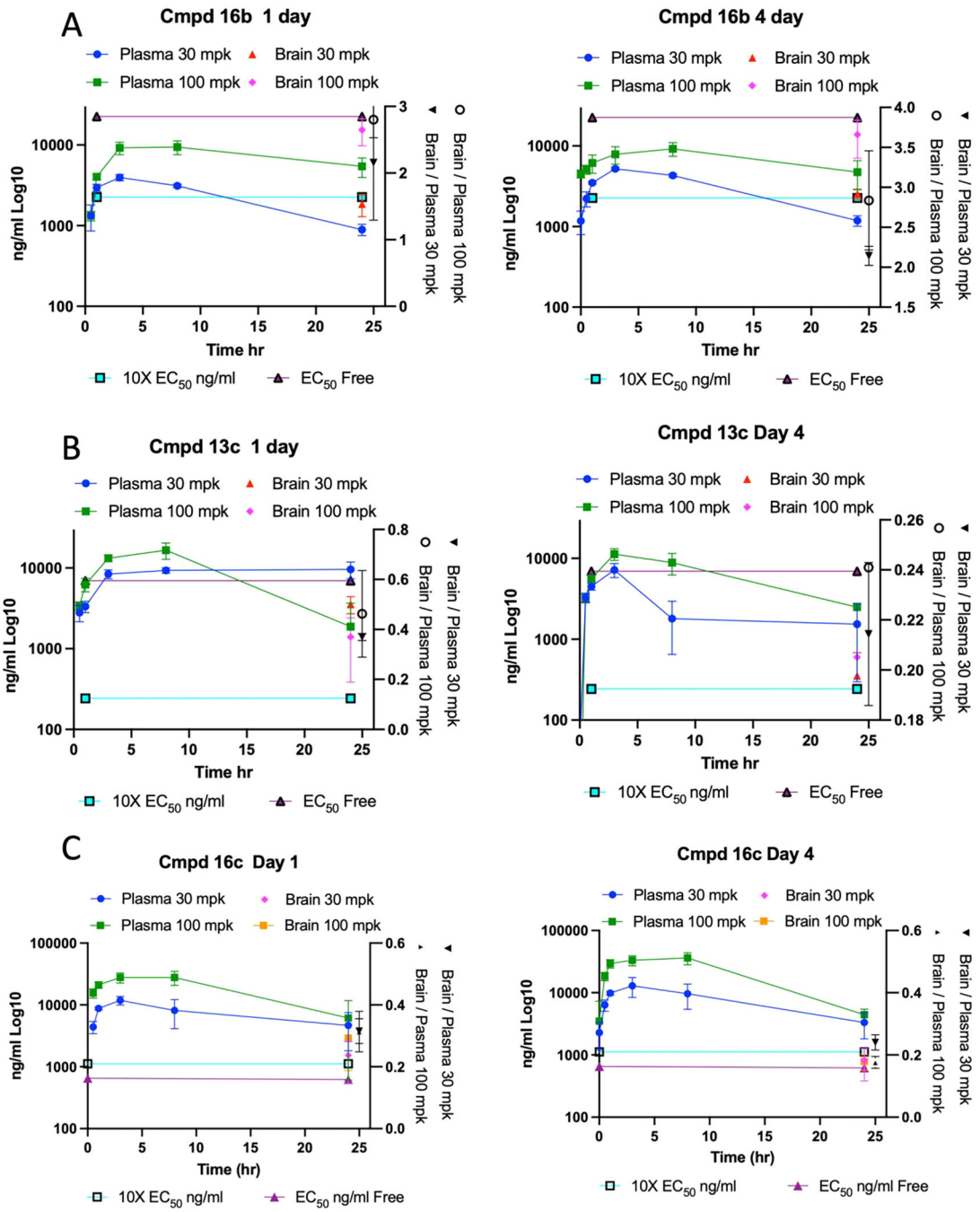

Figure 5.

Summary of repeated dose PK. (A) Plasma and brain levels for repeated oral dosing of **16c** at 30 mg/kg BID and 100 mg/kg QD for 4 days. Estimates for 10xEC_{50} (total) were based on in vitro growth inhibition assay and graphed as a cyan line. EC_{50} free was estimated from the EC_{50} and the unbound fraction from PBB and are graphed as purple lines. Total brain levels are shown as single points at 24 h and the brain/plasma ratio at 24 h is plotted as an offset at 25 h. (B) PK profiles for repeated oral dosing of **13c**. Labels as in A. (C) PK profile

for repeated oral dosing of **16c**. Labels as in A. $n = 3$ animals per compound. Means ± SD. BID dosing was offset by 10 h. $n = 3$ animals per group.

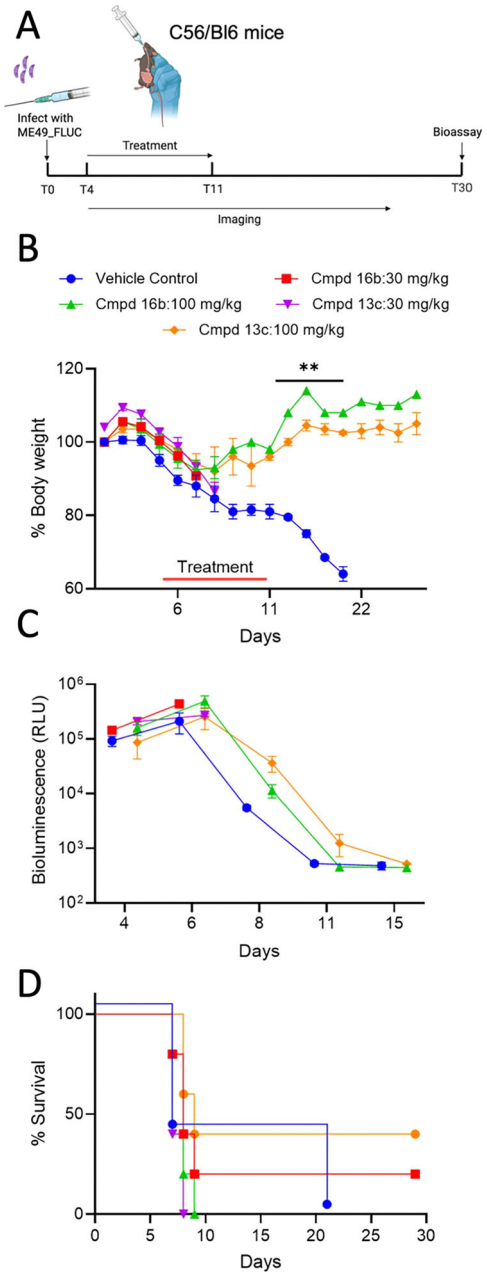

Figure 6.

Performance of top leads 16band 13c in an acute infection model. (A) Diagram of timing (days) for infection and treatment. Dosing: 30 mg/mL BID, 100 mg/kg QD. (B) Weight loss vs time. $^{**}P < 0.01$, one way ANOVA comparing **16b** and **13c** vs vehicle control. (C) Bioluminescence imaging of Fluc-expressing parasites. RLU, relative light units. (D) Cumulative mortality. $n = 3$ animals, Means ± SD.

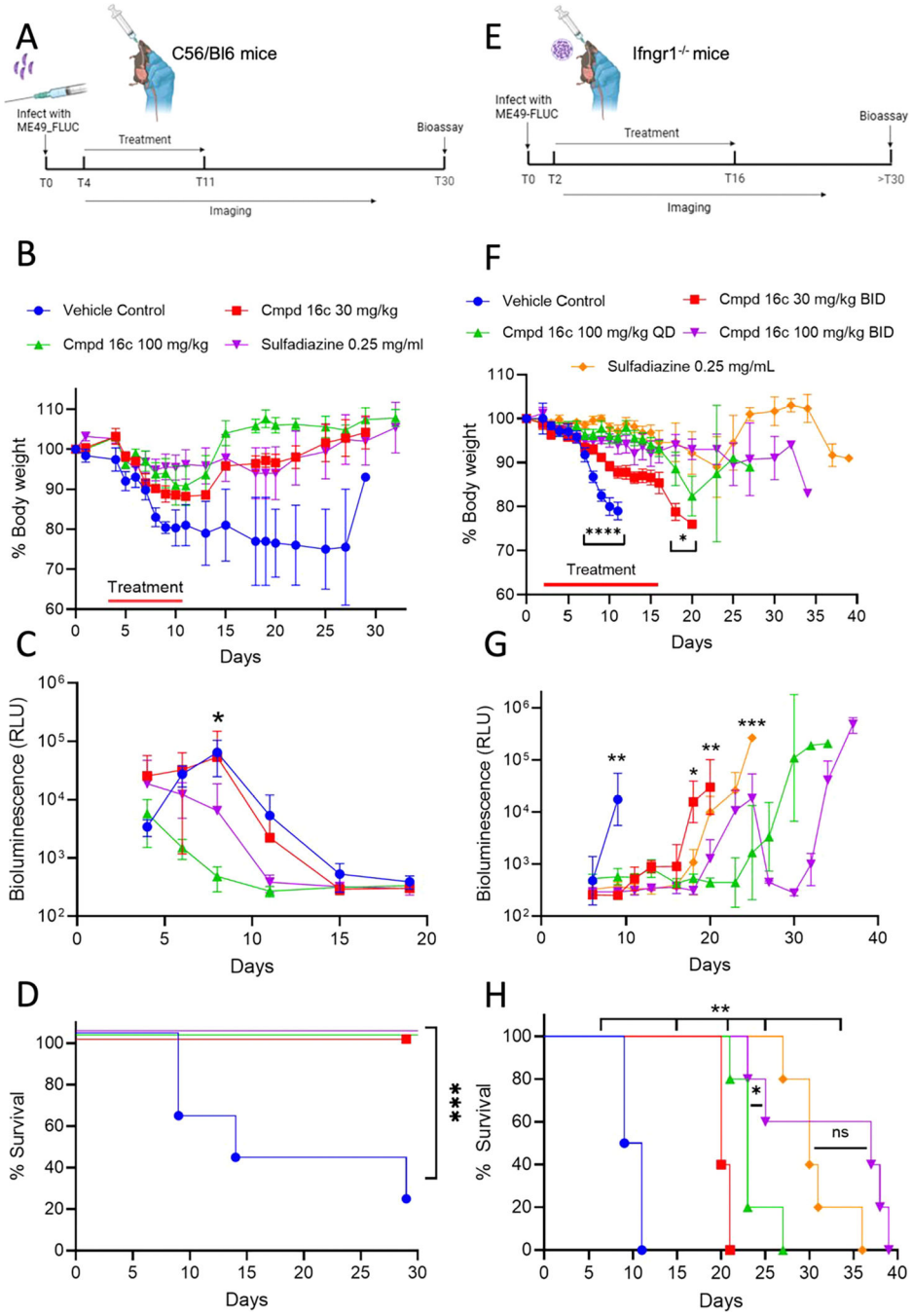

Figure 7.

Efficacy testing of 16c. (A) Diagram of timing for i.p. infection and treatment in acute infection model. Mice were infected by i.p. injection with ME49-FLUC. PO dosing: 30 mg/kg BID, 100 mg/kg QD. (B) Weight loss vs time. Means ± SD. (C) Bioluminescence imaging of Fluc-expressing parasites. RLU, relative light units. * $P < 0.05$ comparing **16c** 30 mg/kg vs 100 mg/kg. Means ± S.D, One-way ANOVA and Dunnett's multiple comparisons test. (D) Cumulative mortality. $n = 5$ animals, *** $P < 0.001$ Mantel Cox test. (E) Diagram of timing for oral infection and treatment in immunocompromised infection model. Mice

were infected by oral gavage with 5 cysts of ME49-FLUC. (F) Weight loss vs time. **** $P < 0.0005$ control vs all groups; * $P < 0.05$ **16c** 30 mg/kg BID vs 100 mg/kg BID and sulfadiazine. Means ± S.D, One-way ANOVA and Dunnett's multiple comparisons test. (G) Bioluminescence imaging of Fluc-expressing parasites. RLU, relative light units. *** $P < 0.001$ control vs all groups; * $P < 0.05$, ** $P < 0.01$ **16c** 30 mg/kg BID vs other groups, *** $P < 0.001$ **16c** 100 mg/kg QD vs other groups. Mean ± S.D, One-way ANOVA and Dunnett's multiple comparisons test. (H) Cumulative mortality. ** $P < 0.01$ control vs all groups. ** $P < 0.01$ **16c** 100 mg/kg BID vs **16c** 100 mg/kg QD. Mantel Cox test. $n = 5$ animals.

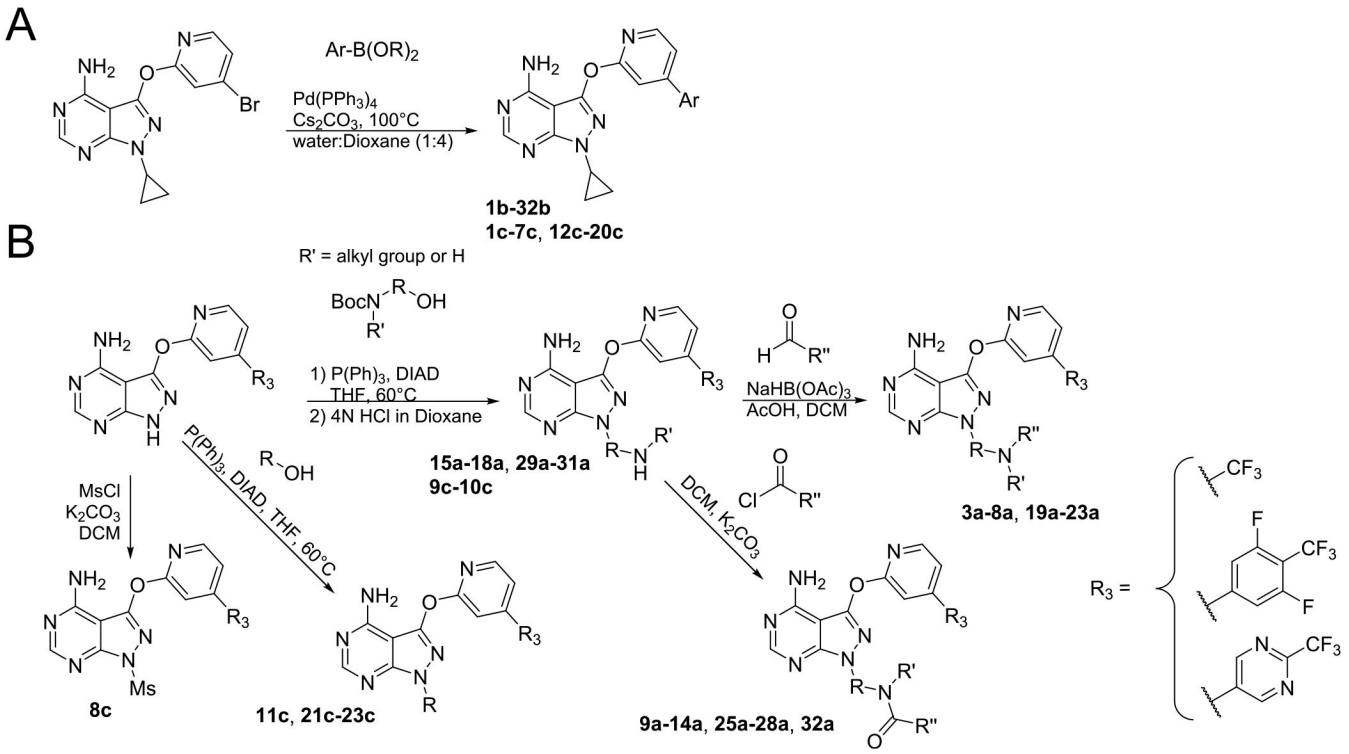

Scheme 1.

Synthesis of PP-O-pyridyl aryl R_3 and Amino R_2 Analogs

Table 1.

SAR of R_2 Amino Moieties for Potency and Metabolic Stability

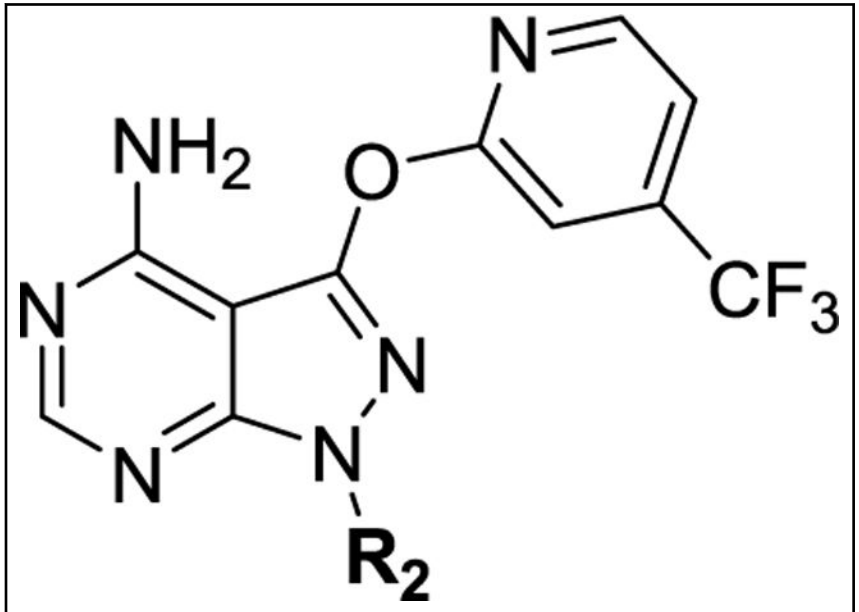

Cmpd	R_2	IC_{50}(nM)[a]	EC_{50}(nM)[a]	MLM/HLM $t_{1/2}$(min)[b]
1a	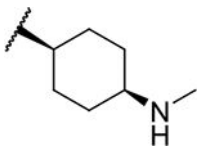	60.2 ± 76.3	41.7	64.8 / 129
2a	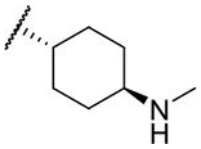	7.22	144	33.4 / >145

J Med Chem. Author manuscript; available in PMC 2026 July 07.

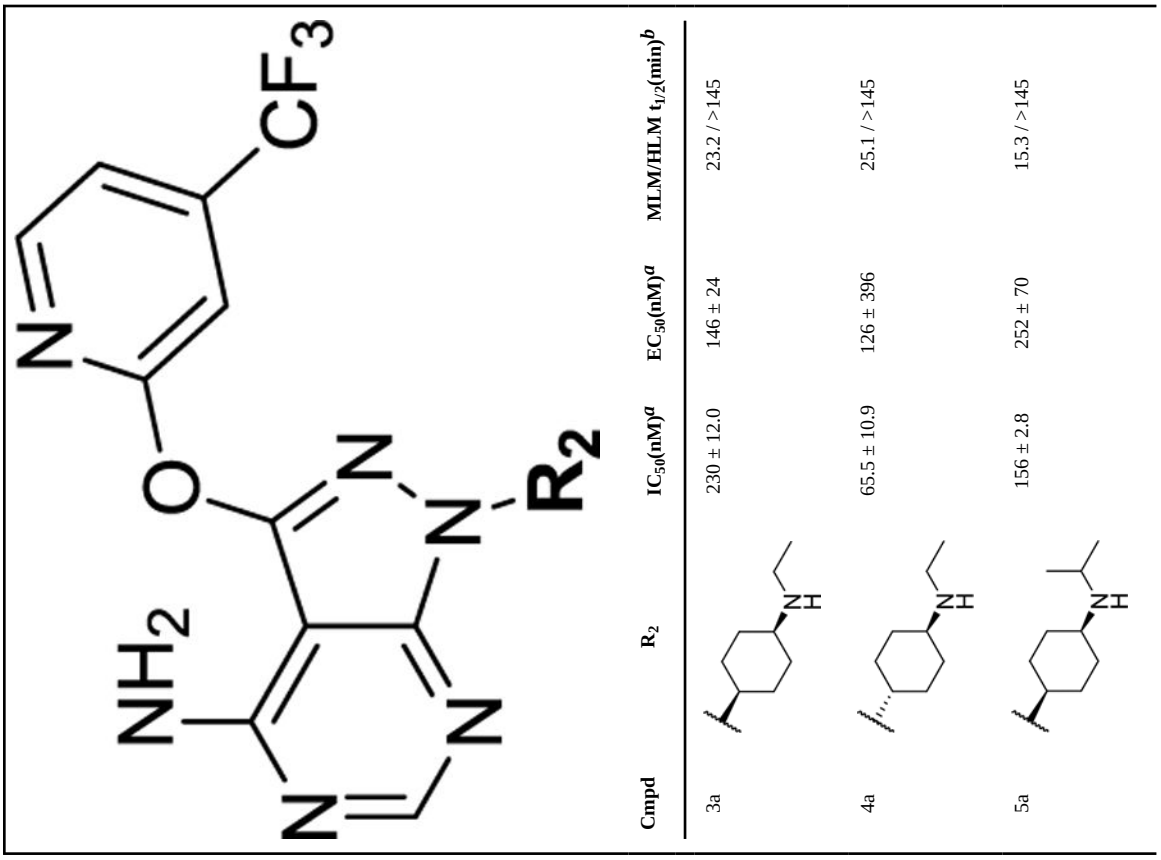

Cmpd	R_2	IC_{50}(nM)[a]	EC_{50}(nM)[a]	MLM/HLM $t_{1/2}$(min)[b]
3a		230 ± 12.0	146 ± 24	23.2 / >145
4a		65.5 ± 10.9	126 ± 396	25.1 / >145
5a		156 ± 2.8	252 ± 70	15.3 / >145

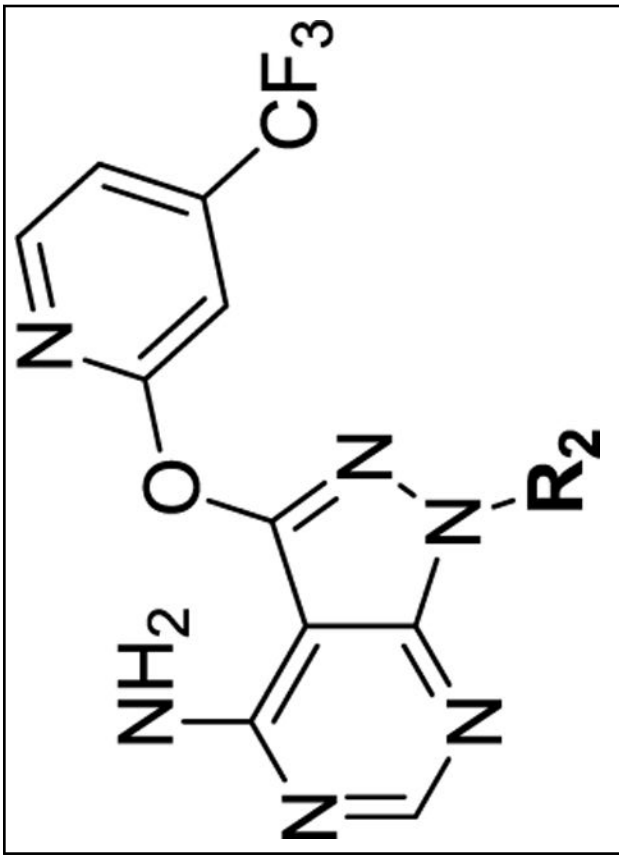

Cmpd	R_2	IC_{50}(nM)[a]	EC_{50}(nM)[a]	MLM/HLM $t_{1/2}$(min)[b]
6a	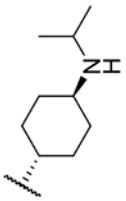	132 ± 2.1	966 ± 280	ND / ND
7a	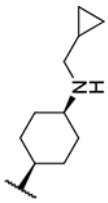	374	ND	ND / ND
8a	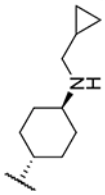	48 ± 33.9	93 ± 35.4	56.9 / >145

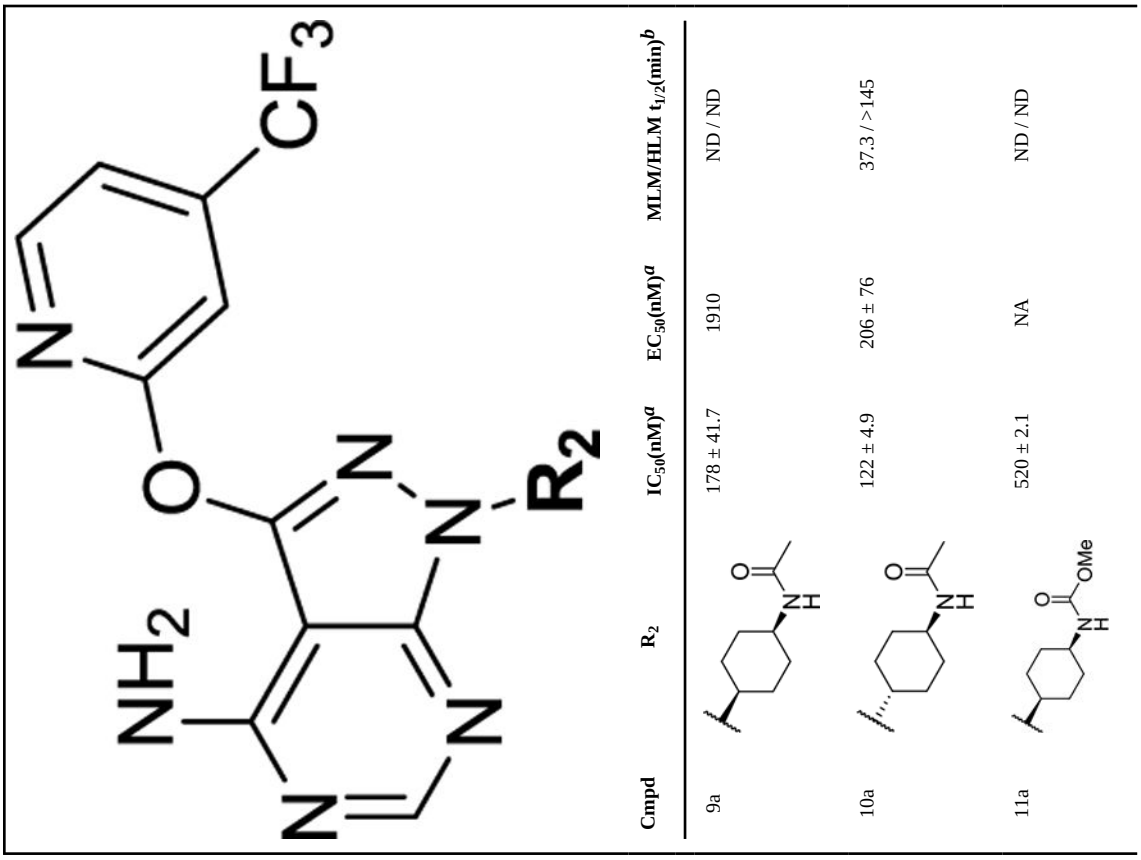

Cmpd	R_2	IC_{50}(nM)[a]	EC_{50}(nM)[a]	MLM/HLM $t_{1/2}$(min)[b]
9a		178 ± 41.7	1910	ND / ND
10a		122 ± 4.9	206 ± 76	37.3 / >145
11a		520 ± 2.1	NA	ND / ND

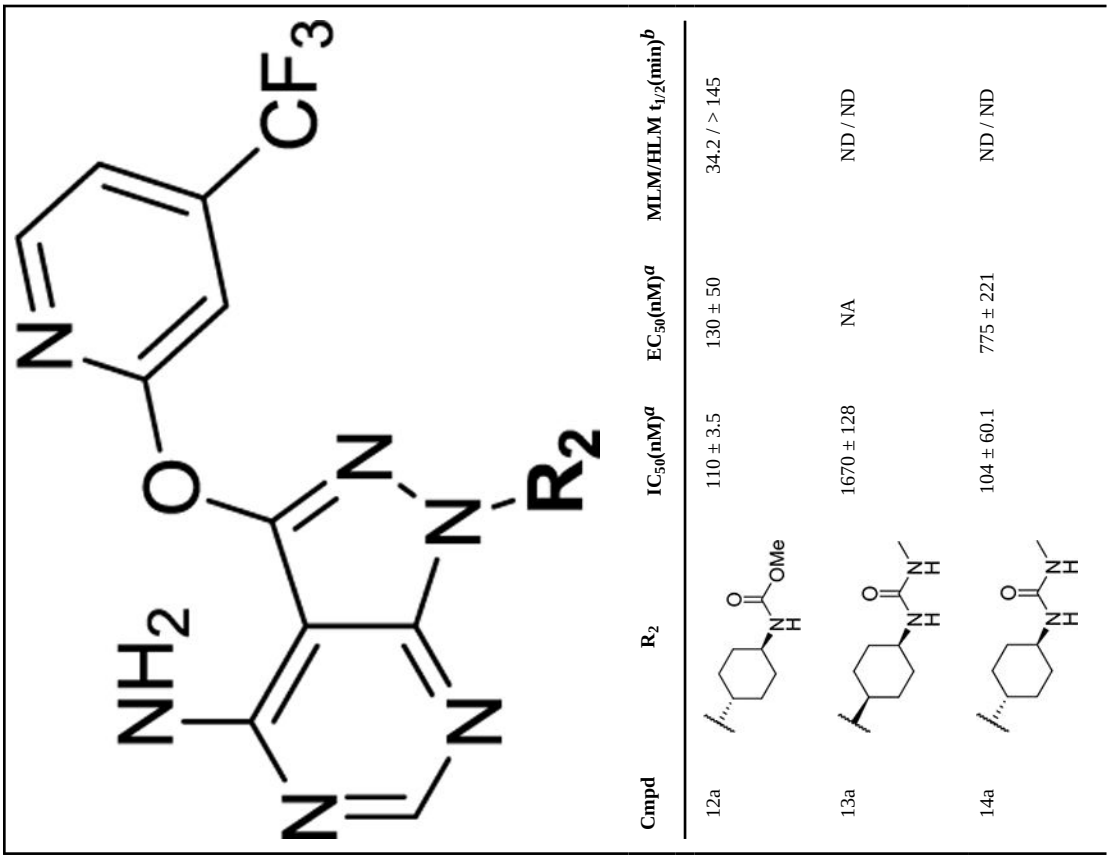

Cmpd	R_2	IC_{50}(nM)[a]	EC_{50}(nM)[a]	MLM/HLM $t_{1/2}$(min)[b]
12a		110 ± 3.5	130 ± 50	34.2 / > 145
13a		1670 ± 128	NA	ND / ND
14a		104 ± 60.1	775 ± 221	ND / ND

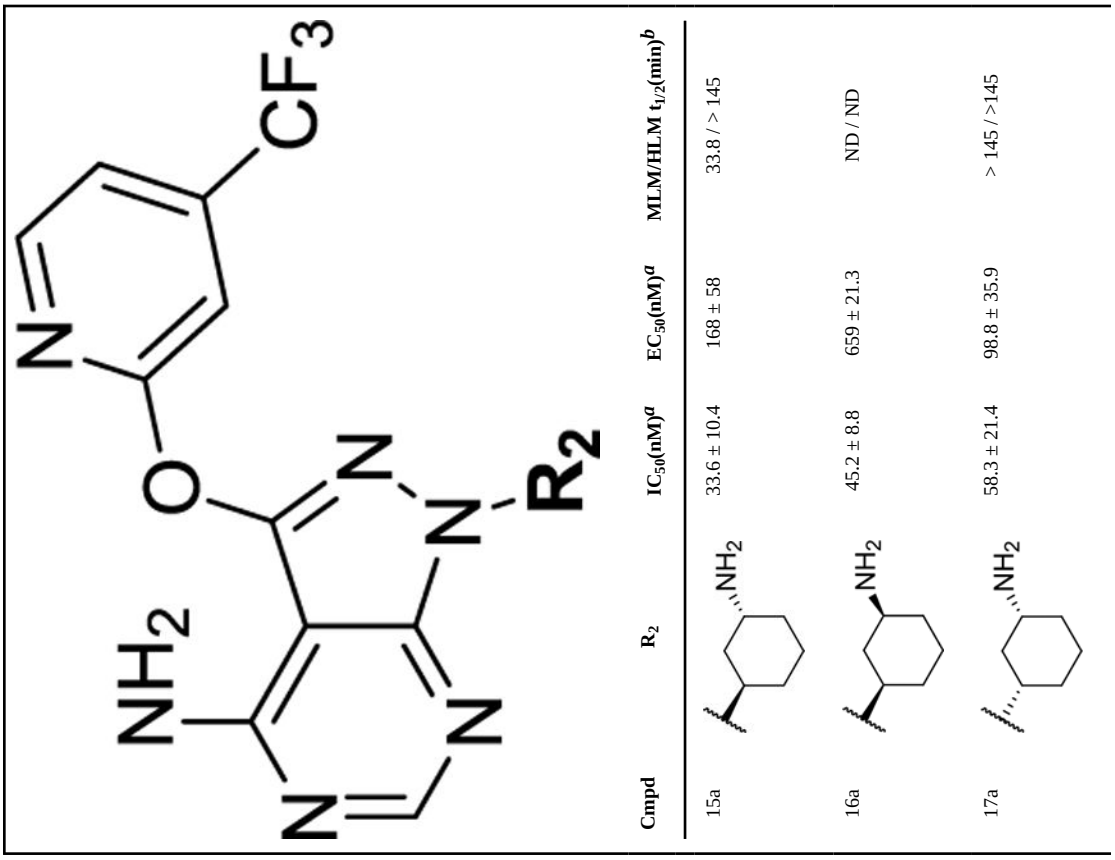

Cmpd	R_2	IC_{50}(nM)[a]	EC_{50}(nM)[a]	MLM/HLM $t_{1/2}$(min)[b]
15a		33.6 ± 10.4	168 ± 58	33.8 / > 145
16a		45.2 ± 8.8	659 ± 21.3	ND / ND
17a		58.3 ± 21.4	98.8 ± 35.9	> 145 / >145

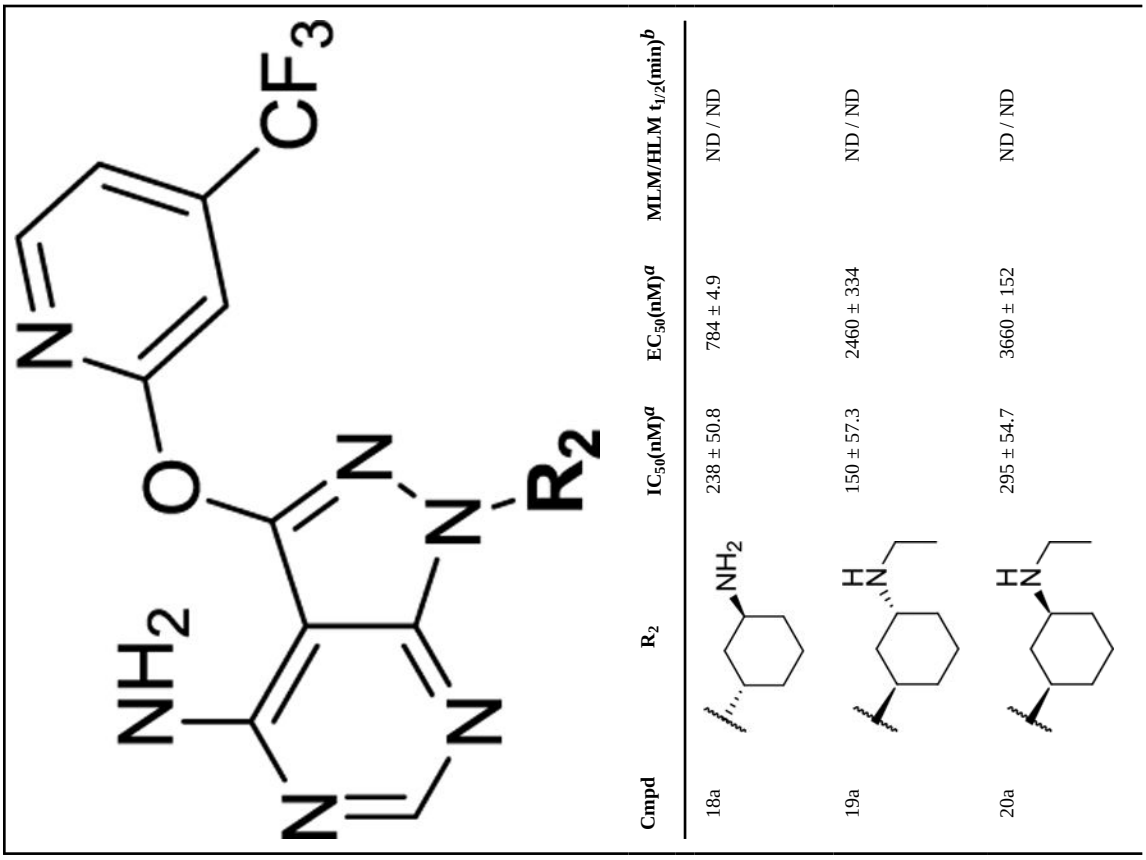

Cmpd	R_2	IC_{50}(nM)[a]	EC_{50}(nM)[a]	MLM/HLM $t_{1/2}$(min)[b]
18a		238 ± 50.8	784 ± 4.9	ND / ND
19a		150 ± 57.3	2460 ± 334	ND / ND
20a		295 ± 54.7	3660 ± 152	ND / ND

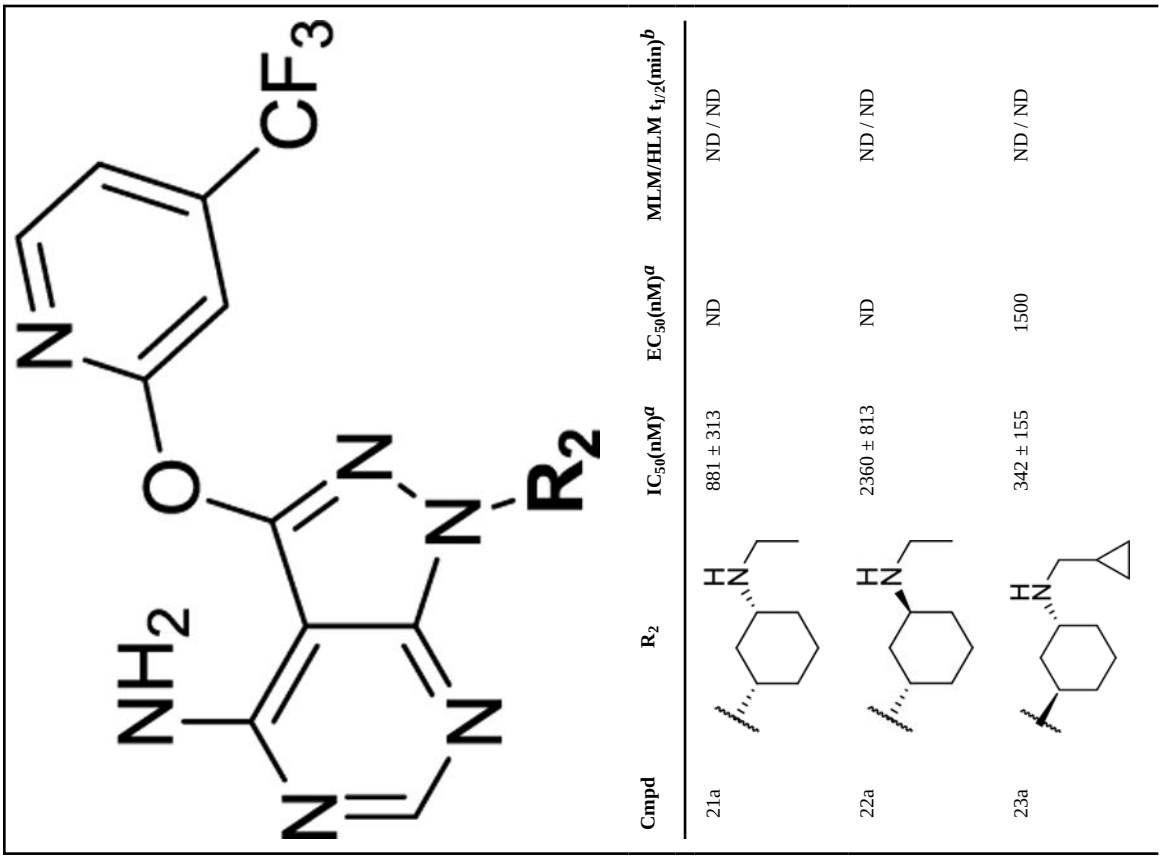

Cmpd	R_2	IC_{50}(nM)[a]	EC_{50}(nM)[a]	MLM/HLM $t_{1/2}$(min)[b]
21a		881 ± 313	ND	ND / ND
22a		2360 ± 813	ND	ND / ND
23a		342 ± 155	1500	ND / ND

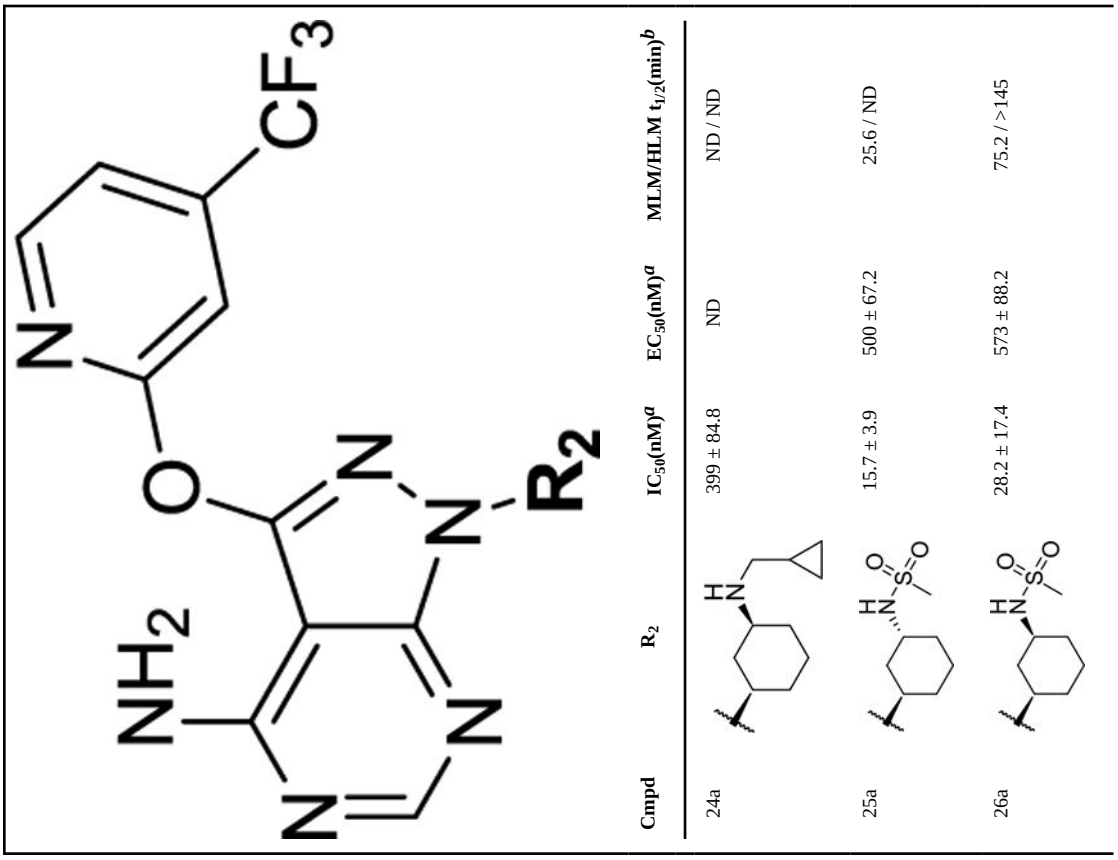

Cmpd	R_2	IC_{50}(nM)[a]	EC_{50}(nM)[a]	MLM/HLM $t_{1/2}$(min)[b]
24a		399 ± 84.8	ND	ND / ND
25a		15.7 ± 3.9	500 ± 67.2	25.6 / ND
26a		28.2 ± 17.4	573 ± 88.2	75.2 / >145

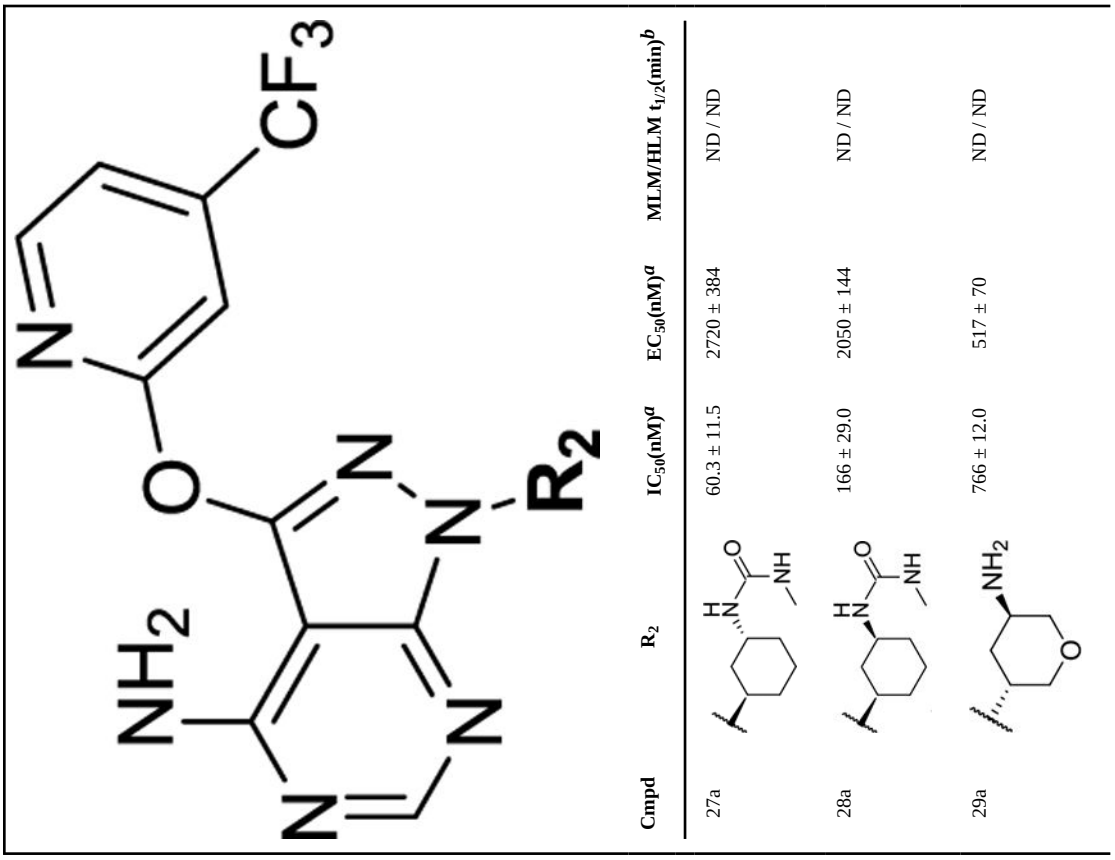

Cmpd	R_2	IC_{50}(nM)[a]	EC_{50}(nM)[a]	MLM/HLM $t_{1/2}$(min)[b]
27a		60.3 ± 11.5	2720 ± 384	ND / ND
28a		166 ± 29.0	2050 ± 144	ND / ND
29a		766 ± 12.0	517 ± 70	ND / ND

Cmpd	R_2	IC_{50}(nM)[a]	EC_{50}(nM)[a]	MLM/HLM $t_{1/2}$(min)[b]
30a		197 ± 3.5	67 ± 98.3	>145 / >145
31a		157 ± 42.8	351 ± 55.6	ND / ND
32a		127 ± 52.5	236 ± 46.8	28.6 / >145

[a]Half maximal inhibitory concentration determined from enzyme and cell-based assay.

[b] Metabolic half-lives. Data are reported as duplicates and triplicates ± standard deviation. Cmpd = compound, ND = not determined.

Table 2.

SAR of R_3 Aryl Moieties for Potency and Metabolic Stability

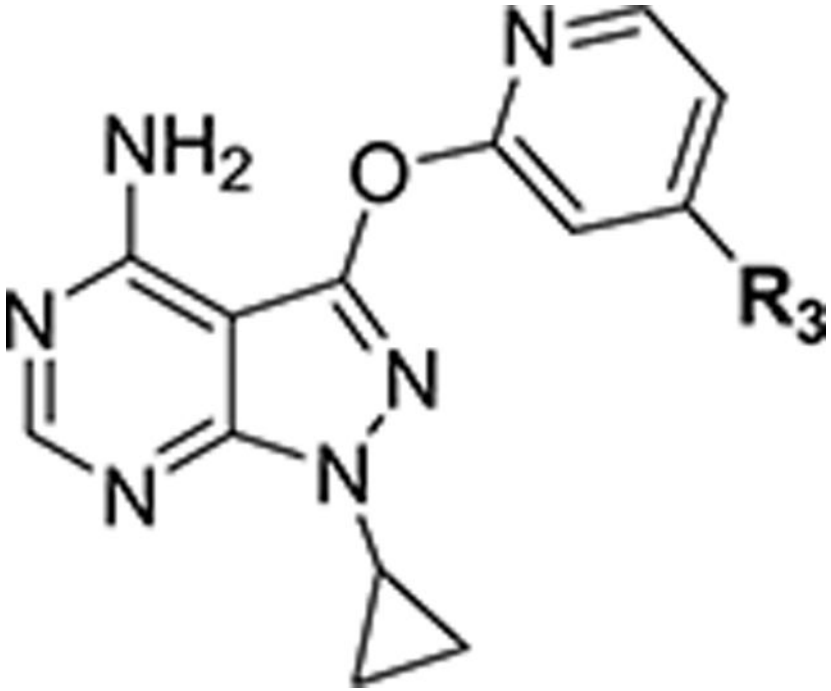

Cmpd	R_3	IC_{50}(nM)[a]	EC_{50}(nM)[a]	MLM/HLM $t_{1/2}$ (min)[b]
1b	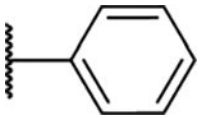	152 ± 140	364	9.8 / 58.9
2b		4.3 ± 1.1	44.8 ± 6.4	2.9 / 8.9

J Med Chem. Author manuscript; available in PMC 2026 July 07.

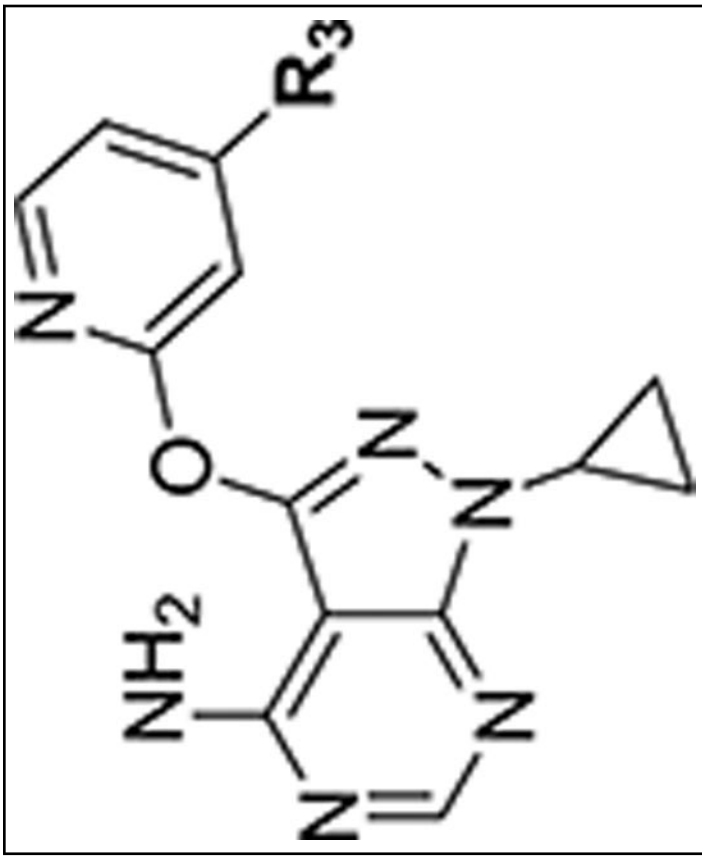

Cmpd	R_3	IC_{50}(nM)[a]	EC_{50}(nM)[a]	MLM/HLM $t_{1/2}$ (min)[b]
3b	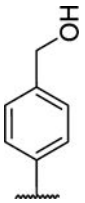	39.6 ± 5.6	304 ± 78.3	6.9 / 107
4b	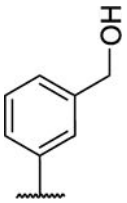	130 ± 43.1	3840 ± 227	ND / ND
5b	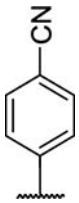	366 ± 54.2	ND	ND / ND

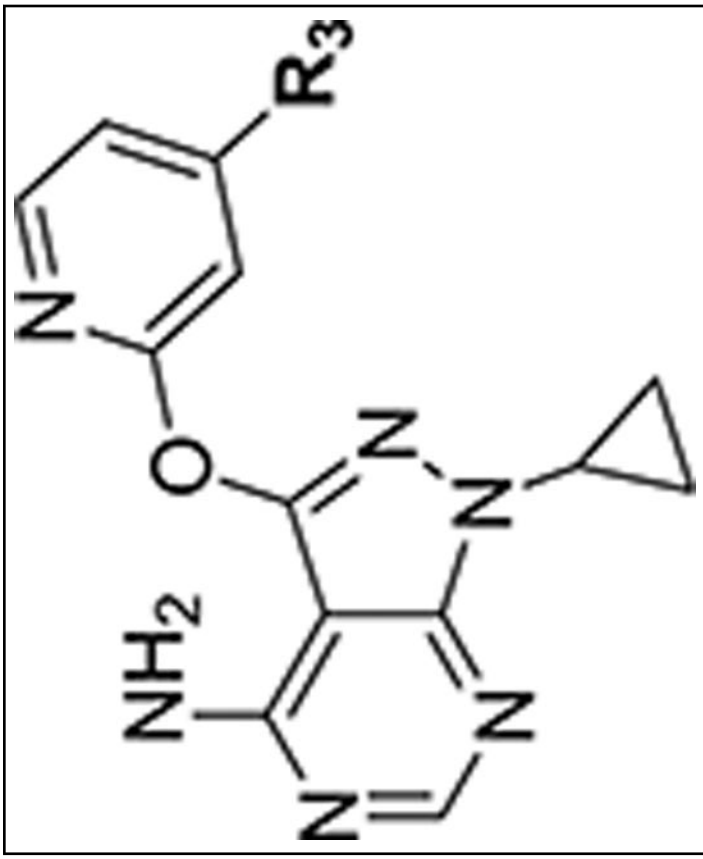

Cmpd	R_3	IC_{50}(nM)[a]	EC_{50}(nM)[a]	MLM/HLM $t_{1/2}$ (min)[b]
6b	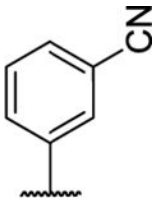	761	ND	ND / ND
7b	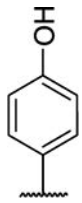	30.3 ± 24.2	304 ± 1.8	7.4 / 101
8b	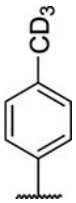	9.41 ± 3.9	168 ± 34.2	5.9 / NA

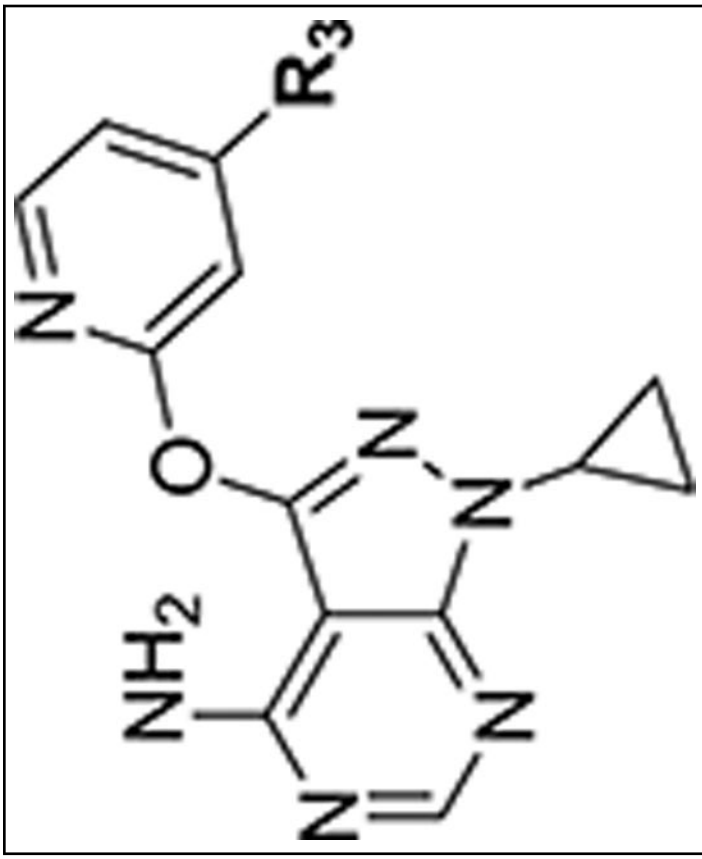

Cmpd	R_3	IC_{50}(nM)[a]	EC_{50}(nM)[a]	MLM/HLM $t_{1/2}$ (min)[b]
9b	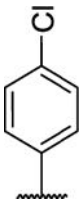	19.5 ± 7.8	188 ± 13.4	8.5 / >145
10b	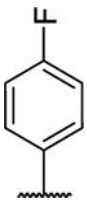	82.2 ± 13.9	391 ± 41.3	24.3 / >145
11b	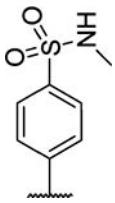	328 ± 12.0	ND	ND / ND

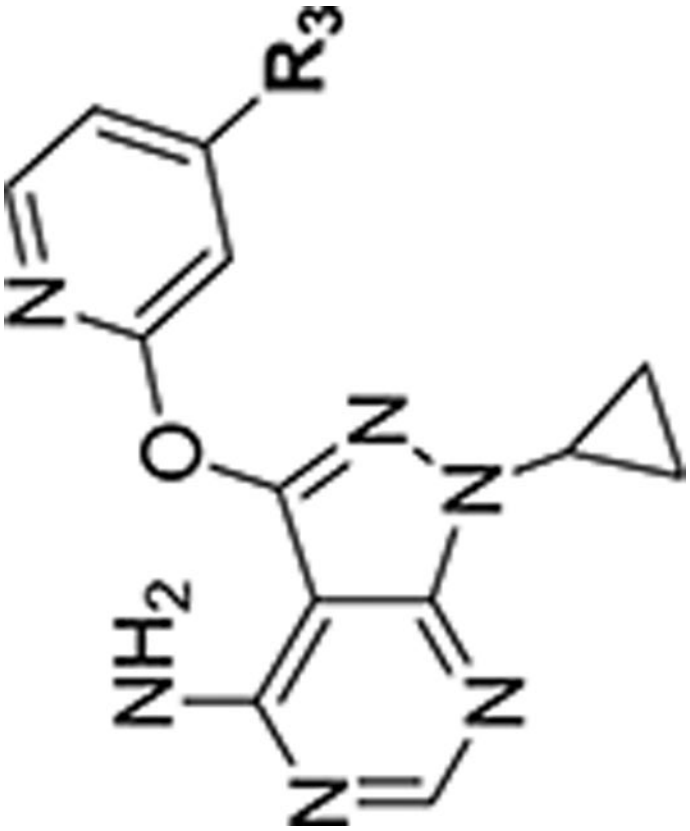

Cmpd	R_3	IC_{50}(nM)[a]	EC_{50}(nM)[a]	MLM/HLM $t_{1/2}$ (min)[b]
12b	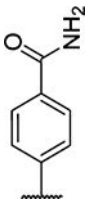	1700 ± 526	ND	ND / ND
13b	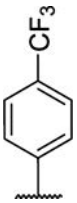	15.5 ± 2.1	175 ± 16.7	68.2 / >145
14b	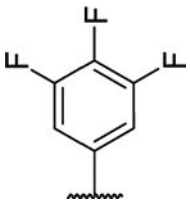	15.9 ± 7.8	677 ± 129	72.1 / 102

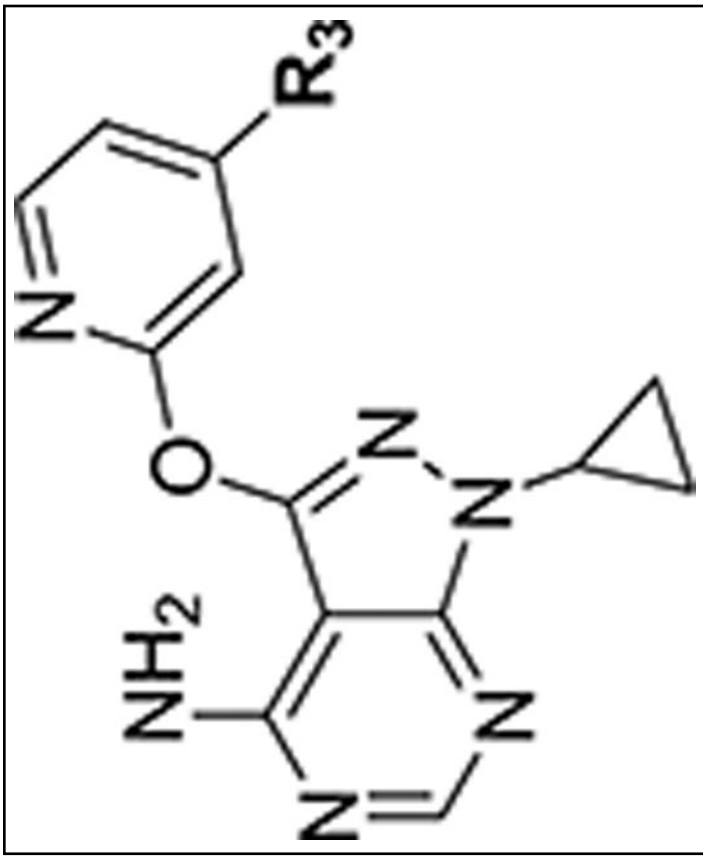

Cmpd	R_3	IC_{50}(nM)[a]	EC_{50}(nM)[a]	MLM/HLM $t_{1/2}$ (min)[b]
15b	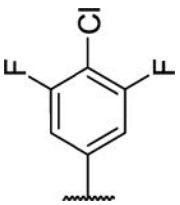	15.2 ± 10.1	112 ± 2.5	85.7 / 127
16b	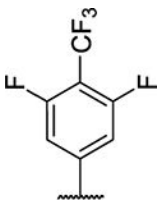	24 ± 13.5	570 ± 281	103 / >145

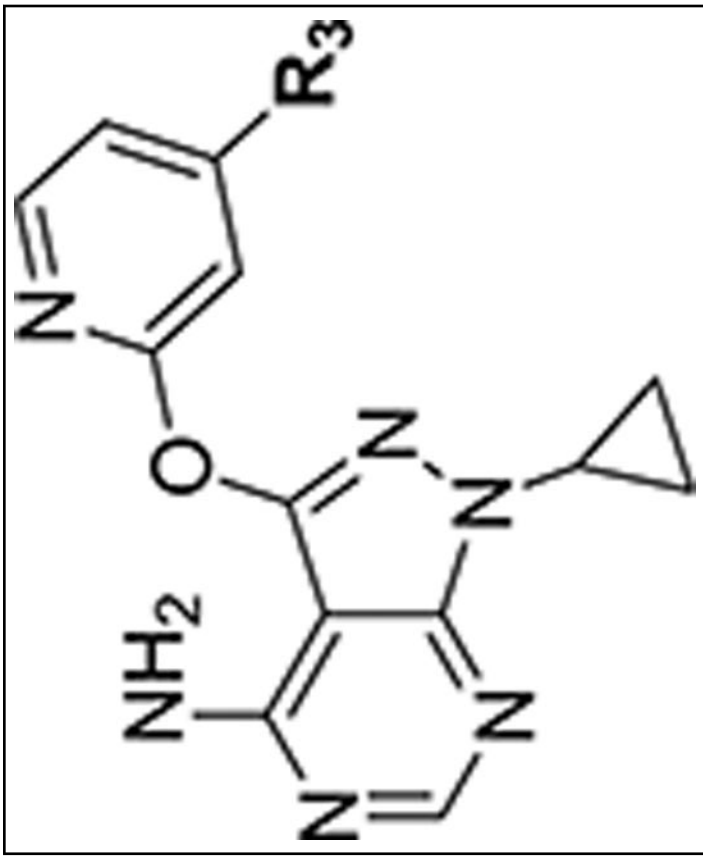

Cmpd	R_3	IC_{50}(nM)[a]	EC_{50}(nM)[a]	MLM/HLM $t_{1/2}$ (min)[b]
17b	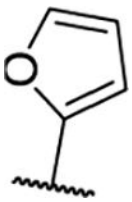	30.7 ± 4.7	214 ± 44.0	2.1 / 10.4
18b	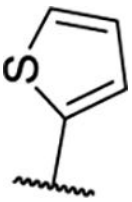	111 ± 9.9	624 ± 131	ND / ND

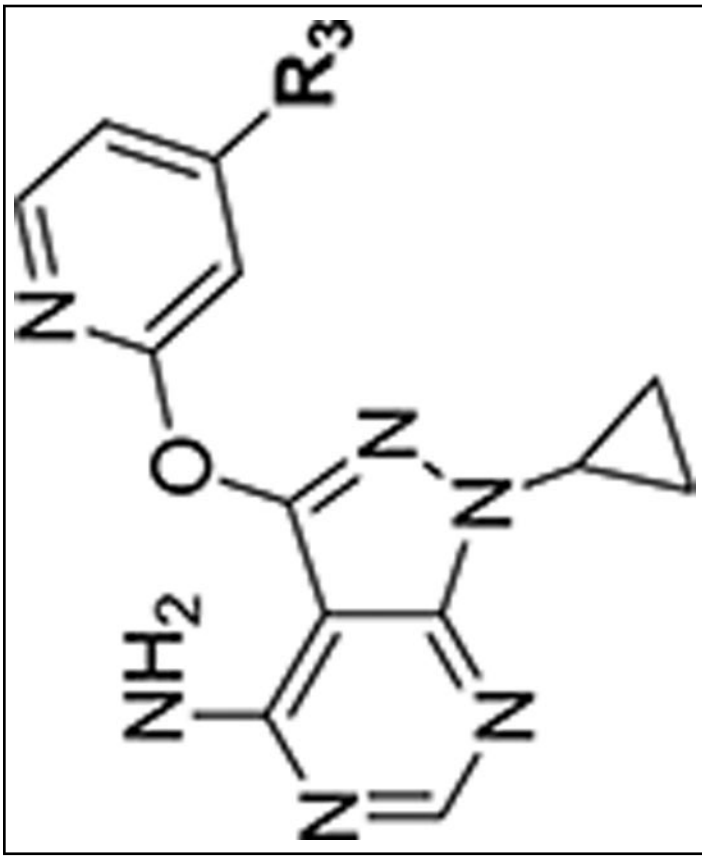

Cmpd	R_3	IC_{50}(nM)[a]	EC_{50}(nM)[a]	MLM/HLM $t_{1/2}$ (min)[b]
19b	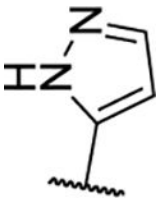	48.3 ± 9.0	243 ± 91.4	4.3 / 73.9
20b		18.2 ± 1.1	244 ± 46.5	5.0 / 28.8

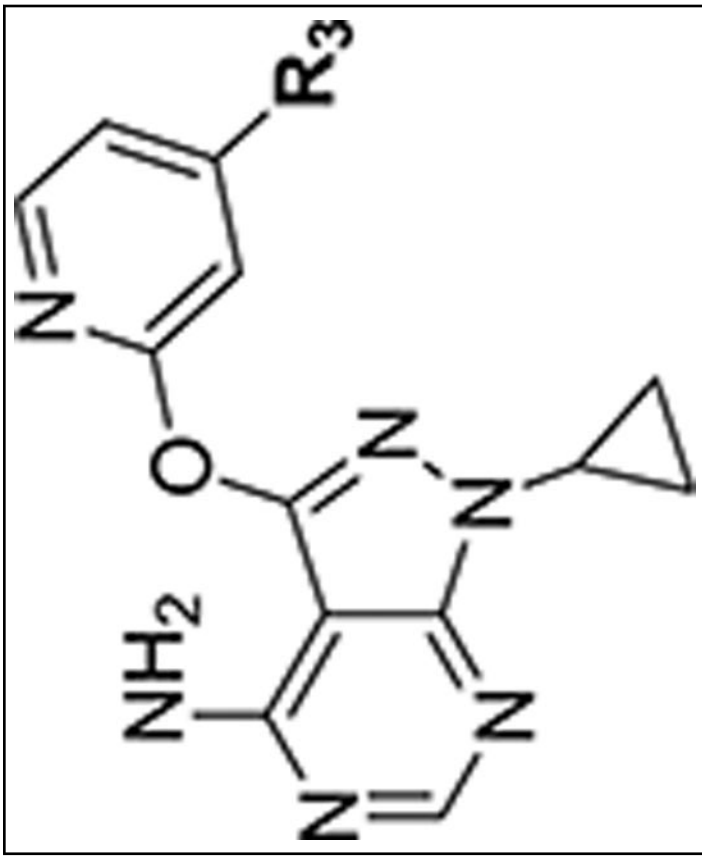

Cmpd	R_3	IC_{50}(nM)[a]	EC_{50}(nM)[a]	MLM/HLM $t_{1/2}$ (min)[b]
21b		38.6 ± 1.9	230 ± 15.3	2.8 / 31.9
22b		600 ± 7.8	ND	ND / ND

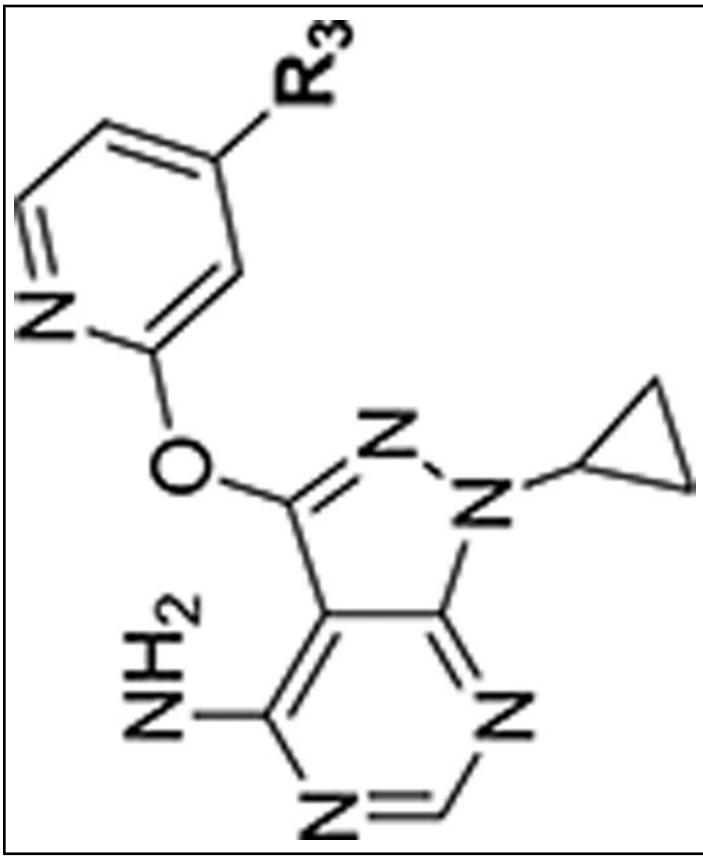

Cmpd	R_3	IC_{50}(nM)[a]	EC_{50}(nM)[a]	MLM/HLM $t_{1/2}$ (min)[b]
23b	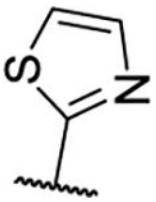	582 ± 277	592 ± 250	ND / ND
24b		355 ± 287	1310 ± 683	ND / ND

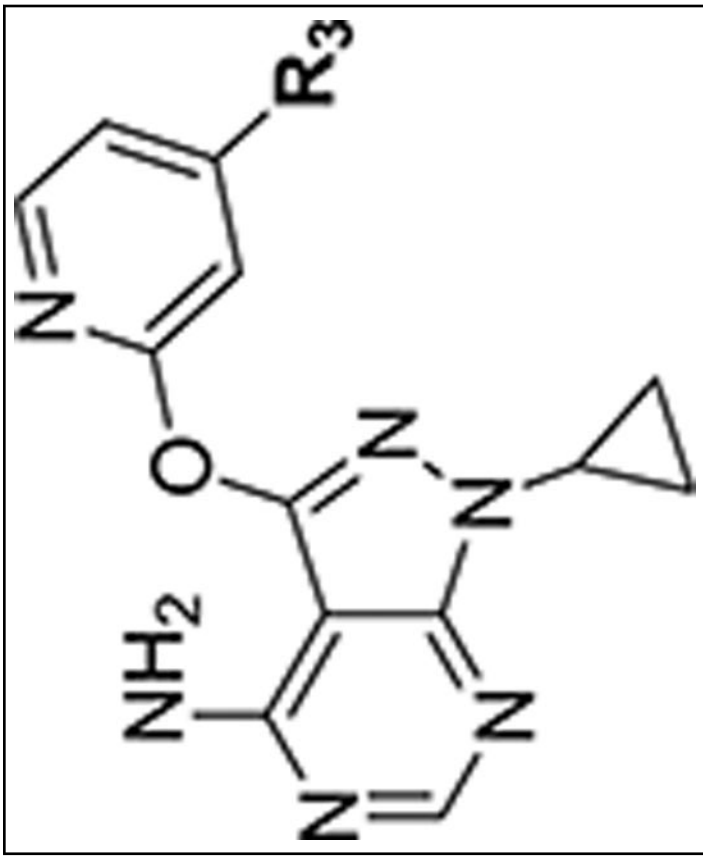

Cmpd	R_3	IC_{50}(nM)[a]	EC_{50}(nM)[a]	MLM/HLM $t_{1/2}$ (min)[b]
25b		306 ± 40.9	10,000	ND / ND
26b	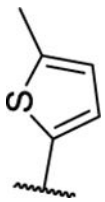	11.1 ± 4.9	133 ± 33.1	9.2 / 7.5
27b	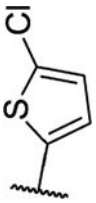	10.7 ± 9.4	209 ± 90.1	8.5 / 38.1

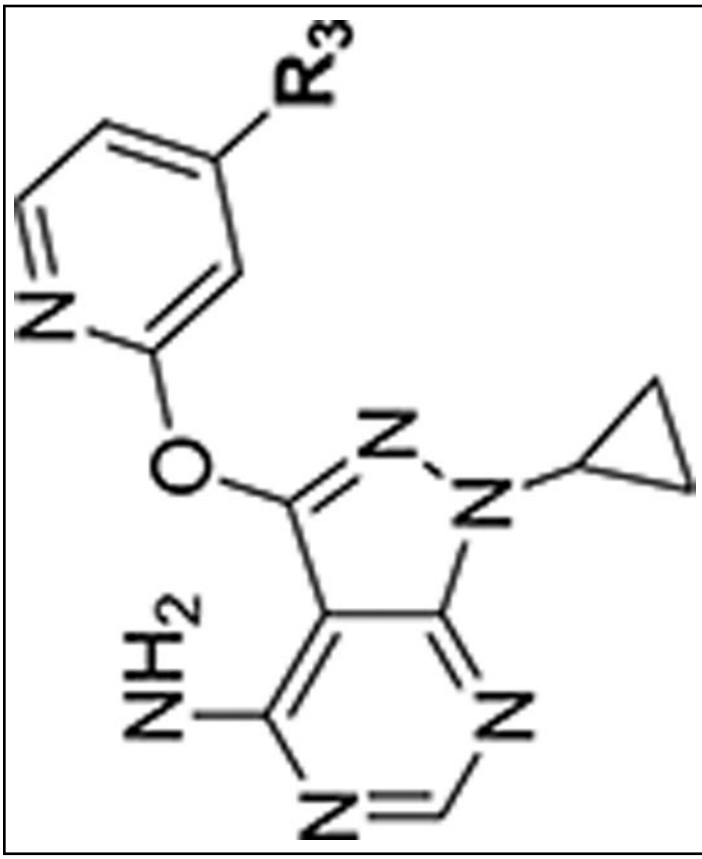

Cmpd	R_3	IC_{50}(nM)[a]	EC_{50}(nM)[a]	MLM/HLM $t_{1/2}$ (min)[b]
28b	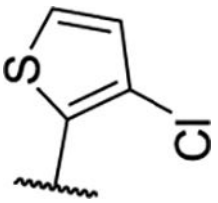	94.4 ± 33.4	698 ± 378	ND / ND
29b	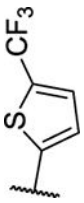	24.4 ± 11.5	314 ± 41.8	6 / 139

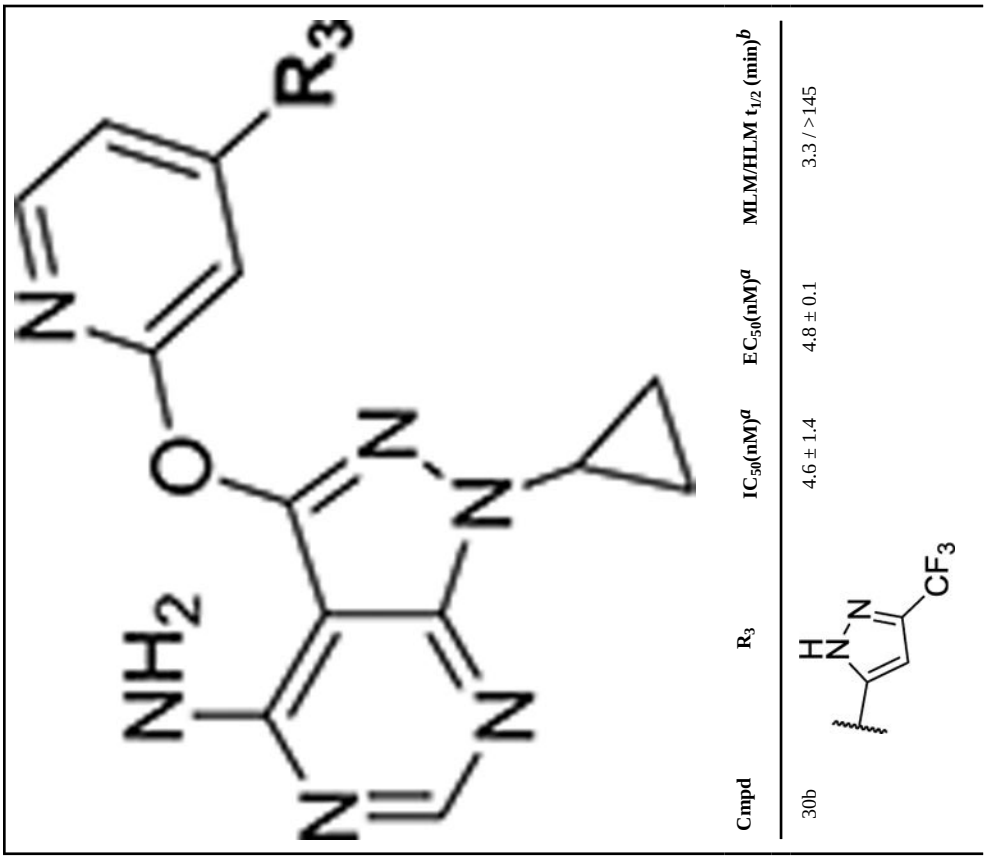

Cmpd	R_3	IC_{50}(nM)[a]	EC_{50}(nM)[a]	MLM/HLM $t_{1/2}$ (min)[b]
30b		4.6 ± 1.4	4.8 ± 0.1	3.3 / >145

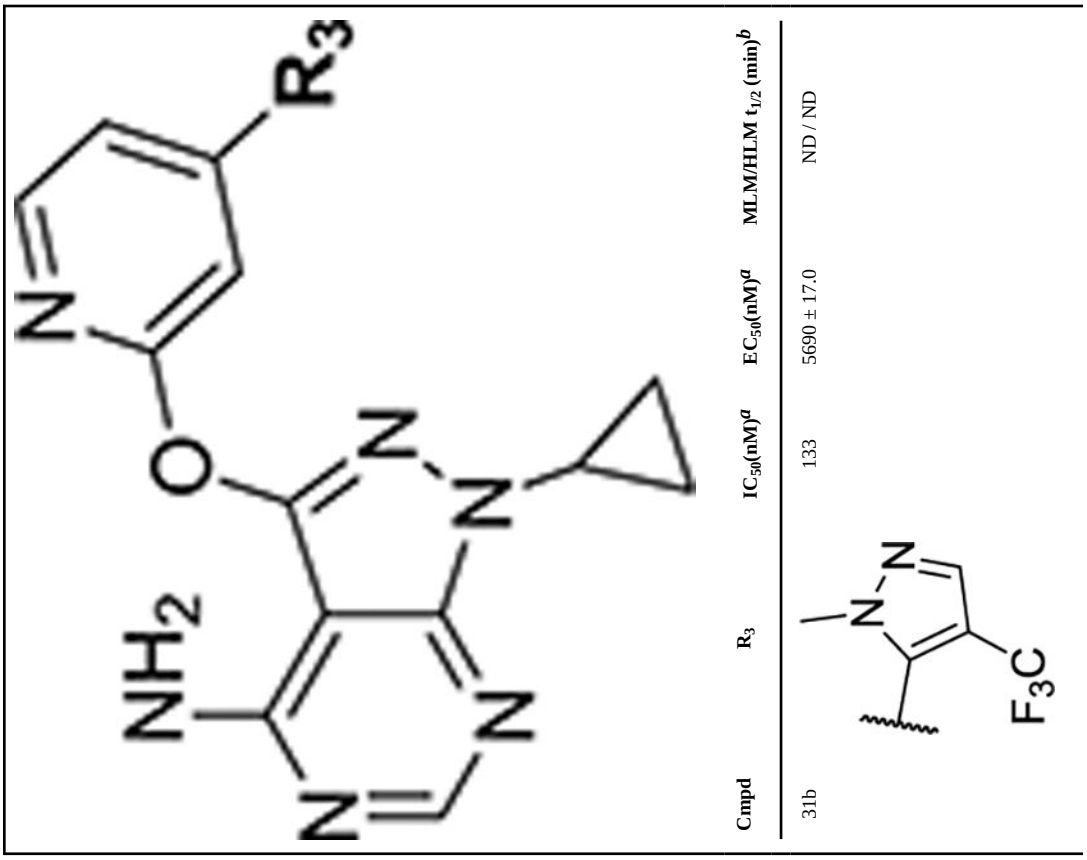

Cmpd	R_3	IC_{50}(nM)[a]	EC_{50}(nM)[a]	MLM/HLM $t_{1/2}$ (min)[b]
31b		133	5690 ± 17.0	ND / ND

Cmpd	R_3	IC_{50}(nM)[a]	EC_{50}(nM)[a]	MLM/HLM $t_{1/2}$ (min)[b]
32b		122 ± 73.6	1330 ± 876	ND / ND

[a] Half maximal inhibitory concentration determined from enzyme and cell-based assay.

[b] Metabolic half-lives. Data are reported as duplicates and triplicates ± standard deviation. Cmpd = compound, ND = not determined.

Table 3.

SAR of PP Biaryl Analogs Optimizing for Reduced Protein Binding

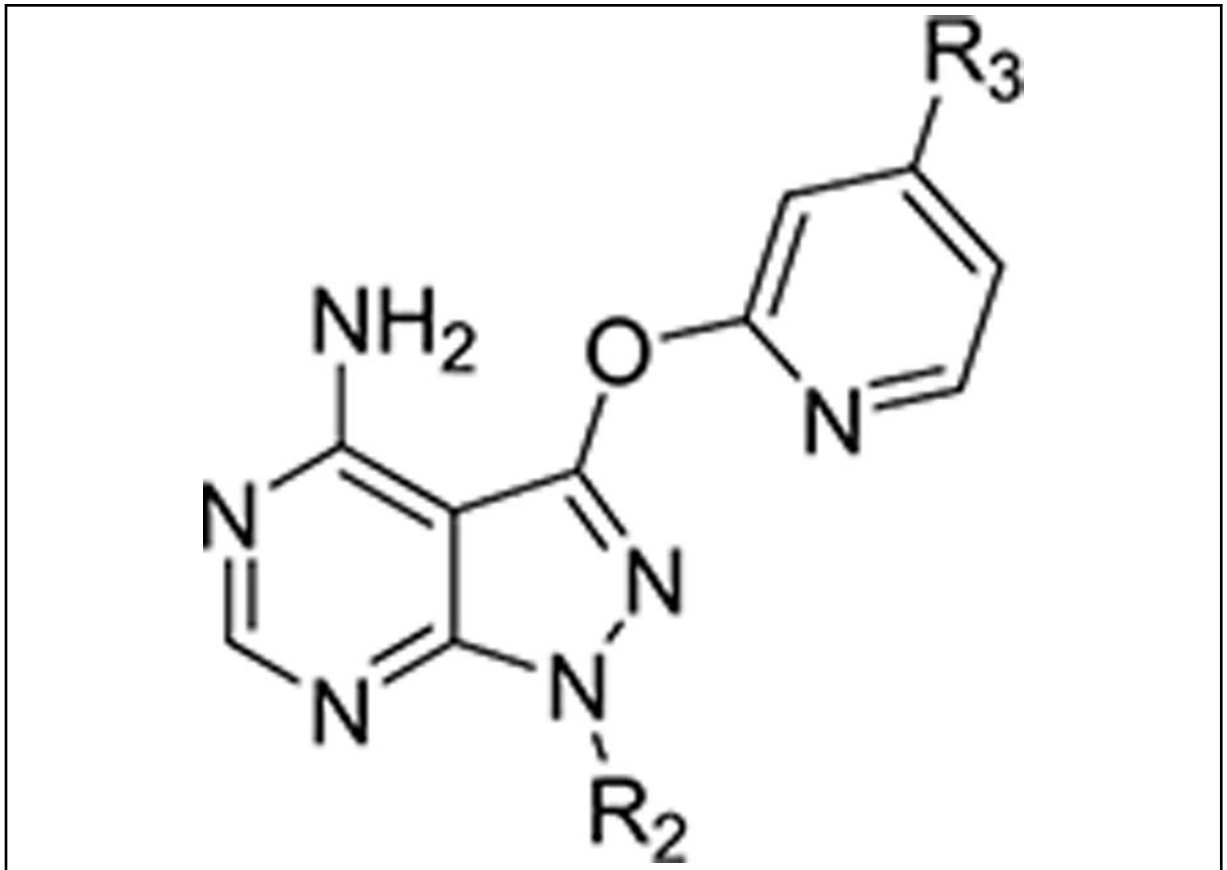

Compound	R_2	R_3	IC_{50}(nM)[a]	EC_{500}(nM)[a]	MLM/HLM $t_{1/2}$(min)[b]	PPB (% bound)[c]
16b	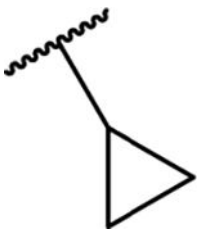	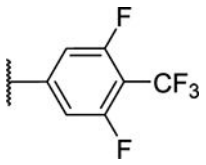	24 ± 13.5	570 ± 281	103 / >145	99.7
1c		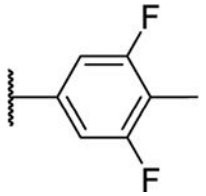	3.8 ± 1.0	86.4 ± 11.8	5.2 / 25.2	99.4

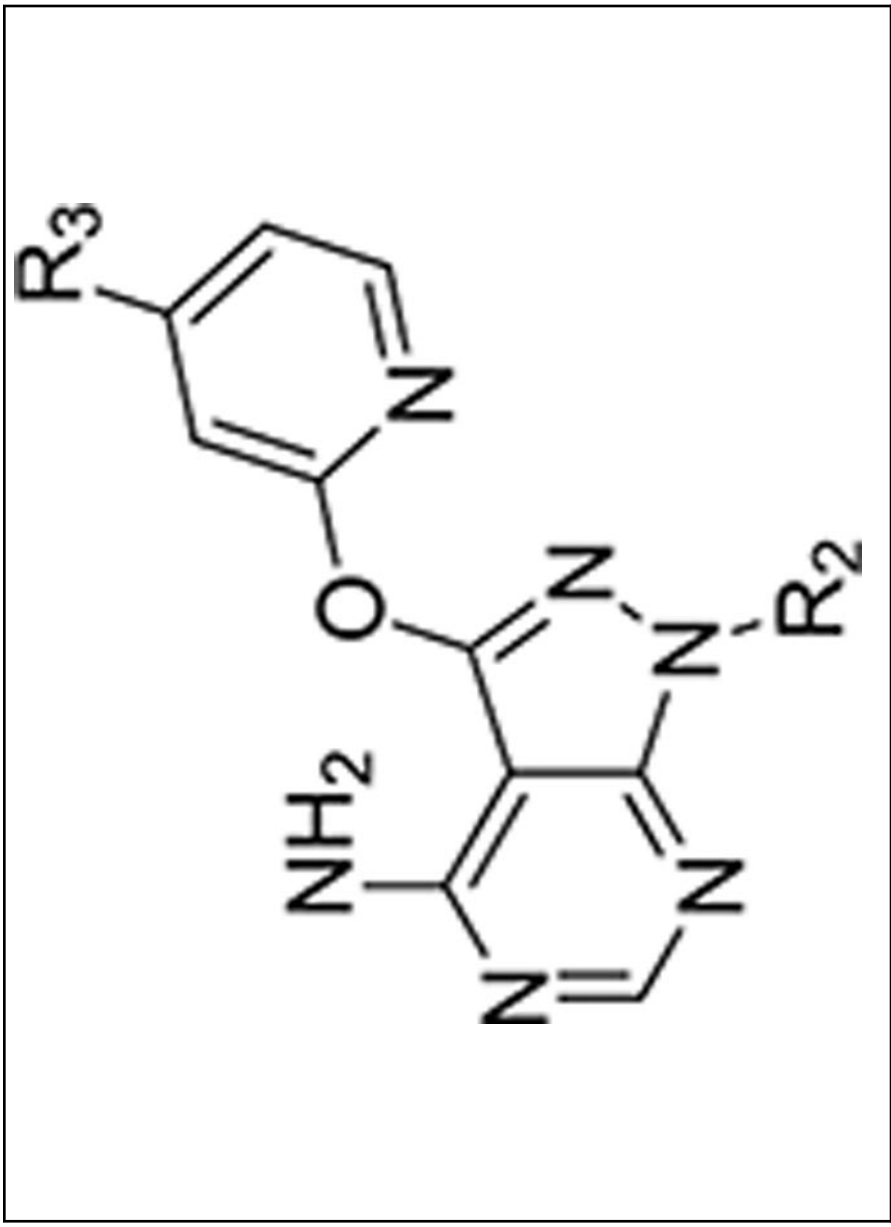

Compound	R_2	R_3	IC_{50}(nM)[a]	EC_{500}(nM)[a]	MLM/HLM $t_{1/2}$(min)[b]	PPB (% bound)[c]
2c		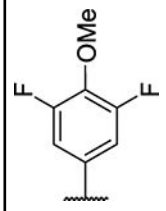	39 ± 41.6	147 ± 9.9	12.4 / NA	97.8

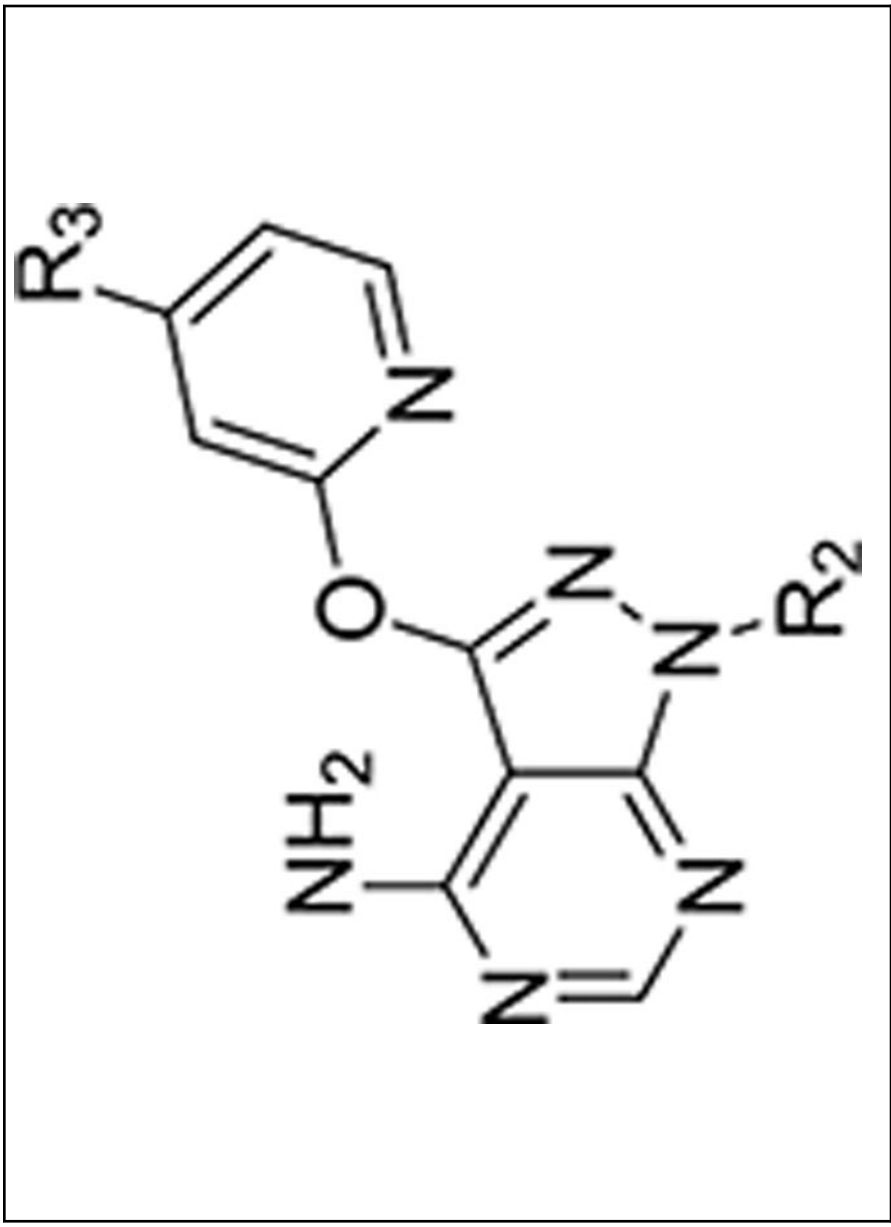

Compound	R_2	R_3	IC_{50}(nM)[a]	EC_{500}(nM)[a]	MLM/HLM $t_{1/2}$(min)[b]	PPB (% bound)[c]
3c		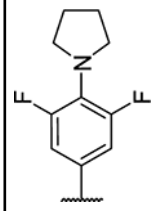	5.5 ± 3.2	17.5 ± 1.8	9.3 / NA	ND

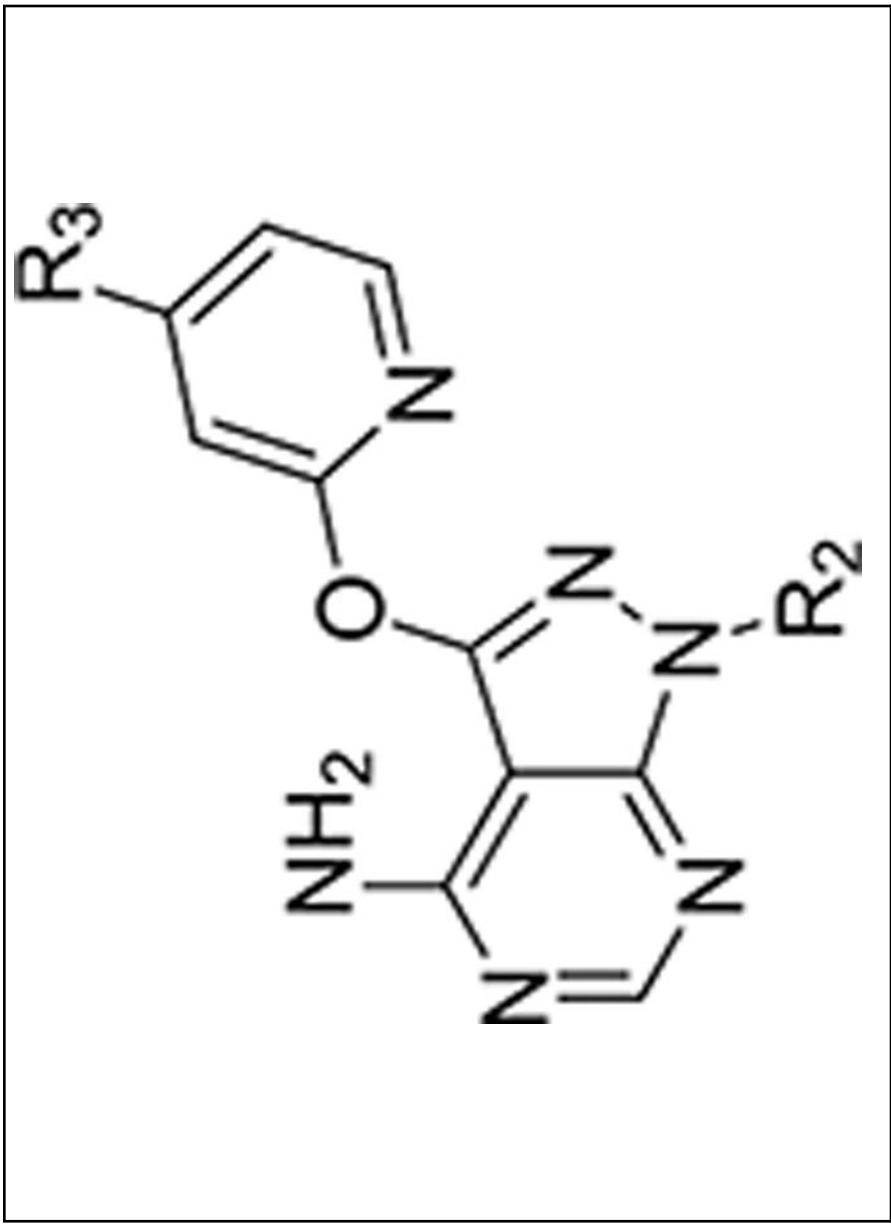

Compound	R_2	R_3	IC_{50}(nM)[a]	EC_{500}(nM)[a]	MLM/HLM $t_{1/2}$(min)[b]	PPB (% bound)[c]
4c		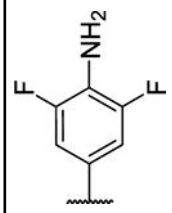	54.8 ± 13.9	1600 ± 764	ND / ND	ND

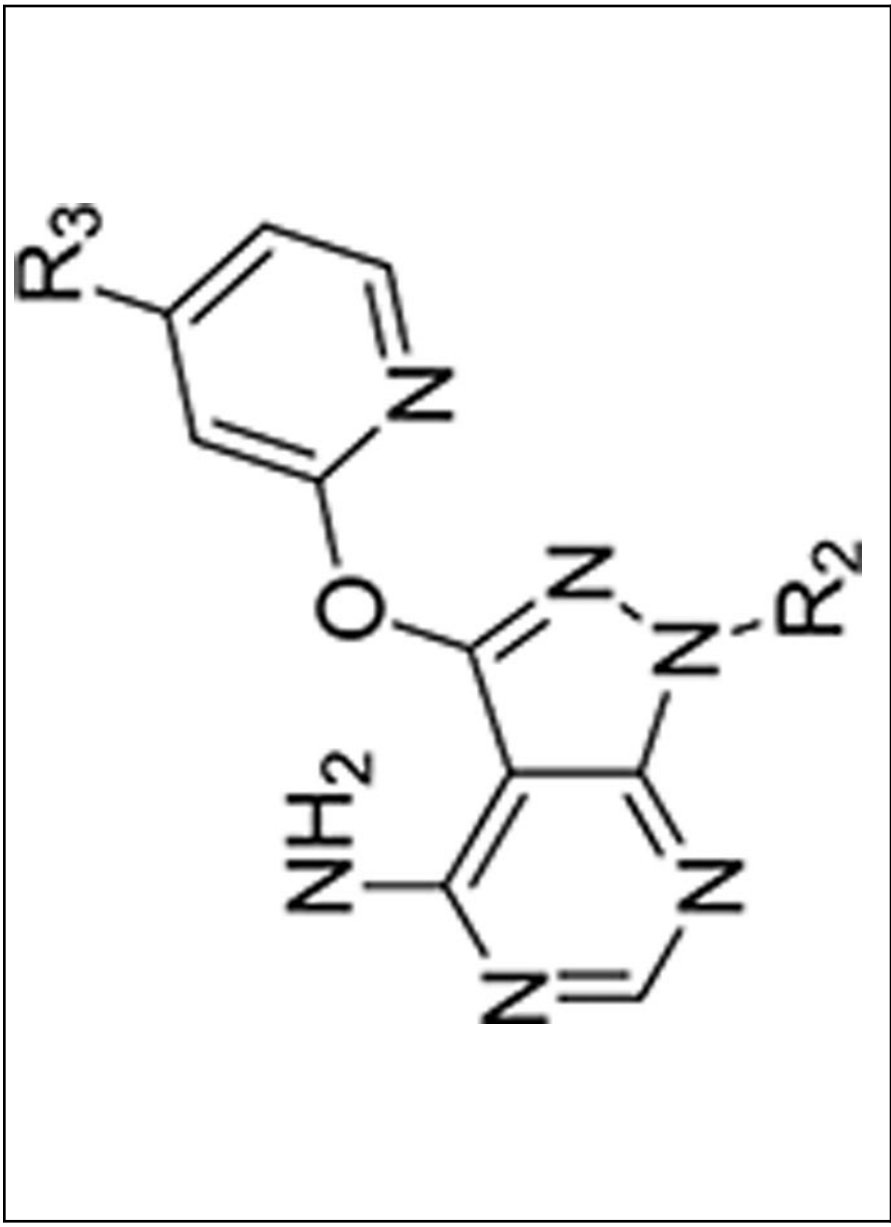

Compound	R_2	R_3	IC_{50}(nM)[a]	EC_{500}(nM)[a]	MLM/HLM $t_{1/2}$(min)[b]	PPB (% bound)[c]
5c		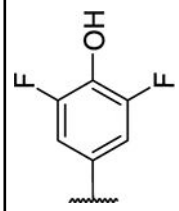	153 ± 89.2	1790 ± 619	ND / ND	ND

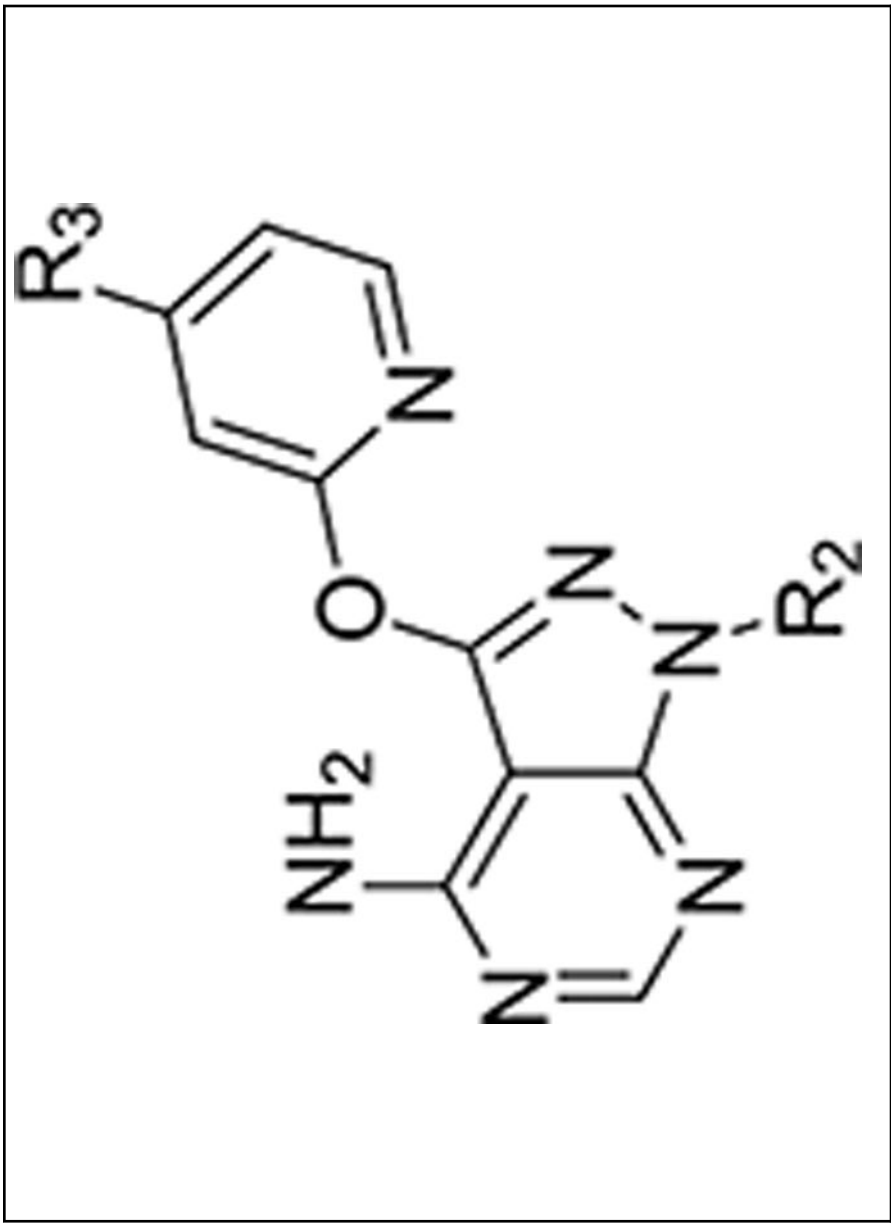

Compound	R_2	R_3	IC_{50}(nM)[a]	EC_{500}(nM)[a]	MLM/HLM $t_{1/2}$(min)[b]	PPB (% bound)[c]
6c		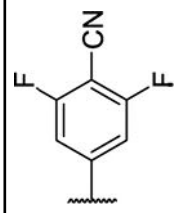	127 ± 30.4	10000	ND / ND	ND

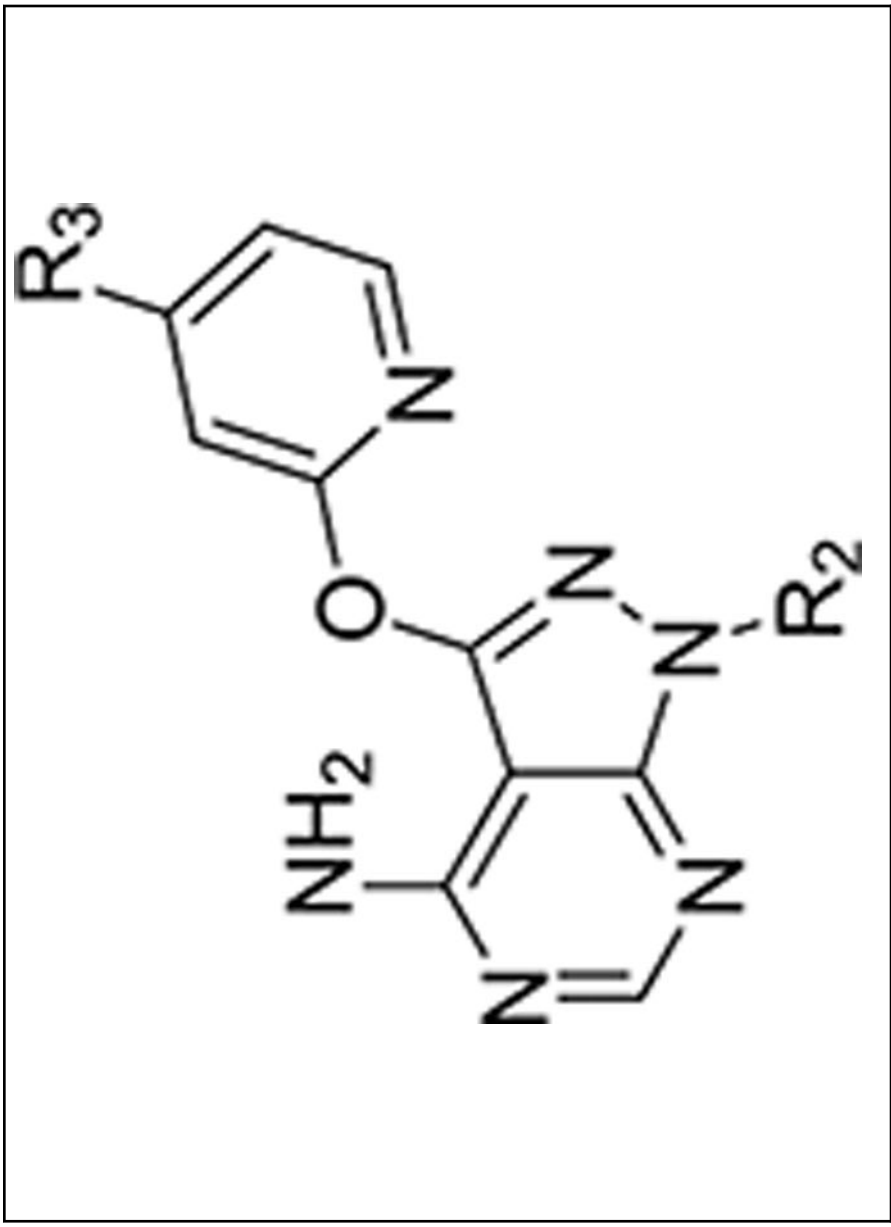

Compound	R_2	R_3	IC_{50}(nM)[a]	EC_{500}(nM)[a]	MLM/HLM $t_{1/2}$(min)[b]	PPB (% bound)[c]
7c		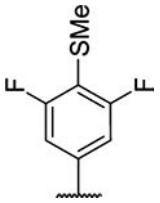	339	ND	ND / ND	ND

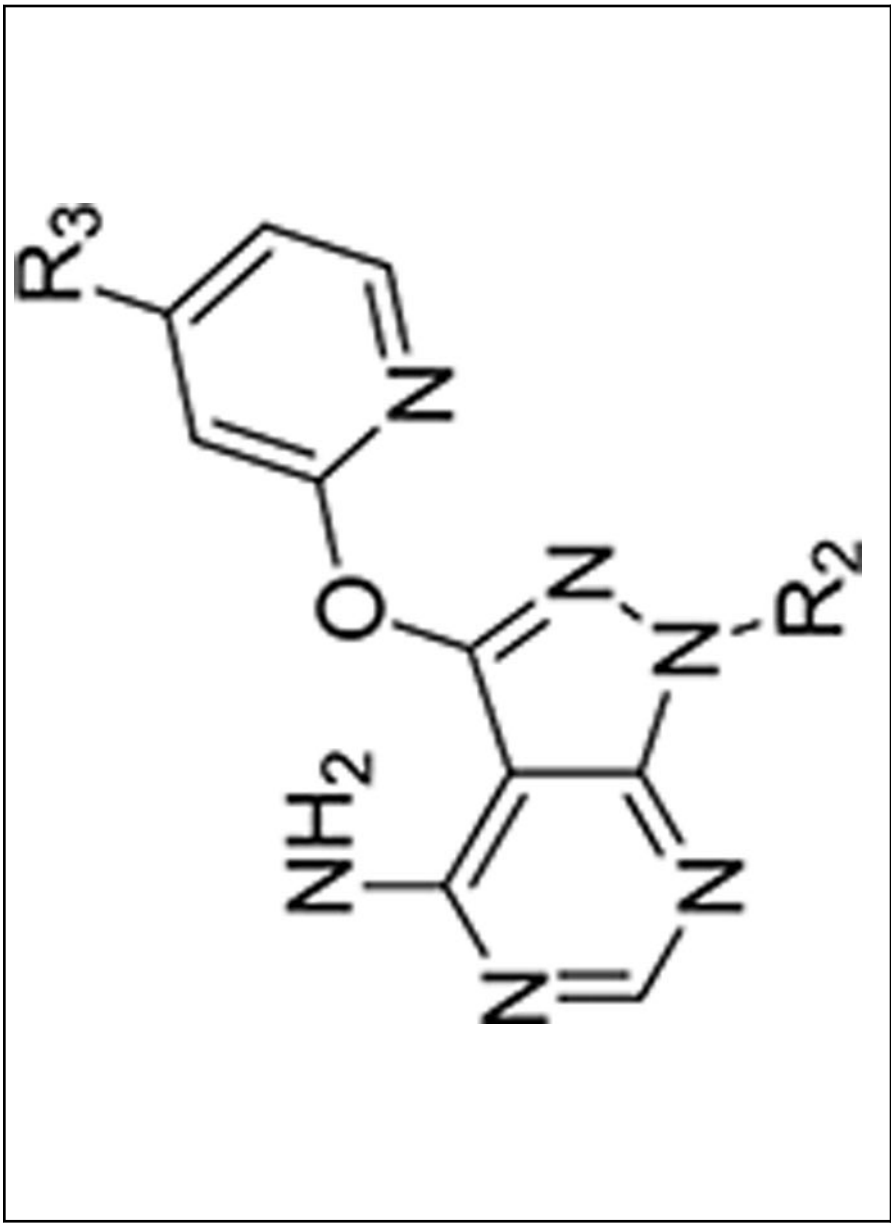

Compound	R_2	R_3	IC_{50}(nM)[a]	EC_{500}(nM)[a]	MLM/HLM $t_{1/2}$(min)[b]	PPB (% bound)[c]
8c	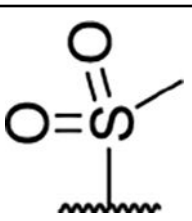	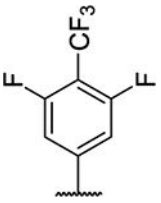	146 ± 53.7	55.1	101 / >145	97.4

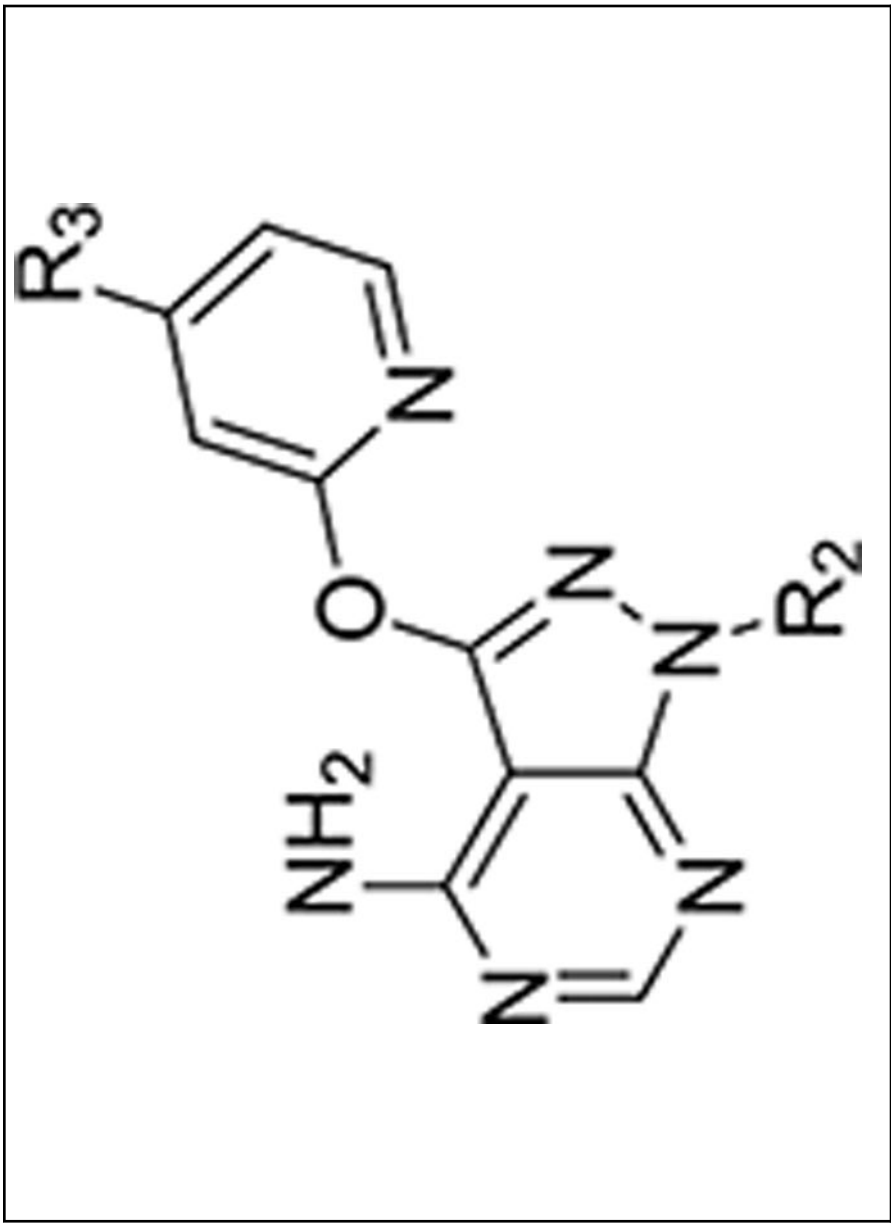

Compound	R_2	R_3	IC_{50}(nM)[a]	EC_{500}(nM)[a]	MLM/HLM $t_{1/2}$(min)[b]	PPB (% bound)[c]
9c	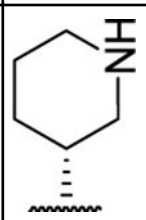		34.2 ± 8.9	377 ± 31.0	95.5 / ND	96.5

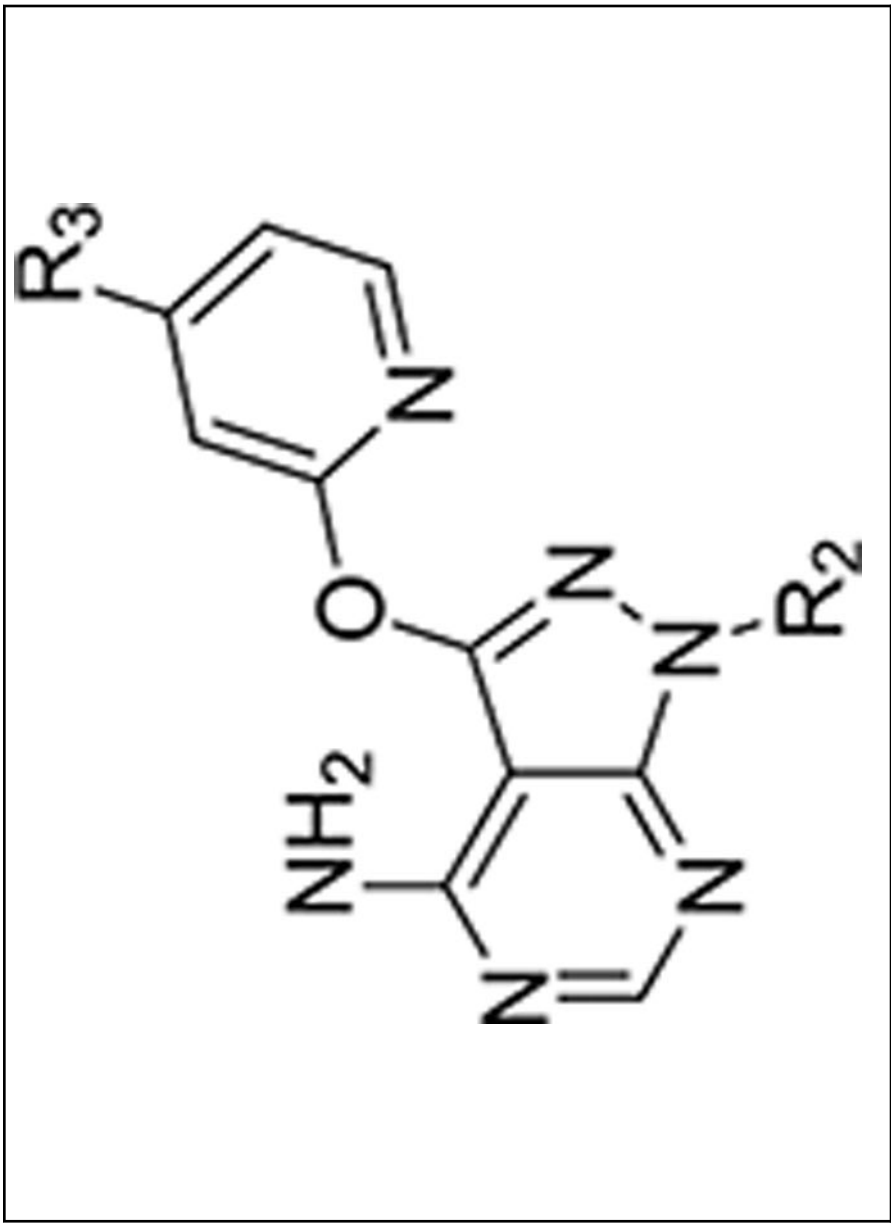

Compound	R_2	R_3	IC_{50}(nM)[a]	EC_{500}(nM)[a]	MLM/HLM $t_{1/2}$(min)[b]	PPB (% bound)[c]
10c	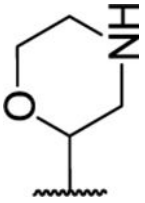		37.8 ± 4.9	602 ± 9.2	30.9 / ND	ND

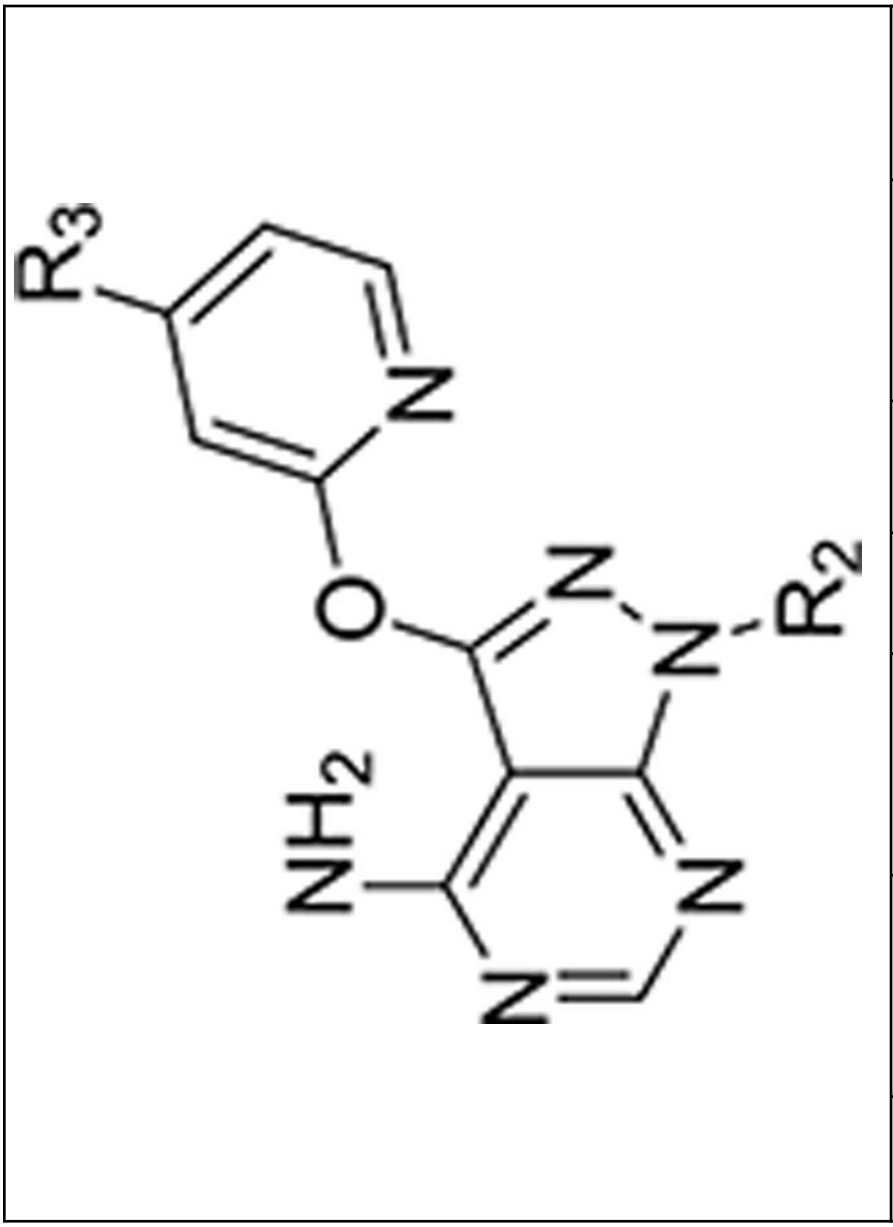

Compound	R_2	R_3	IC_{50}(nM)[a]	EC_{500}(nM)[a]	MLM/HLM $t_{1/2}$(min)[b]	PPB (% bound)[c]
11c	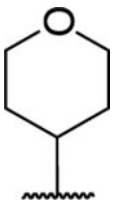		71.1 ± 17.7	309 ± 80.6	38.6 / ND	ND

Compound	R_2	R_3	IC_{50}(nM)[a]	EC_{500}(nM)[a]	MLM/HLM $t_{1/2}$(min)[b]	PPB (% bound)[c]
12c			49.6 ± 26.1	530 ± 13.1	64.9 / ND	96.5
13c			39.6 ± 34.3	638 ± 313	93.9 / >145	96.5

Compound	R_2	R_3	IC_{50}(nM)[a]	EC_{500}(nM)[a]	MLM/HLM $t_{1/2}$(min)[b]	PPB (% bound)[c]
14c			116 ± 52.3	1550 ± 358	8.9 / >145	88.6
15c			49.0 ± 5.6	292 ± 38.2	82.4 / ND	ND

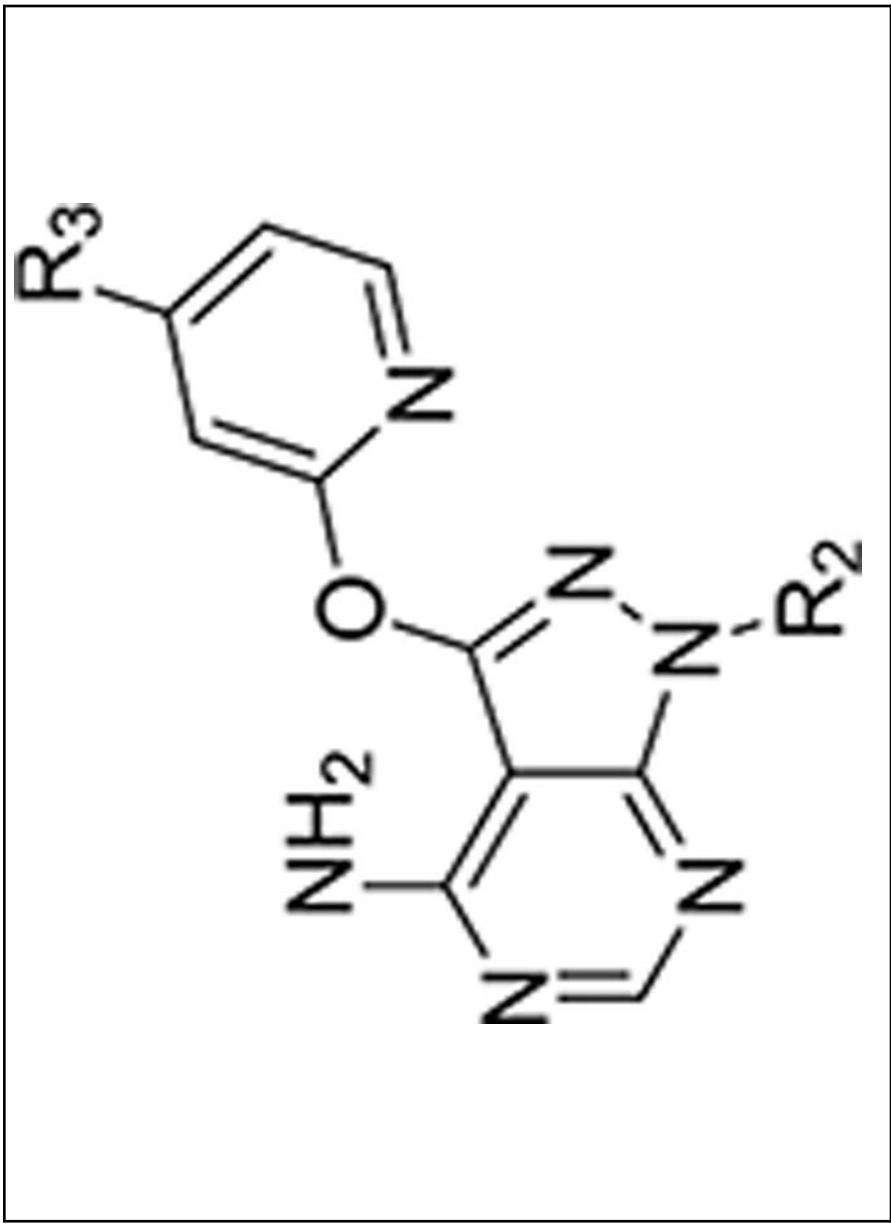

Compound	R_2	R_3	IC_{50}(nM)[a]	EC_{500}(nM)[a]	MLM/HLM $t_{1/2}$(min)[b]	PPB (% bound)[c]
16c		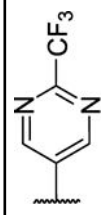	15.7 ± 9.1	270 ± 55.8	108 / >145	82.0
17c		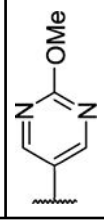	45.0 ± 6.9	684 ± 64.3	ND / ND	ND

Compound	R_2	R_3	IC_{50}(nM)[a]	EC_{500}(nM)[a]	MLM/HLM $t_{1/2}$(min)[b]	PPB (% bound)[c]
18c			6.9 ± 3.1	71.6 ± 25.6	10.0 / ND	ND
19c			11.9 ± 3.7	90 ± 7.5	26.6 / ND	ND

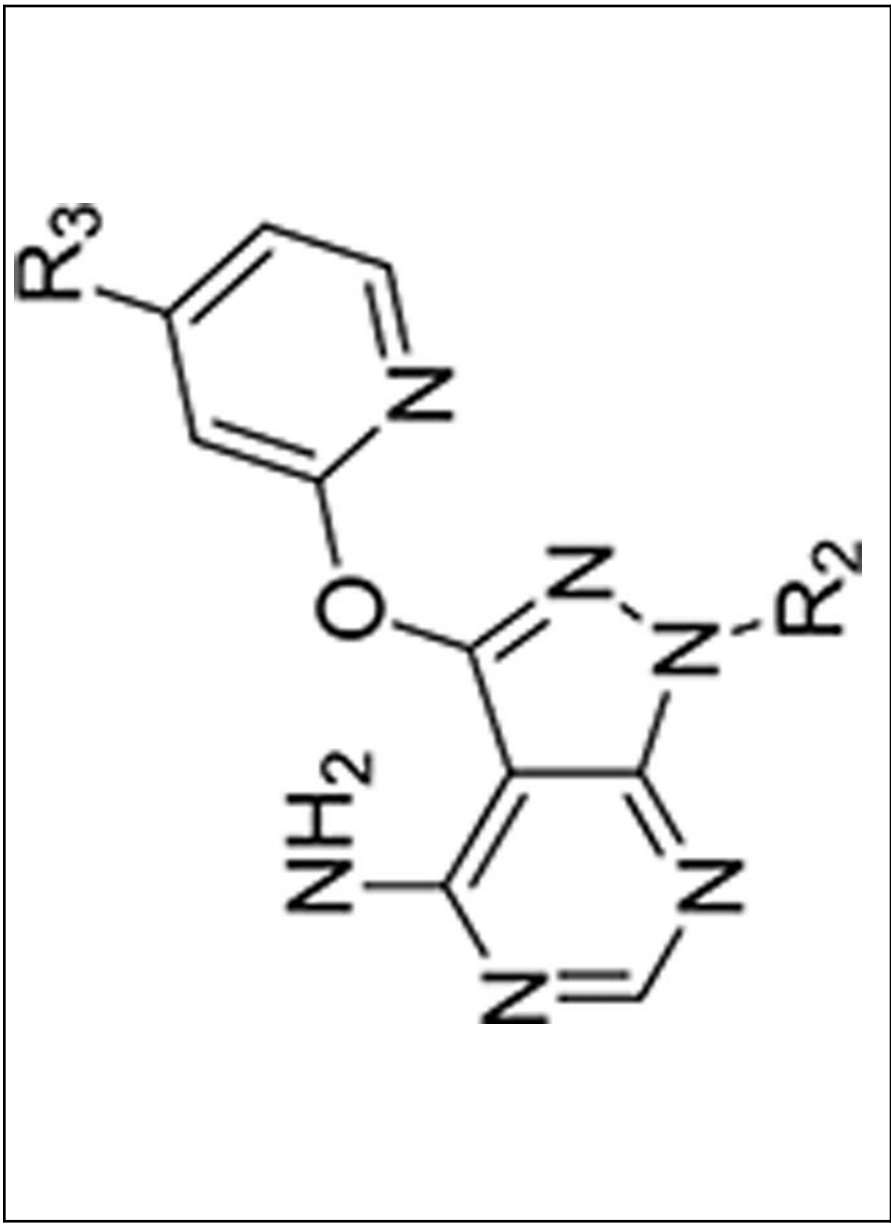

Compound	R_2	R_3	IC_{50}(nM)[a]	EC_{500}(nM)[a]	MLM/HLM $t_{1/2}$(min)[b]	PPB (% bound)[c]
20c		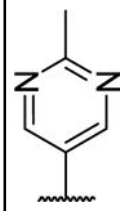	36.1 ± 8.8	403 ± 14.1	>145 / 92.8	ND

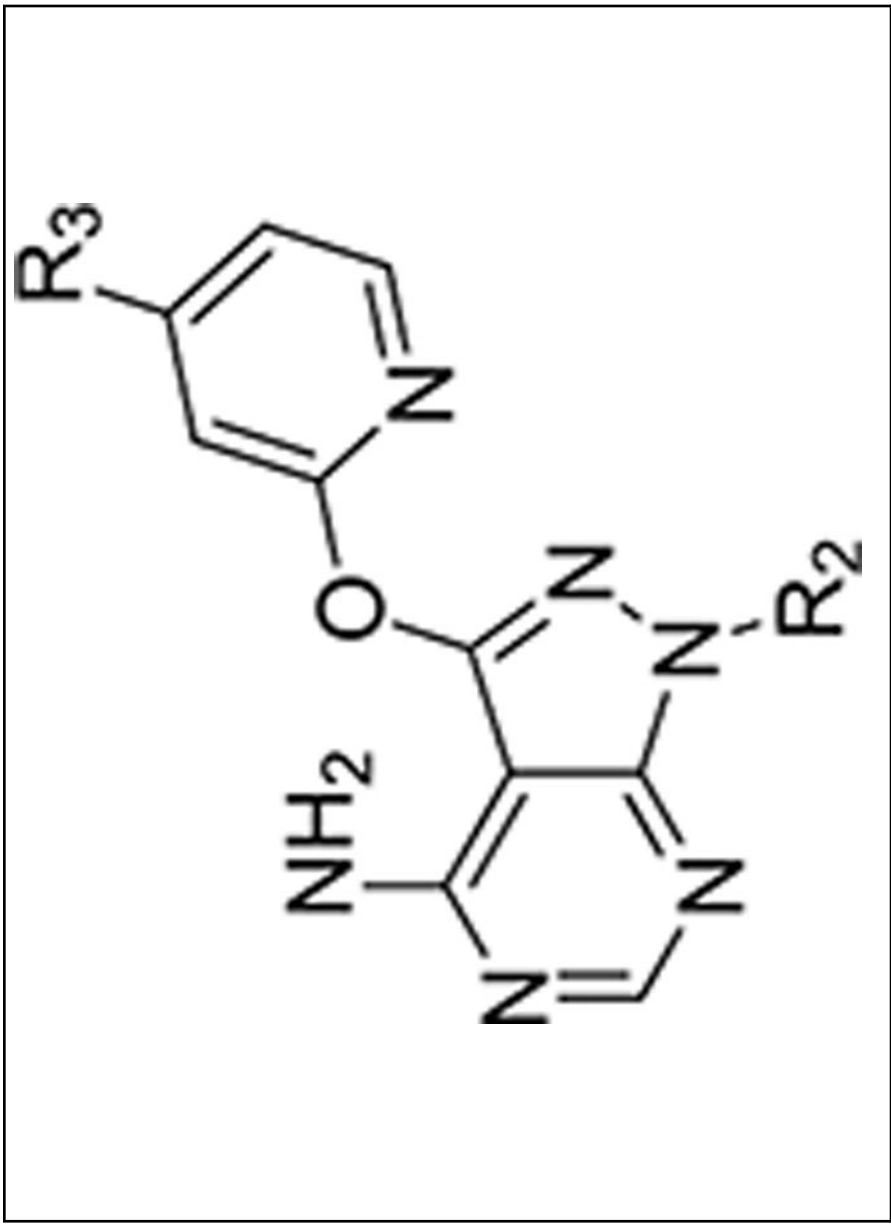

Compound	R_2	R_3	IC_{50}(nM)[a]	EC_{500}(nM)[a]	MLM/HLM $t_{1/2}$(min)[b]	PPB (% bound)[c]
21c	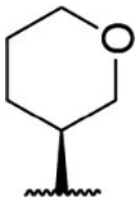	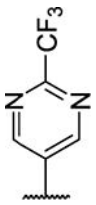	15.3 ± 9.0	273 ± 111	>145 / 130	ND

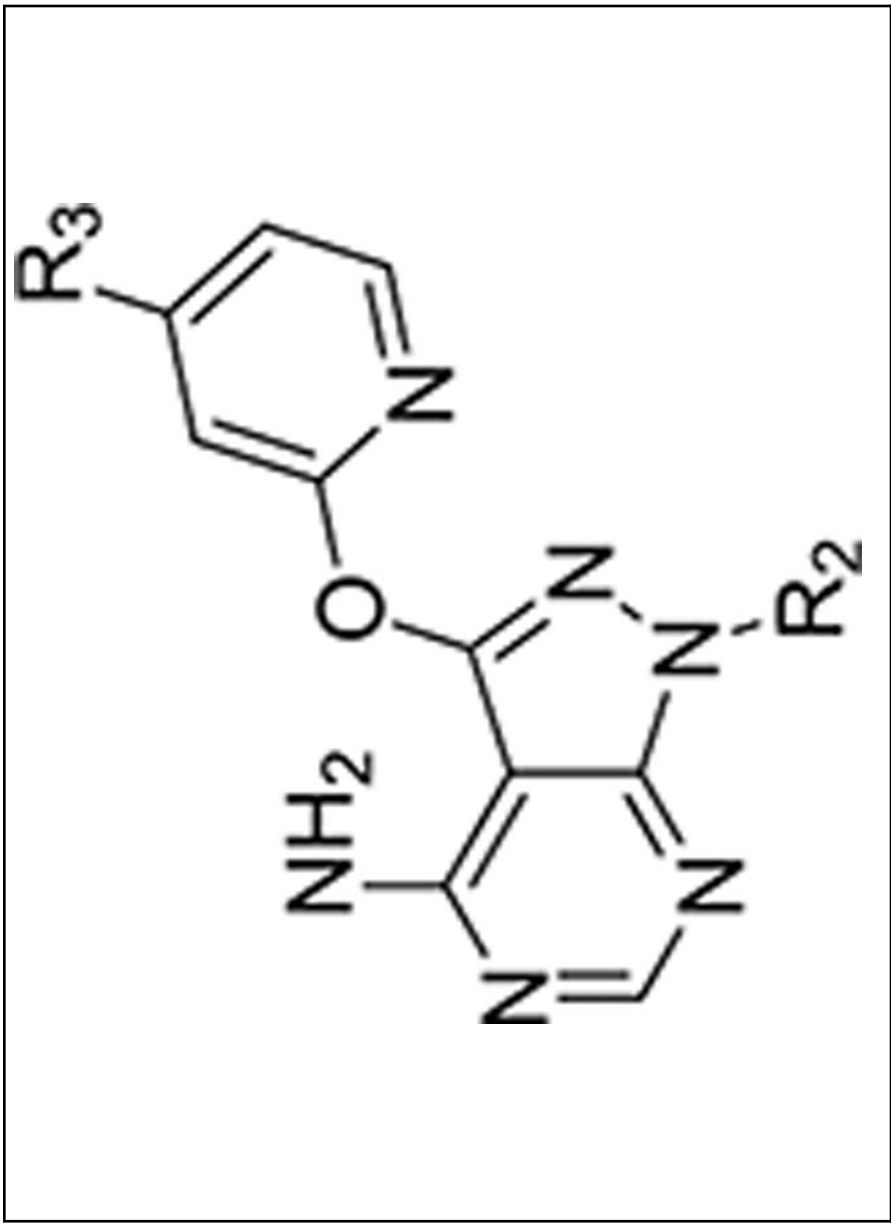

Compound	R_2	R_3	IC_{50}(nM)[a]	EC_{500}(nM)[a]	MLM/HLM $t_{1/2}$(min)[b]	PPB (% bound)[c]
22c			3.6 ± 0.6	239 ± 69.0	54.2 / ND	ND

Compound	R_2	R_3	IC_{50}(nM)[a]	EC_{500}(nM)[a]	MLM/HLM $t_{1/2}$(min)[b]	PPB (% bound)[c]
23c			2.9 ± 0.3	147 ± 47.9	29.8 / ND	ND

[a] Half maximal inhibitory concentration determined from enzyme and cell-based assay.

[b] Metabolic half-lives.

[c] Plasma Data are reported as duplicates and triplicates ± standard deviation. ND = not determined.

Table 4.

Summary of Surviving Animals in Acute Challenge Model

trial	compound	dosage (mg/kg)	frequency	number of animals	number of survivors	ELISA[c]	outgrowth on HFF[d]
1	vehicle control		BID	5	0		
1	**16b**	30[a]	BID	5	0		
1	**16b**	100[a]	QD	5	1	1.22	1/1
1	**13c**	30[a]	BID	5	0		
1	**13c**	100[a]	QD	5	2	0.88	2/2
2	vehicle control		BID	5	1	0.74	1/1
2	**16c**	30[a]	BID	5	5	1.74	5/5
2	**16c**	100[a]	QD	5	5	2.23	0/5
2	sulfadiazine	0.25[b]	ad lib	5	5	2.18	3/5

[a] mg/kg.

[b] mg/mL.

[c] OD450 nm.

[d] Number of positive/number of surviving mice.